JAAVSO

The Journal of
The American Association
of Variable Star Observers

Volume 38
Number 1
2010

ISSN 0271-9053

49 Bay State Road
Cambridge, MA 02138
U. S. A.

The *Journal of the American Association of Variable Star Observers* is a refereed scientific journal published by the American Association of Variable Star Observers, 49 Bay State Road, Cambridge, Massachusetts 02138, USA. The *Journal* is made available to all AAVSO members and subscribers.

In order to speed the dissemination of scientific results, selected papers that have been refereed and accepted for publication in the *Journal* will be posted on the internet at the *eJAAVSO* website as soon as they have been typeset and edited. These electronic representations of the *JAAVSO* articles are automatically indexed and included in the NASA Astrophysics Data System (ADS). *eJAAVSO* papers may be referenced as *J. Amer. Assoc. Var. Star Obs., in press,* until they appear in the concatonated electronic issue of *JAAVSO*. The *Journal* cannot supply reprints of papers.

Page Charges

Unsolicited papers by non-Members will be assessed a charge of $15 per page.

Instructions for Submissions

The *Journal* welcomes papers from all persons concerned with the study of variable stars and topics specifically related to variability. All manuscripts should be written in a style designed to provide clear expositions of the topic. Contributors are strongly encouraged to submit digitized text in LATEX+POSTSCRIPT, MS WORD, or plain-text format. Manuscripts may be mailed electronically to journal@aavso.org or submitted by postal mail to *JAAVSO*, 49 Bay State Road, Cambridge, MA 02138, USA.

Manuscripts must be submitted according to the following guidelines, or they will be returned to the author for correction:

Manuscripts must be:
1) original, unpublished material;
2) written in English;
3) accompanied by an abstract of no more than 100 words.
4) not more than 2,500–3,000 words in length (10–12 pages double-spaced).

Figures for publication must:
1) be camera-ready or in a high-contrast, high-resolution, standard digitized image format;
2) have all coordinates labeled with division marks on all four sides;
3) be accompanied by a caption that clearly explains all symbols and significance, so that the reader can understand the figure without reference to the text.

Maximum published figure space is 4.5" by 7". When submitting original figures, be sure to allow for reduction in size by making all symbols and letters sufficiently large.

Photographs and halftone images will be considered for publication if they directly illustrate the text.

Tables should be:
1) provided separate from the main body of the text;
2) numbered sequentially and referred to by Arabic number in the text, e.g., Table 1.

References:
1) References should relate directly to the text.
2) References should be keyed into the text with the author's last name and the year of publication, e.g., (Smith 1974; Jones 1974) or Smith (1974) and Jones (1974).
3) In the case of three or more joint authors, the text reference should be written as follows: (Smith *et al.* 1976).
4) All references must be listed at the end of the text in alphabetical order by the author's last name and the year of publication, according to the following format:
   Brown, J., and Green, E. B. 1974, *Astrophys. J.*, **200**, 765.
   Thomas, K. 1982, *Phys. Report*, **33**, 96.
5) Abbreviations used in references should be based on recent issues of the Journal or the listing provided at the beginning of *Astronomy and Astrophysics Abstracts* (Springer-Verlag).

Miscellaneous:
1) Equations should be written on a separate line and given a sequential Arabic number in parentheses near the right-hand margin. Equations should be referred to in the text as, e.g., equation (1).
2) Magnitude will be assumed to be visual unless otherwise specified.
3) Manuscripts may be submitted to referees for review without obligation of publication.

Journal of the American Association of Variable Star Observers
Volume 38, Number 1, 2010

Table of Contents continued on next page

Abstracts of Papers and Posters Presented at the 98th Annual Meeting of the AAVSO, Held in Newton, Massachusetts, November 6–7, 2009

Secular Variation of the Mode Amplitude-Ratio of the Double-Mode RR Lyrae Star NSVS 5222076

David A. Hurdis
76 Harbour Island Road, Narragansett, RI 02882; hurdisd@cox.net

Tom Krajci
P.O. Box 1351, Cloudcroft, NM 88317; tom_krajci@tularosa.net

Presented at the 98th Annual Meeting of the AAVSO, November 7, 2009
Received November 9, 2009; revised November 19, 2009; accepted November 19, 2009

Abstract In 2008, a campaign of time-series observations (Hurdis 2009) was conducted in the *V* and *I* bands for NSVS 5222076, a double-mode RR Lyrae (RRd) field star in Bootes. Comparison of those results with the earlier observations of Oaster, Smith, and Kinemuchi (2006) suggested that a rapid and significant decrease might be occurring in the amplitude ratio, A_0/A_1, of the star's fundamental and first-overtone pulsation modes. To follow up on this interesting result, another campaign of time-series observations was conducted in 2009. We find that the amplitude ratio has indeed decreased in the *V*-band, from 1.93 in 2005 to 1.76 in 2008 to 1.48 in 2009.

1. Introduction

In his earlier paper on NSVS 5222076 (= GSC 03059-00636), Hurdis (2009) described the discovery by Oaster (2005) of the star's double-mode variability in Northern Sky Variability Survey (NSVS; Woźniak *et al.* 2004) data, and the subsequent series of 1,570 *V*-band observations of it by Oaster, Smith, and Kinemuchi (2006, cited as OSK hereafter). He further described how NSVS 5222076 is unusual among RRd stars in that its fundamental mode is dominant. OSK had measured the amplitude ratio for the fundamental and first-overtone modes, A_0/A_1, to be approximately 2, and had pointed out that this unusually high amplitude ratio makes NSVS 5222076 a rarity, even among those RRd stars that have relatively strong fundamental mode pulsation.

From his 2008 observations, Hurdis (2009) had estimated the amplitude ratio, A_0/A_1, to be about 1.4 for both the *V* and *Ic* bands. That number was estimated by eye with a ruler, from phase plots of the deconvolved pulsation modes that had been created with PERANSO version 2.20 (Vanmunster 2005). The estimate was made difficult by having caught only four good maxima over the fourteen nights of observation. Nevertheless, the data were sufficiently good for it to be clear that the amplitude ratio was definitely less than OSK's value of "approximately 2." This seeming decrease in A_0/A_1, if correct, signified a gain in strength of the first-overtone mode relative to the fundamental mode. It became apparent that

more observations were needed, both to verify the result and to determine whether NSVS 5222076 is, perhaps, in the process of changing its dominant pulsation mode from fundamental to first-overtone.

In the globular cluster, M3, a few double-mode RR Lyrae stars have been observed to undergo changes in the relative strengths of the two pulsation modes (Clementini *et al.* 2004). In four such cases in M3 (V79, V166, V200, and V251), switching from one mode being dominant to the other has been observed (Corwin *et al*. 1999; Clementini *et al*. 2004; Clement and Thompson 2007). Clementini *et al.* (2004) observed that these changes can occur rapidly, over the span of a single year. They suggest that those stars are undergoing rapid evolutionary changes. The remarkable case of V79 in M3 is recounted by Clement and Thompson (2007). V79 has been observed for over a century, and has exhibited many changes, including an abrupt change of its fundamental period in 1897, and a switch in 1992 from being a single-mode (fundamental) pulsator to a double-mode pulsator with dominant first-overtone. Recent observations (Goranskij and Barsukova 2007), have revealed that a reverse switch has occurred, with the star returning to single-mode (fundamental) pulsation.

Observations of RRd stars are useful to modelers, because their two independent pulsation periods allow a unique determination of the star's mass (Clementini *et al.* 2004; Cox 1980). Observations of RRd mode switching, as described above, can provide even more information about a star's interior and evolution. To date, however, the only RRd stars that have been observed to have switched modes have been located in the crowded field of M3. On the other hand, NSVS 5222076 is a field star, located well out of the Galactic plane in Bootes. It is moderately bright (average $m_V = 12.94$), and well-placed for Northern Hemisphere observers. If it were, indeed, on the verge of undergoing a mode switch, it would provide a unique opportunity to study the event, unimpeded by the crowded star field of a globular cluster.

Having determined the need for more observations of NSVS 5222076 to verify that its amplitude ratio, A_0/A_1, is decreasing, it was decided to request time on the AAVSO Robotic Telescope Network (AAVSONet). The proposal was accepted, and the project was assigned to the robotic 28-cm Celestron telescope known as the Wright28, managed by coauthor Tom Krajci.

2. Objectives

The objectives for the work reported herein were as follows: a. Observe NSVS 5222076 in the *V*-band over a sufficiently long baseline, and including enough maxima, to allow the amplitude ratio, A_0/A_1, of the two pulsation modes to be accurately determined. b. Contiguously with the above *V*-band observations, observe the star in the *I*-band. c. By combining our *V*-band data with both the *V*-band data from the 2008 observing season (Hurdis 2009) and the *V*-band photometric data of OSK, expand the time baseline of observations, thereby

permitting more precise determinations of the pulsation periods and their ratio, P_1/P_0. d. Determine the ratio of amplitudes, A_0/A_1, of the deconvolved fundamental and first-overtone modes for both wavelength bands.

3. Equipment and methods

Two telescopes were used for our observations. The Wright28 is a 28-cm (11-in) Celestron C11 Schmidt-Cassegrain, located at Tom Krajci's Astrokolkhoz Observatory at an elevation of 2,877 meters (9,440 feet) near Cloudcroft, New Mexico. It is equipped with an f/6.2 focal reducer, giving it a focal length of 1,720 mm. Its images were taken with a Santa Barbara Instrument Group (SBIG) ST-7XME CCD camera, with its pixels binned 2 × 2 to increase sensitivity. The filters used were Johnson-V and Cousins-I interference filters from Astrodon.

The second telescope was a Meade 40-cm (16-in) Schmidt-Cassegrain, permanently mounted at the first author's Toby Point Observatory, near sea-level on the south coast of Rhode Island. Its focal ratio of f/10 gives it a focal length of 4,064 mm. It is equipped with an SBIG ST-8XME CCD camera, with its pixels binned 2 × 2 to increase sensitivity. The photometric filters used were Johnson-V and Cousins-I from Custom Scientific.

Our observing procedure was to take continuous, alternating *V*-band and *I*-band exposures of 90-second duration throughout the night for as long as the star was at an air mass of 2.0 or less. To maximize the number of pulsation maxima captured in our data, the choice of observing nights was guided by an ephemeris created from the most accurate value available for the fundamental pulsation period (Hurdis 2009). With the Wright28 telescope, 1,186 *V*-band images and 1,154 *I*-band images were taken on thirteen nights, between JD 2454883 and JD 2454964. With the Meade telescope, 296 *V*-band and 304 *I*-band images were taken on four nights, between JD 2454938 and JD 2455023.

Differential photometry of NSVS 5222076 was performed with AIP4WIN version 2.3.0 (Berry and Burnell 2005). GSC 03059-00534 was used as the comparison star for all images, where $V = 14.035$, $I = 13.385$, and $V–I = 0.650$. For the Wright28 images, GSC-03060-00055 was used as the check star, for which $V = 13.576$, $I = 12.810$, and $V–I = 0.766$. For the Meade images, GSC-03060- 00569 was used as the check star, for which $V = 12.969$, $I = 12.313$, and $V–I = 0.656$. Henden (2008) performed the photometric calibration of the star field in April 2008, using the robotic telescope at Sonoita Research Observatory near Sonoita, Arizona. This calibration is available at ftp://ftp.aavso.org/public/calib/g3059.dat.

Two software packages were used to perform period analysis of the photometric data extracted from the images. These were PERANSO version 2.20 (Vanmunster 2005) and PERIOD04 (Lenz and Breger 2005).

4. Results

Photometry from the 1,482 *V*-band images from this year's study were combined with those from the 1,102 *V*-band images from 2008 (Hurdis 2009) and with the 1,570 points from Michigan State's *V*-band photometry (OSK 2006). The time baseline for this combined dataset was 1,609 days, permitting an improved determination of the pulsation periods. By use of the Deeming DFT algorithm in PERANSO, the fundamental and first-overtone periods were, respectively, determined to be $P_0 = 0.494050 \pm 0.000037$ day and $P_1 = 0.366894 \pm 0.000010$ day. The period ratio, P_1 / P_0 is, therefore, $= 0.7426 \pm 0.0001$, in good agreement with the 0.743 value found by OSK. Determination of P_0 and P_1 with PERIOD04 produced virtually identical results.

Figure 1 shows the PERANSO phase curve resulting from differential photometry of the 1,482 *V*-band images from this year's study. It is plotted for the calculated fundamental period of 0.494050 day. The different symbols for the data points indicate the seventeen different observation nights. Figures 2 and 3 show *V*-band phase curves for the deconvolved pulsation modes of NSVS 5222076. Figure 2 is plotted for the fundamental period of 0.494050 day, while Figure 3 is plotted for the first-overtone period of 0.366894 day. Here also, the different symbols for the data points indicate the seventeen different observation nights.

Figure 4 shows the phase curve for the 1,458 *I*-band images from this year's study, while Figures 5 and 6 show the *I*-band phase curves for the deconvolved pulsation modes.

The amplitude ratio, A_0/A_1, of the fundamental and first overtone pulsation components of a dataset can be accurately determined by using PERIOD04 to achieve a least-squares-fit of the calculated Fourier components to the light curve. This provides a more accurate estimate of modal amplitudes than the method previously used by Hurdis (2009). Therefore, the A_0/A_1 values reported in that reference for the 2008 observations are superseded by the values herein. Light curve fitting with PERIOD04 was done for each of the three data-sets, namely, the 2005 observations of OSK, the 2008 observations (Hurdis 2009), and the most recent 2009 observations. The fit to the 2009 *V*-band data is presented in Table 1, while that to the 2009 *I*-band data is presented in Table 2.

The amplitude ratio results were as follows. In the *V*-band, A_0/A_1 decreased from 1.93 ± 0.02 in 2005 to 1.76 ± 0.03 in 2008 to 1.48 ± 0.01 in 2009. This change is the result of both a decrease in the amplitude of the fundamental mode, A_0, and an increase in the amplitude of the first overtone mode, A_1. Amplitude ratio uncertainties were derived from the standard deviations calculated by PERIOD04 for the least-squares fits of the Fourier components to the measured light curves. The propagation-of-errors formula for quotients was used to determine the uncertainty of the ratio, A_0/A_1. These results are graphically illustrated in Figure 7, where the upper half of the figure shows the number and distribution of the time-series observations, while the lower half shows the time variation of A_0/A_1. In the *I*-

band, A_0/A_1 was virtually constant, at 1.56 ± 0.06 in 2008 and 1.52 ± 0.03 in 2009. (OSK did not observe in the I-band.) These results are illustrated in Figure 8.

The cause of the night-to-night modulation in amplitude and phase evident in Figures 2, 3, 5, and 6, is not yet clear. A PERIOD04 analysis of NSVS 5222076 data by Templeton (2009) suggests the presence of Blazhko-like amplitude modulation, but no Blazhko period can be found in the data. Another proposed cause of this amplitude and phase modulation is the influence of interaction terms involving both frequencies, such as $f_0 + f_1$, $2f_0 + f_1$, $f_1 - f_0$, etc. However, those terms had been removed from the data used to plot Figures 2, 3, 5, and 6, yet the amplitude and phase modulation remains. A remarkable example of amplitude modulation can be seen in Figure 1 for the pulsation maximum of JD 2454956 (2009 May 4–5) denoted by the diamond-shaped symbols. As shown in Figure 2, even when the effect of the first overtone mode has been removed from the data, the amplitude of that particular maximum was much below the norm. One can conjecture that this amplitude and phase modulation is due to random, non-periodic irregularities in the pulsation behavior of the star as it approaches a mode switch. Continued monitoring of NSVS 5222076 will be required to unravel the cause of this puzzling behavior. Interestingly, Blazhko-like amplitude modulation has also been reported for V79 in M3 (Goranskij and Barsukova 2007). The highly irregular behavior of V79 was mentioned above.

In conclusion, in the *V*-band at least, A_0/A_1 has been shown to be decreasing, so NSVS 5222076 may be evolving toward a mode switch in which the first-overtone mode becomes dominant. Continued observation of NSVS 5222076 will be needed to determine whether a mode switch is indeed imminent.

5. Acknowledgements

The authors gratefully acknowledge AAVSO Director Arne Henden for providing his Sonoita Research Observatory photometric calibration of the star field. They also thank Prof. Horace Smith of Michigan State University for his useful comments on amplitude-modulation and mode-switching in RR Lyrae stars. They are indebted, as well, to AAVSO Staff Astronomer Matthew Templeton for helpful discussions on PERIOD04, and for his use of that program to explore their NSVS 5222076 data for Blazhko-like effects.

References

Berry, R., and Burnell, J. 2005, AIP4WIN, astronomical image processing software provided with *The Handbook of Astronomical Image Processing*, 2nd ed., Willmann-Bell, Richmond, VA.

Clement, C. M., and Thompson, M. 2007, *J. Amer. Assoc. Var. Star Obs.*, **35**, 336.

Clementini, G., Corwin, T. M., Carney, B. W., and Sumerel, A. N. 2004, *Astron. J.*, **127**, 938.

Corwin, T. M., Carney, B. W., and Allen, D. M. 1999, *Astron. J.*, **117**, 1332.
Cox, J. P. 1980, *Theory of Stellar Pulsation*, Princeton Univ. Press, Princeton, NJ.
Goranskij, V. P., and Barsukova, E. A. 2007, *Astron. Telegram*, No. 1120.
Henden, A. A. 2008, Sonoita Calibration of NSVS 5222076 Star Field.
Hurdis, D. A. 2009, *J. Amer. Assoc. Var. Star Obs.*, **37**, 28.
Lenz, P., and Breger, M. 2005, *Commun. Asteroseismology*, **146**, 53.
Oaster, L. 2005, Senior Thesis, Michigan State Univ.
Oaster, L., Smith, H. A., and Kinemuchi, K. 2006, *Publ. Astron. Soc. Pacific*, **118**, 405.
Templeton, M. R. 2009, private communication.
Vanmunster, T. 2005, PERANSO period analysis software, www.peranso.com
Woźniak, P. R. *et al.* 2004, *Astron. J.*, **127**, 2436.

Table 1. PERIOD04 fit to 2009 *V*-band data on NSVS 5222076.

Frequency (cycles/day)	*Amplitude (magnitude)*	*Frequency (cycles/day)*	*Amplitude (magnitude)*
2.02409 (=f_0)	0.165	$4f_0$	0.023
2.72558 (=f_1)	0.112	$5f_0$	0.015
$2f_0$	0.070	$2f_1$	0.015
f_0+f_1	0.032	$4f_0+f_1$	0.011
f_1-f_0	0.031	$3f_0+f_1$	0.011
$3f_0$	0.029	$6f_0$	0.005
$2f_0+f_1$	0.028		

Table 2. PERIOD04 fit to 2009 *I*-band data on NSVS 5222076.

Frequency (cycles/day)	*Amplitude (magnitude)*	*Frequency (cycles/day)*	*Amplitude (magnitude)*
2.02409 (=f_0)	0.107	$4f_0$	0.012
2.72558 (=f_1)	0.070	$2f_1$	0.012
$2f_0$	0.051	$3f_0+f_1$	0.008
$3f_0$	0.018	$4f_0+f_1$	0.007
$2f_0+f_1$	0.017	$3f_1$	0.007
f_0+f_1	0.016	$4f_1$	0.006
f_1-f_0	0.015	$6f_0$	0.005

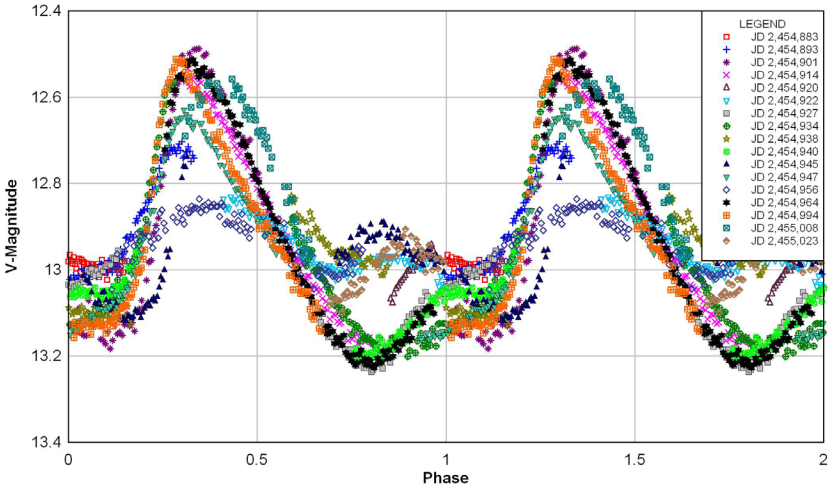

Figure 1. Phase curve of NSVS 5222076 resulting from differential photometry of 1,482 *V*-band images, plotted for fundamental period of 0.494050 day. Different symbols for data points indicate the seventeen different observation nights.

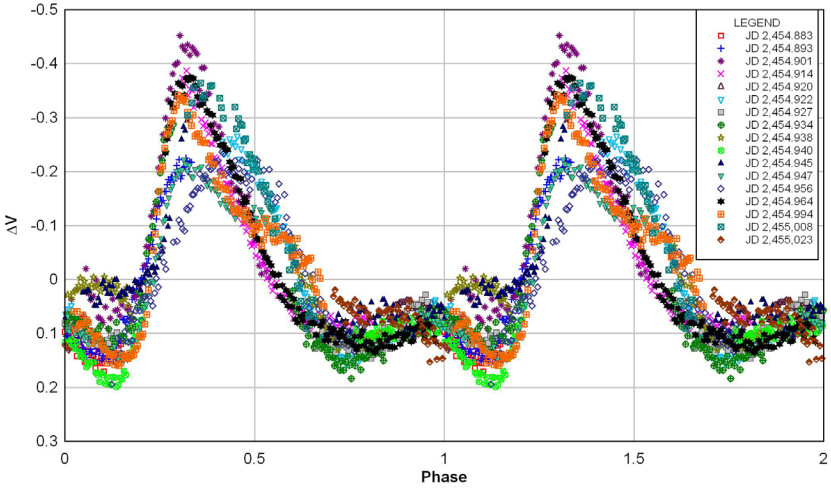

Figure 2. Deconvolved fundamental mode of NSVS 5222076. Phase curve for photometry of 1,482 *V*-band images, plotted for fundamental period of 0.494050 day.

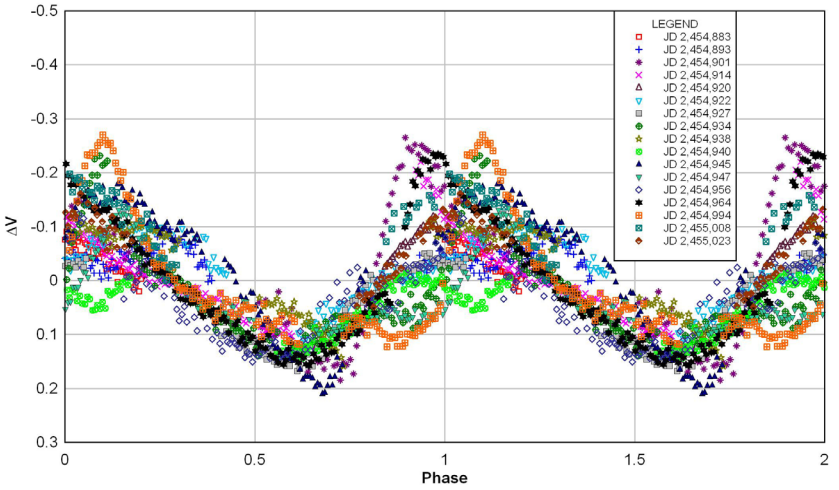

Figure 3. Deconvolved first-overtone mode of NSVS 5222076. Phase curve for photometry of 1,482 *V*-band images, plotted for the first-overtone period of 0.366894 day.

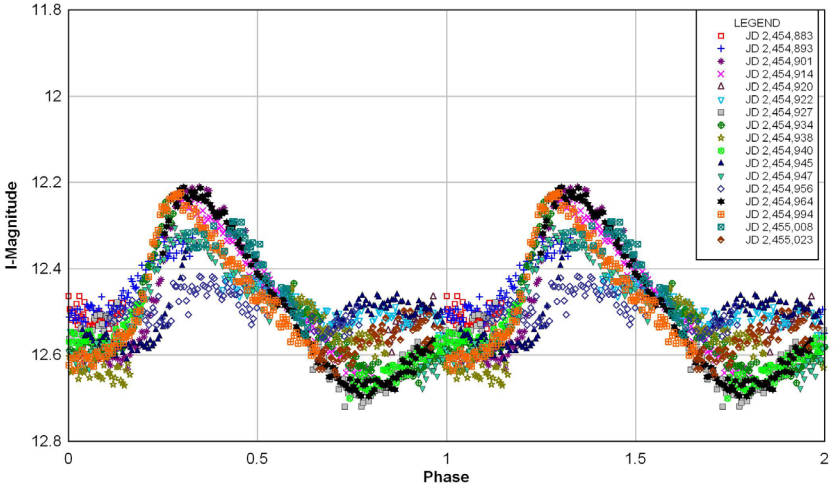

Figure 4. Phase curve resulting from differential photometry of 1,458 *I*-band images, plotted for fundamental period of 0.494050 day. Different symbols for data points indicate the seventeen different observation nights.

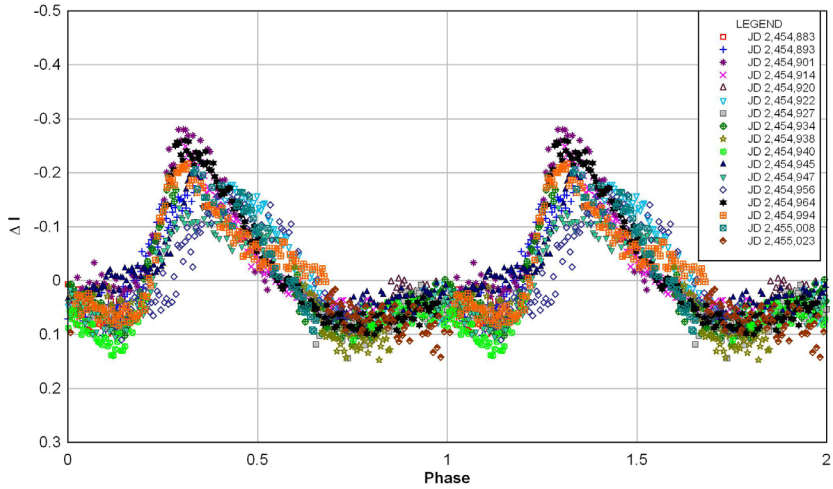

Figure 5. Deconvolved fundamental mode of NSVS 5222076. Phase curve for photometry of 1,458 *I*-band images, plotted for fundamental period of 0.494050 day.

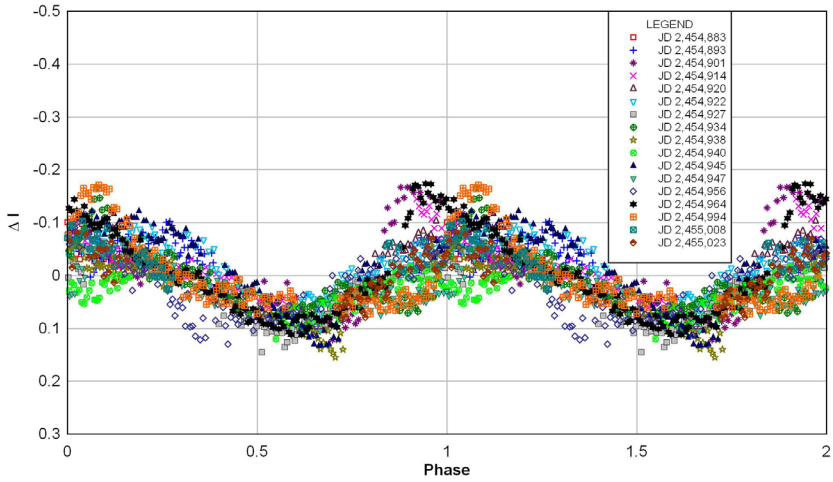

Figure 6. Deconvolved first-overtone mode of NSVS 5222076. Phase curve for photometry of 1,458 *I*-band images, plotted for the first-overtone period of 0.366894 day.

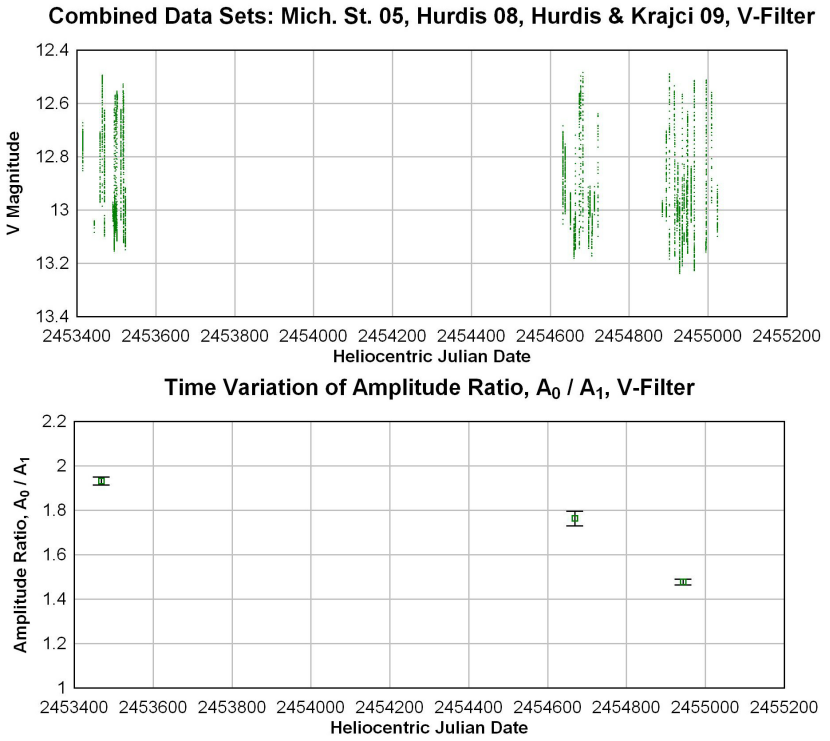

Figure 7. Secular variation of mode amplitude ratio, A_0/A_1, for *V*-band.

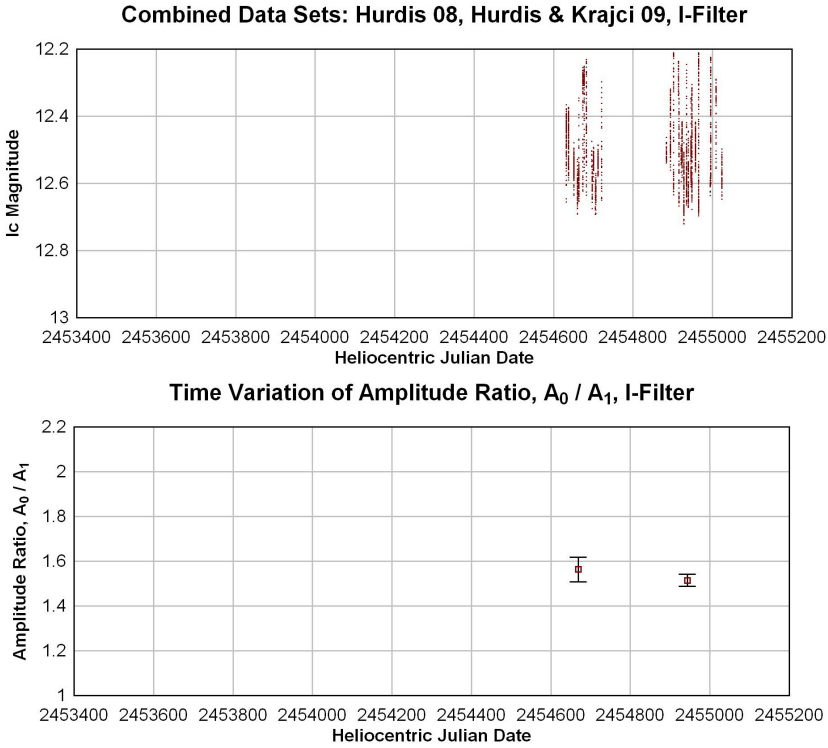

Figure 8. Secular variation of mode amplitude ratio, A_0/A_1, for *I*-band.

Recent Maxima of 64 Short Period Pulsating Stars

Gerard Samolyk
P.O. Box 20677, Greenfield, WI 53220; gsamolyk@wi.rr.com

Received January 7, 2010; revised March 1, 2010; accepted March 1, 2010

Abstract This paper contains times of maxima for 64 short period pulsating stars (primarily RR Lyrae and δ Scuti stars). This represents a portion of the CCD observations received by the AAVSO Short Period Pulsator (SPP) section through December 2009.

1. Recent observations

The accompanying list contains times of maxima calculated from CCD observations made by participants in the AAVSO's RR Lyrae program, now known as the AAVSO Short Period Pulsator Section (SPP). This list will be web-archived and made available through the AAVSO ftp site at ftp://ftp.aavso.org/public/datasets/jsamog381.txt. These observations were reduced by the writer using the PERANSO program (Vanmunster 2007). The error estimate is included.

The linear elements in the *General Catalogue of Variable Stars* (GCVS; Kholopov *et al.* 1985) were used to compute the O–C values for all stars except RZ Cap and DG Hya. For RZ Cap and DG Hya, the GCVS elements are missing or are in significant error. For these two stars, the following light elements were calculated using PERANSO and the times of maxima listed in this paper:

RZ CapTime of maximum: (JD) = 2451384.8279 + 0.40100719 E
±0.0005 0.00000010

DG HyaTime of maximum: (JD) = 2452374.565 + 0.7542427 E
±0.002 0.0000011

References

Kholopov, P. N., *et al.* 1985, *General Catalogue of Variable Stars*, 4th ed., Moscow.
Vanmunster, T. 2007, PERANSO period analysis software, http://www.peranso.com

Table 1. Recent times of maxima of stars in the AAVSO RR Lyrae program.

Star	*JD (max) Hel. 2400000+*	*Cycle*	*O-C*	*Observer**	*Error*
SW And	53398.5405	79737	–0.2878	SAH	0.0012
SW And	54717.8059	82720	–0.3420	MZK	0.0009
SW And	54830.5826	82975	–0.3466	SNE	0.0010
XX And	54423.6372	21220	–0.4942	BIZ	0.0021
XX And	54454.7150	21263	–0.4945	BIZ	0.0020
AT And	52219.6072	16010	–0.6184	SAH	0.0026
AT And	54454.6841	19633	–0.6237	BIZ	0.0035
AT And	55080.8561	20648	–0.6202	MZK	0.0013
AT And	55158.5817	20774	–0.6258	MZK	0.0023
SW Aqr	52902.6721	60538	–0.0009	SAH	0.0013
SW Aqr	53239.8017	61272	0.0002	SAH	0.0013
SW Aqr	53315.5860	61437	–0.0006	SAH	0.0013
SW Aqr	55138.5600	65406	–0.0009	SAH	0.0012
TZ Aqr	53323.5842	27617	0.0112	SAH	0.0019
TZ Aqr	54379.7226	29466	0.0114	BIZ	0.0052
YZ Aqr	53284.6038	32468	0.0499	BIZ	0.0025
YZ Aqr	53289.5678	32477	0.0465	SAH	0.0017
YZ Aqr	53588.7156	33019	0.0472	HES	0.0023
YZ Aqr	54316.7181	34338	0.0515	HES	0.0022
YZ Aqr	54422.6962	34530	0.0587	BIZ	0.0030
AA Aqr	52999.5632	52967	–0.1037	SAH	0.0014
AA Aqr	53238.8549	53360	–0.1058	SAH	0.0021
AA Aqr	53251.6435	53381	–0.1039	BIZ	0.0049
AA Aqr	54392.6891	55255	–0.1184	BIZ	0.0019
BO Aqr	53315.5824	16850	0.1170	SAH	0.0032
BO Aqr	54417.7114	18438	0.1445	BIZ	0.0023
BR Aqr	52581.5498	31015	–0.1309	SAH	0.0016
BR Aqr	54439.6450	34871	–0.1592	BIZ	0.0015
BR Aqr	55115.7129	36274	–0.1668	SAH	0.0021
DN Aqr	53615.7636	39748	0.0296	BIZ	0.0032
DN Aqr	54413.6719	41007	0.0416	BIZ	0.0020
DN Aqr	55112.7021	42110	0.0412	SAH	0.0036
TZ Aur	52316.6504	82758	0.0102	SAH	0.0011
TZ Aur	52374.6172	82906	0.0092	SAH	0.0009
TZ Aur	53077.6734	84701	0.0094	HES	0.0010
TZ Aur	53724.7223	86353	0.0119	PRX	0.0010
TZ Aur	54071.7455	87239	0.0114	PRX	0.0011
TZ Aur	54394.8764	88064	0.0107	SAH	0.0010

Table continued on following pages

Table 1. Recent times of maxima of stars in the AAVSO RR Lyrae program, cont.

Star	*JD (max) Hel. 2400000+*	*Cycle*	*O-C*	*Observer**	*Error*
TZ Aur	54518.6483	88380	0.0134	BIZ	0.0014
TZ Aur	55185.6690	90083	0.0123	PRX	0.0008
BH Aur	51544.5939	19279	–0.0034	SAH	0.0013
BH Aur	52998.6095	22467	–0.0020	SAH	0.0017
BH Aur	53345.6968	23228	0.0009	BKS	0.0027
BH Aur	53355.7292	23250	–0.0007	BKS	0.0034
BH Aur	53357.5562	23254	0.0020	BKS	0.0029
BH Aur	53644.8890	23884	–0.0018	SAH	0.0014
BH Aur	53762.5601	24142	–0.0019	SAH	0.0017
BH Aur	54170.7569	25037	–0.0054	BIZ	0.0014
BH Aur	54441.6780	25631	–0.0017	PRX	0.0023
BH Aur	54509.6359	25780	–0.0011	BIZ	0.0014
BH Aur	54831.6369	26486	0.0005	PRX	0.0013
BH Aur	55136.7600	27155	–0.0005	SAH	0.0015
BH Aur	55178.7183	27247	–0.0025	PRX	0.0011
RS Boo	52224.7065	27705	0.0406	GHS	0.0010
RS Boo	52785.7734	29192	0.0045	SAH	0.0014
RS Boo	53130.6564	30106	–0.0003	BIZ	0.0012
RS Boo	54611.7181	34031	0.0060	MZK	0.0012
RS Boo	54651.7147	34137	0.0046	GHS	0.0010
RS Boo	54887.5385	34762	–0.0084	VJA	0.0008
RS Boo	54904.8985	34808	–0.0060	MZK	0.0009
RS Boo	54946.7787	34919	–0.0104	MZK	0.0011
ST Boo	52133.7145	52953	0.0698	SAH	0.0021
ST Boo	54591.7889	56903	0.0959	SAH	0.0013
ST Boo	54596.7685	56911	0.0972	SAH	0.0016
ST Boo	54619.7893	56948	0.0933	BIZ	0.0014
SW Boo	51749.7388	17874	0.1775	SAH	0.0014
SW Boo	52029.6227	18419	0.1886	SAH	0.0012
SW Boo	52126.6832	18608	0.1923	SAH	0.0013
SW Boo	52735.7555	19794	0.2203	SAH	0.0016
SW Boo	54177.8079	22602	0.2858	SAH	0.0015
SW Boo	54212.7287	22670	0.2867	PRX	0.0014
SW Boo	54230.7029	22705	0.2874	BIZ	0.0013
SW Boo	54267.6812	22777	0.2917	GHS	0.0018
SW Boo	54571.7043	23369	0.3061	BIZ	0.0027
SW Boo	54610.7352	23445	0.3089	GHS	0.0014
SW Boo	54933.7594	24074	0.3239	SAH	0.0017

Table continued on following pages

Table 1. Recent times of maxima of stars in the AAVSO RR Lyrae program, cont.

Star	*JD (max) Hel. 2400000+*	*Cycle*	*O-C*	*Observer**	*Error*
SZ Boo	54215.6914	50831	0.0071	PRX	0.0016
SZ Boo	54560.7538	51491	0.0085	BIZ	0.0013
SZ Boo	54938.7471	52214	0.0031	MZK	0.0011
SZ Boo	54938.7489	52214	0.0049	SAH	0.0016
TV Boo	54578.7362	95883	0.0921	BIZ	0.0030
TV Boo	54919.7417	96974	0.0953	PRX	0.0030
TW Boo	53863.6307	50674	–0.0469	BM	0.0013
TW Boo	54227.7020	51358	–0.0504	BIZ	0.0013
TW Boo	54557.7070	51978	–0.0548	BIZ	0.0013
TW Boo	54597.6257	52053	–0.0566	MZK	0.0011
TW Boo	54631.6964	52117	–0.0514	GHS	0.0016
UU Boo	52426.7726	35766	0.1440	HES	0.0013
UU Boo	52469.7215	35860	0.1424	SNE	0.0017
UU Boo	52804.6596	36593	0.1577	SAH	0.0027
UU Boo	53154.6632	37359	0.1602	BIZ	0.0014
UU Boo	53170.6558	37394	0.1606	BIZ	0.0013
UU Boo	53884.8429	38957	0.1810	SAH	0.0010
UU Boo	54209.7240	39668	0.1916	PRX	0.0012
UU Boo	54245.8220	39747	0.1929	BIZ	0.0011
UU Boo	54565.6769	40447	0.2034	BIZ	0.0013
UU Boo	54660.7195	40655	0.2066	GHS	0.0015
UU Boo	54940.8182	41268	0.2130	PRX	0.0010
UY Cam	52762.681	64400	–0.085	SNE	0.003
UY Cam	52791.795	64509	–0.078	SNE	0.002
UY Cam	52975.519	65197	–0.079	SAH	0.002
UY Cam	52975.785	65198	–0.080	SAH	0.003
UY Cam	52979.526	65212	–0.078	SAH	0.003
UY Cam	52979.792	65213	–0.079	SAH	0.002
UY Cam	52986.730	65239	–0.084	SAH	0.004
UY Cam	53046.553	65463	–0.079	SAH	0.002
UY Cam	53098.631	65658	–0.074	BIZ	0.003
UY Cam	53232.676	66160	–0.084	SNE	0.005
UY Cam	53463.671	67025	–0.081	SNE	0.004
UY Cam	53463.672	67025	–0.080	SNE	0.004
UY Cam	53691.724	67879	–0.082	PRX	0.008
UY Cam	53712.553	67957	–0.082	SNE	0.002
UY Cam	54055.707	69242	–0.078	PRX	0.006
UY Cam	54079.725	69332	–0.094	SAH	0.004

Table continued on following pages

Table 1. Recent times of maxima of stars in the AAVSO RR Lyrae program, cont.

Star	*JD (max) Hel. 2400000+*	*Cycle*	*O-C*	*Observer**	*Error*
UY Cam	54191.620	69751	–0.089	PRX	0.002
UY Cam	54398.579	70526	–0.088	SAH	0.003
UY Cam	54402.578	70541	–0.095	SAH	0.004
UY Cam	54402.849	70542	–0.091	SAH	0.003
UY Cam	54403.651	70545	–0.090	SAH	0.004
UY Cam	54403.926	70546	–0.082	SAH	0.004
UY Cam	54522.755	70991	–0.087	BIZ	0.002
UY Cam	54771.639	71923	–0.086	SAH	0.004
UY Cam	54933.732	72530	–0.088	SAH	0.004
UY Cam	55105.702	73174	–0.093	SAH	0.003
RW Cnc	54480.8324	27275	–0.3343	SAH	0.0018
RW Cnc	54484.6620	27282	–0.3351	SAH	0.0024
RW Cnc	54507.6455	27324	–0.3340	SAH	0.0017
RW Cnc	54519.6816	27346	–0.3363	SAH	0.0027
RW Cnc	54536.6498	27377	–0.3312	SAH	0.0019
RW Cnc	54554.7004	27410	–0.3382	SAH	0.0028
RW Cnc	54554.7051	27410	–0.3335	BIZ	0.0038
RW Cnc	54861.6922	27971	–0.3250	PRX	0.0035
RW Cnc	54867.7054	27982	–0.3310	PRX	0.0021
RW Cnc	54867.7098	27982	–0.3266	SAH	0.0019
RW Cnc	54891.7901	28026	–0.3231	SAH	0.0028
RW Cnc	54907.6445	28055	–0.3374	SAH	0.0020
TT Cnc	53799.7041	24590	0.1164	SAH	0.0033
TT Cnc	54128.7230	25174	0.0808	BIZ	0.0018
TT Cnc	54128.7230	25174	0.0808	PRX	0.0017
TT Cnc	54532.7441	25891	0.1087	BIZ	0.0017
TT Cnc	54571.5986	25960	0.0852	MZK	0.0016
TT Cnc	54865.7248	26482	0.0908	PRX	0.0023
VZ Cnc	54527.5345	82024	0.0054	MZK	0.0008
VZ Cnc	54544.6614	82120	0.0094	BIZ	0.0022
SS CVn	53818.6688	29667	–0.3187	PRX	0.0015
SS CVn	53952.6545	29947	–0.3189	HES	0.0039
SS CVn	54261.7872	30593	–0.3108	BIZ	0.0012
SS CVn	54564.6831	31226	–0.3186	BIZ	0.0009
RV Cap	52489.7018	41556	–0.0103	SAH	0.0028
RV Cap	52533.6124	41654	0.0214	SAH	0.0016
RV Cap	53581.7557	43995	–0.0040	SAH	0.0018
RV Cap	53589.8102	44013	–0.0089	SAH	0.0018

Table continued on following pages

Table 1. Recent times of maxima of stars in the AAVSO RR Lyrae program, cont.

Star	*JD (max) Hel. 2400000+*	*Cycle*	*O-C*	*Observer**	*Error*
RV Cap	53603.6908	44044	–0.0084	SAH	0.0020
RV Cap	53616.6673	44073	–0.0165	SAH	0.0018
RV Cap	54708.7210	46512	–0.0104	SAH	0.0014
RV Cap	55093.7862	47372	–0.0050	HES	0.0015
RZ Cap	51384.8299	0	0.0020	SAH	0.0016
RZ Cap	51411.6955	67	0.0001	SAH	0.0013
RZ Cap	51452.5976	169	–0.0005	SAH	0.0014
RZ Cap	51804.6835	1047	0.0011	SAH	0.0015
RZ Cap	51837.5636	1129	–0.0014	SAH	0.0019
RZ Cap	52179.6215	1982	–0.0027	SAH	0.0016
RZ Cap	52468.7501	2703	–0.0002	SAH	0.0018
RZ Cap	52517.6739	2825	0.0007	SAH	0.0019
RZ Cap	52562.5866	2937	0.0006	SAH	0.0017
RZ Cap	53197.7825	4521	0.0011	SAH	0.0017
RZ Cap	53224.6489	4588	0.0000	SAH	0.0015
RZ Cap	53277.5817	4720	–0.0001	SAH	0.0015
RZ Cap	53539.8387	5374	–0.0018	SAH	0.0013
RZ Cap	53588.7631	5496	–0.0003	GHS	0.0020
RZ Cap	53932.8288	6354	0.0012	SAH	0.0019
RZ Cap	54016.6392	6563	0.0011	SAH	0.0021
RZ Cap	54366.7189	7436	0.0015	SAH	0.0017
RZ Cap	54688.7261	8239	0.0000	SAH	0.0014
RZ Cap	55044.8192	9127	–0.0013	SAH	0.0013
VW Cap	52163.659	85133	0.162	SAH	0.006
VW Cap	52489.820	86171	0.122	SAH	0.006
VW Cap	52559.572	86393	0.108	SAH	0.004
VW Cap	52581.591	86463	0.129	SAH	0.007
VW Cap	52950.537	87637	0.133	SAH	0.007
VW Cap	53232.765	88535	0.156	SAH	0.006
VW Cap	53618.690	89763	0.170	SAH	0.006
RR Cet	53323.7984	36422	0.0035	MKE	0.0017
RR Cet	53672.7616	37053	0.0059	SAH	0.0022
RR Cet	55157.6478	39738	0.0116	SAH	0.0018
RU Cet	54416.6541	24886	0.0790	PRX	0.0044
RU Cet	54477.6414	24990	0.0932	BIZ	0.0024
RU Cet	54783.6855	25512	0.0991	PRX	0.0021
RU Cet	54786.6124	25517	0.0946	PRX	0.0020
RU Cet	55163.6016	26160	0.1058	SAH	0.0017

Table continued on following pages

Table 1. Recent times of maxima of stars in the AAVSO RR Lyrae program, cont.

Star	*JD (max) Hel. 2400000+*	*Cycle*	*O-C*	*Observer**	*Error*
RU Cet	55167.7078	26167	0.1080	PRX	0.0019
RU Cet	55177.6625	26184	0.0960	SAH	0.0019
RV Cet	54418.7233	24551	0.1932	PRX	0.0023
RV Cet	54418.7256	24551	0.1955	BIZ	0.0026
RV Cet	54438.6664	24583	0.1875	PRX	0.0018
RV Cet	54438.6712	24583	0.1923	BIZ	0.0037
RX Cet	52996.6644	22435	0.0899	SAH	0.0035
RX Cet	54424.7261	24924	0.2327	BIZ	0.0032
RX Cet	55155.6669	26198	0.2901	PRX	0.0024
RZ Cet	52663.5678	36734	–0.0991	SAH	0.0024
RZ Cet	53001.5765	37396	–0.1147	SAH	0.0031
RZ Cet	53363.5994	38105	–0.1148	SAH	0.0017
RZ Cet	53722.5532	38808	–0.1204	SAH	0.0019
RZ Cet	54066.6883	39482	–0.1369	PRX	0.0019
RZ Cet	54448.6149	40230	–0.1472	BIZ	0.0018
RZ Cet	54449.6429	40232	–0.1404	PRX	0.0019
RZ Cet	54833.6143	40984	–0.1483	SAH	0.0017
RZ Cet	55169.5748	41642	–0.1696	PRX	0.0024
UU Cet	52902.7862	19295	–0.1227	SAH	0.0022
UU Cet	53265.8309	19894	–0.1205	SAH	0.0022
UU Cet	54407.6740	21778	–0.1340	BIZ	0.0030
UU Cet	54413.7339	21788	–0.1349	BIZ	0.0024
UU Cet	54424.6457	21806	–0.1326	PRX	0.0025
XX Cyg	52581.5595	60254	0.0025	SNE	0.0007
XX Cyg	52581.6929	60255	0.0010	SNE	0.0007
XX Cyg	52839.6918	62168	0.0030	HES	0.0010
XX Cyg	53017.5772	63487	0.0013	BIZ	0.0007
XX Cyg	53270.5843	65363	0.0014	BIZ	0.0010
XX Cyg	53540.7200	67366	0.0023	PRX	0.0007
XX Cyg	53584.6852	67692	0.0015	PRX	0.0007
XX Cyg	53612.6030	67899	0.0022	SAH	0.0006
XX Cyg	54261.8442	72713	0.0027	SAH	0.0006
XX Cyg	54372.5684	73534	0.0027	GHS	0.0007
XX Cyg	54612.7625	75315	0.0020	MZK	0.0008
XX Cyg	54729.6917	76182	0.0032	MZK	0.0006
XX Cyg	55011.6952	78273	0.0037	SAH	0.0008
XX Cyg	55011.8286	78274	0.0022	SAH	0.0007
XX Cyg	55079.6654	78777	0.0019	MZK	0.0005

Table continued on following pages

Table 1. Recent times of maxima of stars in the AAVSO RR Lyrae program, cont.

Star	*JD (max) Hel. 2400000+*	*Cycle*	*O-C*	*Observer**	*Error*
XX Cyg	55092.6133	78873	0.0027	MZK	0.0005
XZ Cyg	52885.6945	18776	–1.5047	SAH	0.0009
XZ Cyg	52900.6262	18808	–1.5074	BIZ	0.0012
XZ Cyg	52950.5530	18915	–1.5175	SAH	0.0012
XZ Cyg	52957.5503	18930	–1.5207	SAH	0.0013
XZ Cyg	53214.6426	19481	–1.5801	BIZ	0.0022
XZ Cyg	53363.4898	19800	–1.6102	SAH	0.0015
XZ Cyg	53463.8147	20015	–1.6258	SAH	0.0012
XZ Cyg	53540.7918	20180	–1.6542	SAH	0.0013
XZ Cyg	53603.7836	20315	–1.6669	SAH	0.0013
XZ Cyg	53798.8291	20733	–1.7020	SAH	0.0014
XZ Cyg	53834.7482	20810	–1.7188	SAH	0.0020
XZ Cyg	53890.7416	20930	–1.7294	SAH	0.0011
XZ Cyg	54226.7006	21650	–1.7944	SAH	0.0008
XZ Cyg	54232.7615	21663	–1.8006	SAH	0.0013
XZ Cyg	54248.6231	21697	–1.8068	SAH	0.0018
XZ Cyg	54260.7618	21723	–1.8023	SAH	0.0013
XZ Cyg	54266.8329	21736	–1.7983	SAH	0.0014
XZ Cyg	54289.6838	21785	–1.8157	GHS	0.0023
XZ Cyg	54631.7064	22518	–1.8842	BIZ	0.0017
XZ Cyg	54651.7668	22561	–1.8919	SAH	0.0015
XZ Cyg	54652.7023	22563	–1.8898	GHS	0.0022
XZ Cyg	54657.8317	22574	–1.8941	SAH	0.0010
XZ Cyg	54701.6826	22668	–1.9130	MZK	0.0014
XZ Cyg	55008.7186	23326	–1.9656	SAH	0.0009
XZ Cyg	55056.7754	23429	–1.9789	SAH	0.0013
XZ Cyg	55058.6459	23433	–1.9752	MZK	0.0007
XZ Cyg	55092.7025	23506	–1.9877	SAH	0.0013
DM Cyg	52501.6456	23625	0.0471	SAH	0.0014
DM Cyg	53239.7660	25383	0.0536	SAH	0.0014
DM Cyg	53316.5998	25566	0.0530	SAH	0.0013
DM Cyg	54255.8301	27803	0.0565	BIZ	0.0018
DM Cyg	54310.8354	27934	0.0602	SAH	0.0014
DM Cyg	54643.7850	28727	0.0608	MZK	0.0014
DM Cyg	55018.7269	29620	0.0677	SAH	0.0013
RW Dra	54246.7329	33571	0.1753	PRX	0.0013
RW Dra	54599.7546	34368	0.1921	BIZ	0.0017
RW Dra	54941.6969	35140	0.2025	PRX	0.0013

Table continued on following pages

Table 1. Recent times of maxima of stars in the AAVSO RR Lyrae program, cont.

Star	*JD (max) Hel. 2400000+*	*Cycle*	*O-C*	*Observer**	*Error*
XZ Dra	54223.7910	25804	–0.1116	BIZ	0.0014
XZ Dra	54629.7610	26656	–0.1170	BIZ	0.0016
RX Eri	52995.6290	53305	–0.0098	SAH	0.0016
RX Eri	53322.7273	53862	–0.0076	SAH	0.0021
RX Eri	53766.6809	54618	–0.0121	PRX	0.0016
RX Eri	53772.5568	54628	–0.0087	SAH	0.0023
RX Eri	54096.7137	55180	–0.0117	PRX	0.0016
RX Eri	54416.7630	55725	–0.0116	BIZ	0.0027
RX Eri	54466.6809	55810	–0.0096	PRX	0.0016
RX Eri	54503.6774	55873	–0.0097	BIZ	0.0018
RX Eri	54823.7277	56418	–0.0085	SAH	0.0020
RX Eri	55190.7559	57043	–0.0092	SAH	0.0018
BB Eri	53747.6832	24896	0.2116	PRX	0.0017
BB Eri	54090.7683	25498	0.2181	BIZ	0.0017
BB Eri	54094.7568	25505	0.2173	PRX	0.0015
BB Eri	54457.7925	26142	0.2280	BIZ	0.0015
BB Eri	54468.6207	26161	0.2281	BIZ	0.0029
BB Eri	54843.6207	26819	0.2352	PRX	0.0018
RX For	54411.7739	24410	–0.0478	BIZ	0.0020
RX For	54831.6822	25113	–0.0513	SAH	0.0031
RX For	55114.7976	25587	–0.0627	SAH	0.0024
SS For	52993.7256	28914	–0.1462	SAH	0.0014
SS For	53387.5996	29709	–0.1407	HES	0.0013
SS For	54456.7470	31867	–0.1355	BIZ	0.0016
RR Gem	52713.6425	28584	–0.2887	HES	0.0010
RR Gem	53042.5973	29412	–0.3071	NMI	0.0009
RR Gem	53046.5745	29422	–0.3030	BIZ	0.0011
RR Gem	53084.7119	29518	–0.3074	NMI	0.0009
RR Gem	53090.6719	29533	–0.3070	NMI	0.0010
RR Gem	53469.6852	30487	–0.3281	GHS	0.0013
RR Gem	54107.7321	32093	–0.3620	PRX	0.0012
RR Gem	54453.7709	32964	–0.3807	PRX	0.0013
RR Gem	54465.6919	32994	–0.3790	BIZ	0.0012
RR Gem	54465.6926	32994	–0.3783	PRX	0.0011
RR Gem	54484.7597	33042	–0.3821	MZK	0.0012
RR Gem	54490.7218	33057	–0.3797	SAH	0.0011
RR Gem	54498.6637	33077	–0.3840	PRX	0.0007
RR Gem	54525.6820	33145	–0.3828	BIZ	0.0009

Table continued on following pages

Table 1. Recent times of maxima of stars in the AAVSO RR Lyrae program, cont.

Star	*JD (max) Hel. 2400000+*	*Cycle*	*O-C*	*Observer**	*Error*
RR Gem	54527.6647	33150	–0.3867	MZK	0.0010
RR Gem	54846.6901	33953	–0.4017	PRX	0.0009
RR Gem	55153.7936	34726	–0.4193	SRIC	0.0010
RR Gem	55154.9801	34729	–0.4247	SRIC	0.0014
RR Gem	55155.7759	34731	–0.4235	SRIC	0.0017
RR Gem	55183.9849	34802	–0.4236	SRIC	0.0007
RR Gem	55188.7533	34814	–0.4229	MZK	0.0006
TW Her	51714.6338	75499	–0.0085	SAH	0.0008
TW Her	52042.7059	76320	–0.0080	SAH	0.0009
TW Her	52184.5633	76675	–0.0087	SAH	0.0008
TW Her	52892.6542	78447	–0.0092	PRX	0.0018
TW Her	52898.6470	78462	–0.0104	BIZ	0.0010
TW Her	54243.7001	81828	–0.0112	PRX	0.0010
TW Her	54591.7517	82699	–0.0113	BIZ	0.0009
TW Her	54673.6687	82904	–0.0123	MZK	0.0009
TW Her	55009.7325	83745	–0.0122	SAH	0.0008
VX Her	52163.5740	66787	0.1068	SAH	0.0009
VX Her	52489.6135	67503	0.0993	SAH	0.0022
VX Her	52525.5856	67582	0.0970	SAH	0.0009
VX Her	52861.6424	68320	0.0886	SAH	0.0020
VX Her	53539.6724	69809	0.0685	SNE	0.0011
VX Her	54231.8176	71329	0.0470	BIZ	0.0009
VX Her	54619.7851	72181	0.0369	SAH	0.0013
VZ Her	51722.6706	33915	0.0522	SAH	0.0008
VZ Her	52884.7028	36554	0.0591	PRX	0.0012
VZ Her	53179.7242	37224	0.0608	BIZ	0.0010
VZ Her	53570.7344	38112	0.0599	PRX	0.0017
VZ Her	53630.6212	38248	0.0621	GHS	0.0012
VZ Her	53884.6913	38825	0.0630	HES	0.0010
VZ Her	54219.7830	39586	0.0651	SAH	0.0012
VZ Her	54241.7979	39636	0.0637	BIZ	0.0010
VZ Her	54245.7607	39645	0.0635	PRX	0.0011
VZ Her	54547.8278	40331	0.0657	MZK	0.0009
VZ Her	54577.7721	40399	0.0677	BIZ	0.0010
VZ Her	54630.6104	40519	0.0666	MZK	0.0009
VZ Her	54965.7010	41280	0.0677	MZK	0.0008
VZ Her	55009.7368	41380	0.0707	SAH	0.0013
AR Her	52017.6559	22476	–1.0404	SAH	0.0016

Table continued on following pages

Table 1. Recent times of maxima of stars in the AAVSO RR Lyrae program, cont.

Star	*JD (max) Hel. 2400000+*	*Cycle*	*O-C*	*Observer**	*Error*
AR Her	52021.8942	22485	–1.0324	SAH	0.0013
AR Her	52025.6675	22493	–1.0193	SAH	0.0025
AR Her	52069.8184	22587	–1.0510	SAH	0.0010
AR Her	52126.7106	22708	–1.0322	SAH	0.0012
AR Her	52398.8106	23287	–1.0784	SAH	0.0050
AR Her	52416.6889	23325	–1.0612	SAH	0.0008
AR Her	52495.6493	23493	–1.0655	SAH	0.0029
AR Her	52517.7225	23540	–1.0836	SAH	0.0011
AR Her	52559.5584	23629	–1.0802	SAH	0.0058
AR Her	52728.7674	23989	–1.0813	SAH	0.0014
AR Her	52735.8107	24004	–1.0884	SAH	0.0015
AR Her	52769.6470	24076	–1.0941	SAH	0.0015
AR Her	52785.6478	24110	–1.0743	SAH	0.0014
AR Her	52791.7543	24123	–1.0781	SAH	0.0023
AR Her	52839.6565	24225	–1.1188	SAH	0.0017
AR Her	52894.6742	24342	–1.0944	SAH	0.0028
AR Her	52919.5564	24395	–1.1237	PRX	0.0021
AR Her	53175.7276	24940	–1.1177	SAH	0.0011
AR Her	53215.6636	25025	–1.1341	BIZ	0.0018
AR Her	53239.6450	25076	–1.1241	SAH	0.0012
AR Her	53463.8246	25553	–1.1479	SAH	0.0016
AR Her	53511.7223	25655	–1.1930	SAH	0.0014
AR Her	53559.7016	25757	–1.1566	SAH	0.0017
AR Her	53574.7002	25789	–1.1989	SAH	0.0017
AR Her	53630.6543	25908	–1.1781	SAH	0.0016
AR Her	53792.7959	26253	–1.1962	SAH	0.0016
AR Her	53798.8872	26266	–1.2152	SAH	0.0021
AR Her	53840.7748	26355	–1.1601	SAH	0.0014
AR Her	53863.7466	26404	–1.2197	BM	0.0013
AR Her	53878.8313	26436	–1.1759	SAH	0.0011
AR Her	53894.7665	26470	–1.2217	SAH	0.0016
AR Her	53903.7485	26489	–1.1702	SAH	0.0015
AR Her	53910.7872	26504	–1.1819	SAH	0.0012
AR Her	53919.6999	26523	–1.1997	SAH	0.0012
AR Her	54176.7702	27070	–1.2348	PRX	0.0019
AR Her	54200.7602	27121	–1.2162	SAH	0.0014
AR Her	54206.8604	27134	–1.2264	SAH	0.0013
AR Her	54207.7958	27136	–1.2310	SAH	0.0017

Table continued on following pages

Table 1. Recent times of maxima of stars in the AAVSO RR Lyrae program, cont.

Star	*JD (max) Hel. 2400000+*	*Cycle*	*O-C*	*Observer**	*Error*
AR Her	54208.7336	27138	–1.2333	PRX	0.0017
AR Her	54210.6053	27142	–1.2417	SAH	0.0020
AR Her	54216.7108	27155	–1.2465	PRX	0.0019
AR Her	54218.6100	27159	–1.2275	SAH	0.0019
AR Her	54224.7516	27172	–1.1962	SAH	0.0020
AR Her	54231.7756	27187	–1.2226	BIZ	0.0009
AR Her	54231.7795	27187	–1.2187	SAH	0.0012
AR Her	54248.6682	27223	–1.2510	SAH	0.0017
AR Her	54577.7018	27923	–1.2370	SAH	0.0018
AR Her	54583.8007	27936	–1.2485	SAH	0.0017
AR Her	54585.6811	27940	–1.2482	SAH	0.0015
AR Her	54590.8385	27951	–1.2611	SAH	0.0014
AR Her	54591.7744	27953	–1.2653	BIZ	0.0013
AR Her	54601.6323	27974	–1.2780	SAH	0.0023
AR Her	54615.7630	28004	–1.2481	SAH	0.0013
AR Her	54624.6712	28023	–1.2704	SAH	0.0015
AR Her	54631.7004	28038	–1.2917	SAH	0.0015
AR Her	54879.8772	28566	–1.2896	MZK	0.0015
AR Her	54930.6672	28674	–1.2627	SAH	0.0013
AR Her	54937.7020	28689	–1.2783	SAH	0.0013
AR Her	54959.7982	28736	–1.2734	SAH	0.0013
AR Her	54962.6302	28742	–1.2616	SAH	0.0022
AR Her	55045.7632	28919	–1.3235	SAH	0.0016
AR Her	55062.7285	28955	–1.2792	SAH	0.0011
DY Her	52448.8224	127896	–0.0196	SAH	0.0011
DY Her	52495.6412	128211	–0.0197	SAH	0.0012
DY Her	52885.6477	130835	–0.0219	PRX	0.0013
DY Her	53288.5873	133546	–0.0219	SAH	0.0011
DY Her	53511.8295	135048	–0.0240	SAH	0.0010
DY Her	53581.6875	135518	–0.0227	SAH	0.0008
DY Her	53617.6572	135760	–0.0218	GHS	0.0017
DY Her	53875.6795	137496	–0.0235	SAH	0.0009
DY Her	53946.7267	137974	–0.0221	SAH	0.0014
DY Her	54244.7316	139979	–0.0231	PRX	0.0009
DY Her	54264.6462	140113	–0.0251	SAH	0.0010
DY Her	54264.7958	140114	–0.0241	SAH	0.0009
DY Her	54562.7994	142119	–0.0264	SAH	0.0013
DY Her	54579.7459	142233	–0.0238	BIZ	0.0016

Table continued on following pages

Table 1. Recent times of maxima of stars in the AAVSO RR Lyrae program, cont.

Star	*JD (max) Hel. 2400000+*	*Cycle*	*O-C*	*Observer**	*Error*
DY Her	54616.7547	142482	–0.0242	HAV	0.0013
DY Her	54700.5816	143046	–0.0254	MZK	0.0007
DY Her	54999.7764	145059	–0.0255	MZK	0.0007
DY Her	55008.6942	145119	–0.0256	SAH	0.0009
SZ Hya	51972.6366	21021	–0.1021	SAH	0.0014
SZ Hya	52356.7051	21736	–0.1603	SAH	0.0028
SZ Hya	52370.7181	21762	–0.1156	SAH	0.0015
SZ Hya	52391.6684	21801	–0.1176	SAH	0.0019
SZ Hya	52398.6559	21814	–0.1143	SAH	0.0024
SZ Hya	52597.9622	22185	–0.1241	SAH	0.0018
SZ Hya	52708.6357	22391	–0.1221	SAH	0.0014
SZ Hya	53049.7717	23026	–0.1336	SAH	0.0016
SZ Hya	53077.7063	23078	–0.1355	BIZ	0.0012
SZ Hya	53098.6579	23117	–0.1363	SAH	0.0016
SZ Hya	53354.8623	23594	–0.1955	SAH	0.0026
SZ Hya	53763.7493	24355	–0.1483	SAH	0.0013
SZ Hya	53785.7740	24396	–0.1504	SAH	0.0012
SZ Hya	53792.7551	24409	–0.1534	SAH	0.0019
SZ Hya	53798.6163	24420	–0.2019	SAH	0.0025
SZ Hya	53812.6358	24446	–0.1506	SAH	0.0015
SZ Hya	53820.6703	24461	–0.1747	PRX	0.0019
SZ Hya	53834.6552	24487	–0.1581	SAH	0.0015
SZ Hya	54089.7885	24962	–0.2139	SAH	0.0044
SZ Hya	54117.7774	25014	–0.1615	PRX	0.0018
SZ Hya	54152.6939	25079	–0.1656	PRX	0.0014
SZ Hya	54174.7212	25120	–0.1651	PRX	0.0013
SZ Hya	54485.7456	25699	–0.2028	SAH	0.0055
SZ Hya	54520.6863	25764	–0.1827	SAH	0.0015
SZ Hya	54527.6646	25777	–0.1886	PRX	0.0030
SZ Hya	54564.7342	25846	–0.1885	BIZ	0.0028
SZ Hya	54797.8447	26280	–0.2403	SAH	0.0039
SZ Hya	54827.9712	26336	–0.1992	SAH	0.0020
SZ Hya	54833.8876	26347	–0.1925	SAH	0.0011
SZ Hya	54875.7467	26425	–0.2381	PRX	0.0025
SZ Hya	54881.7011	26436	–0.1934	PRX	0.0016
SZ Hya	54888.6850	26449	–0.1936	PRX	0.0010
SZ Hya	54904.7806	26479	–0.2152	SAH	0.0070
SZ Hya	54917.6953	26503	–0.1943	PRX	0.0017

Table continued on following pages

Table 1. Recent times of maxima of stars in the AAVSO RR Lyrae program, cont.

Star	*JD (max) Hel. 2400000+*	*Cycle*	*O-C*	*Observer**	*Error*
SZ Hya	55179.8655	26991	–0.1973	SAH	0.0016
SZ Hya	55186.8266	27004	–0.2203	SAH	0.0033
DG Hya	52374.5700	0	0.0050	SAH	0.0024
DG Hya	52380.5882	8	–0.0107	SAH	0.0019
DG Hya	52389.6526	20	0.0027	SAH	0.0022
DG Hya	52615.9270	320	0.0043	SAH	0.0031
DG Hya	52739.6183	484	–0.0002	SAH	0.0037
DG Hya	53463.6883	1444	–0.0032	GHS	0.0029
DG Hya	54522.6479	2848	–0.0003	PRX	0.0025
DG Hya	54534.7173	2864	0.0012	BIZ	0.0022
DG Hya	54831.8868	3258	–0.0009	SAH	0.0025
DG Hya	54884.6850	3328	0.0003	PRX	0.0027
DH Hya	52356.7559	43314	0.0439	SAH	0.0015
DH Hya	52698.5731	44013	0.0513	SAH	0.0023
DH Hya	52740.6235	44099	0.0479	SAH	0.0013
DH Hya	53802.7353	46271	0.0556	PRX	0.0015
DH Hya	54135.7458	46952	0.0583	PRX	0.0019
DH Hya	54536.7304	47772	0.0644	BIZ	0.0014
DH Hya	54893.7024	48502	0.0677	PRX	0.0012
RR Leo	53071.6791	21610	0.0579	NMI	0.0010
RR Leo	53152.6592	21789	0.0596	BIZ	0.0011
RR Leo	53405.5534	22348	0.0659	SAH	0.0014
RR Leo	53469.7943	22490	0.0670	SAH	0.0013
RR Leo	53813.6221	23250	0.0759	SAH	0.0012
RR Leo	54173.7308	24046	0.0795	PRX	0.0012
RR Leo	54486.7925	24738	0.0850	MZK	0.0013
RR Leo	54535.6518	24846	0.0859	MZK	0.0011
RR Leo	54539.7270	24855	0.0895	SAH	0.0009
RR Leo	54563.7025	24908	0.0882	BIZ	0.0010
RR Leo	54875.8608	25598	0.0951	SAH	0.0010
RR Leo	54905.7194	25664	0.0957	HES	0.0009
RR Leo	54923.8143	25704	0.0949	PRX	0.0008
SS Leo	54176.7094	19790	–0.0493	BIZ	0.0018
SS Leo	54533.7170	20360	–0.0579	BIZ	0.0018
SS Leo	54592.5941	20454	–0.0571	MZK	0.0021
SS Leo	54932.6919	20997	–0.0642	SAH	0.0019
ST Leo	53810.7272	54160	–0.0205	PRX	0.0017
ST Leo	53842.7521	54227	–0.0205	PRX	0.0009

Table continued on following pages

Table 1. Recent times of maxima of stars in the AAVSO RR Lyrae program, cont.

Star	*JD (max) Hel. 2400000+*	*Cycle*	*O-C*	*Observer**	*Error*
ST Leo	54179.7314	54932	–0.0202	PRX	0.0013
ST Leo	54180.6864	54934	–0.0211	BIZ	0.0012
ST Leo	54212.7101	55001	–0.0224	HES	0.0011
ST Leo	54559.7297	55727	–0.0194	BIZ	0.0012
ST Leo	54561.6413	55731	–0.0197	GHS	0.0014
ST Leo	54882.8480	56403	–0.0185	SAH	0.0010
ST Leo	54906.7444	56453	–0.0213	PRX	0.0011
TV Leo	54520.8638	25978	0.1090	BIZ	0.0026
TV Leo	54905.7411	26550	0.1146	SAH	0.0020
WW Leo	53072.6780	30174	0.0308	NMI	0.0028
WW Leo	54904.7300	33213	0.0360	SAH	0.0025
AA Leo	53405.7774	23067	–0.0686	PRX	0.0020
AA Leo	53405.7782	23067	–0.0678	BIZ	0.0019
AA Leo	54209.7640	24410	–0.0766	BIZ	0.0014
AA Leo	54233.7120	24450	–0.0749	HES	0.0014
AA Leo	54567.7602	25008	–0.0765	BIZ	0.0014
AA Leo	54958.6782	25661	–0.0807	PRX	0.0020
U Lep	53001.6786	20034	0.0384	SAH	0.0013
U Lep	54086.7197	21900	0.0449	SAH	0.0037
U Lep	54100.6733	21924	0.0431	PRX	0.0017
U Lep	54461.7710	22545	0.0441	BIZ	0.0015
U Lep	54496.6563	22605	0.0408	BIZ	0.0016
U Lep	54503.6362	22617	0.0430	BIZ	0.0012
U Lep	54828.6844	23176	0.0460	SAH	0.0023
U Lep	54860.6630	23231	0.0434	PRX	0.0012
U Lep	55185.7104	23790	0.0456	SAH	0.0015
SZ Lyn	52785.6871	121635	0.0239	HES	0.0012
SZ Lyn	53011.5660	123509	0.0203	BIZ	0.0012
SZ Lyn	53051.5825	123841	0.0192	BIZ	0.0012
SZ Lyn	53079.6693	124074	0.0214	NMI	0.0008
SZ Lyn	53644.7348	128762	0.0192	SAH	0.0009
SZ Lyn	53644.8544	128763	0.0183	SAH	0.0009
SZ Lyn	53721.7571	129401	0.0197	PRX	0.0008
SZ Lyn	53745.6239	129599	0.0206	SAH	0.0009
SZ Lyn	53761.5352	129731	0.0213	SAH	0.0007
SZ Lyn	53773.5891	129831	0.0217	SAH	0.0007
SZ Lyn	53801.5531	130063	0.0216	SAH	0.0009
SZ Lyn	53801.6733	130064	0.0212	SAH	0.0009

Table continued on following pages

Table 1. Recent times of maxima of stars in the AAVSO RR Lyrae program, cont.

Star	*JD (max) Hel. 2400000+*	*Cycle*	*O-C*	*Observer**	*Error*
SZ Lyn	53840.6077	130387	0.0228	SAH	0.0007
SZ Lyn	53853.6262	130495	0.0236	SAH	0.0008
SZ Lyn	53871.5881	130644	0.0258	SAH	0.0012
SZ Lyn	53890.6318	130802	0.0250	SAH	0.0009
SZ Lyn	53981.8799	131559	0.0281	SAH	0.0010
SZ Lyn	54009.8443	131791	0.0284	SAH	0.0007
SZ Lyn	54015.8703	131841	0.0277	SAH	0.0011
SZ Lyn	54058.7811	132197	0.0280	PRX	0.0011
SZ Lyn	54079.8751	132372	0.0284	SAH	0.0008
SZ Lyn	54120.8567	132712	0.0282	SAH	0.0008
SZ Lyn	54134.7170	132827	0.0269	SAH	0.0009
SZ Lyn	54168.5878	133108	0.0274	SAH	0.0010
SZ Lyn	54208.6027	133440	0.0247	SAH	0.0007
SZ Lyn	54222.5857	133556	0.0257	SAH	0.0009
SZ Lyn	54261.6365	133880	0.0232	SAH	0.0008
SZ Lyn	54366.8605	134753	0.0202	SAH	0.0008
SZ Lyn	54394.8251	134985	0.0207	SAH	0.0009
SZ Lyn	54414.8334	135151	0.0202	SAH	0.0010
SZ Lyn	54484.6200	135730	0.0171	BIZ	0.0010
SZ Lyn	54484.7384	135731	0.0149	BIZ	0.0012
SZ Lyn	54499.5644	135854	0.0151	HAV	0.0007
SZ Lyn	54506.6801	135913	0.0193	SAH	0.0010
SZ Lyn	54511.5016	135953	0.0194	MZK	0.0009
SZ Lyn	54511.6224	135954	0.0196	MZK	0.0011
SZ Lyn	54511.7420	135955	0.0187	MZK	0.0015
SZ Lyn	54513.6690	135971	0.0172	HAV	0.0008
SZ Lyn	54520.7815	136030	0.0181	SAH	0.0008
SZ Lyn	54525.6041	136070	0.0193	HAV	0.0013
SZ Lyn	54562.7261	136378	0.0165	SAH	0.0008
SZ Lyn	54583.5797	136551	0.0176	SAH	0.0007
SZ Lyn	54768.8438	138088	0.0195	SAH	0.0006
SZ Lyn	54792.8309	138287	0.0202	SAH	0.0010
SZ Lyn	54807.6573	138410	0.0208	SAH	0.0009
SZ Lyn	54837.5508	138658	0.0216	SAH	0.0008
SZ Lyn	54865.6345	138891	0.0207	SAH	0.0009
SZ Lyn	54865.7558	138892	0.0215	SAH	0.0008
SZ Lyn	54903.6043	139206	0.0220	SAH	0.0008
SZ Lyn	54903.7252	139207	0.0224	SAH	0.0009

Table continued on following pages

Table 1. Recent times of maxima of stars in the AAVSO RR Lyrae program, cont.

Star	*JD (max) Hel. 2400000+*	*Cycle*	*O-C*	*Observer**	*Error*
SZ Lyn	54923.6165	139372	0.0254	SAH	0.0009
SZ Lyn	55114.9109	140959	0.0309	SAH	0.0009
SZ Lyn	55163.8484	141365	0.0312	SAH	0.0007
SZ Lyn	55167.7045	141397	0.0302	SRIC	0.0011
SZ Lyn	55167.8271	141398	0.0322	SRIC	0.0012
SZ Lyn	55167.9454	141399	0.0300	SRIC	0.0010
RZ Lyr	53265.6069	23633	–0.0084	BIZ	0.0018
RZ Lyr	53929.7219	24932	0.0029	SAH	0.0016
RZ Lyr	53935.8523	24944	–0.0016	SAH	0.0018
RZ Lyr	54205.7765	25472	–0.0134	BIZ	0.0018
RZ Lyr	54611.7106	26266	–0.0057	BIZ	0.0013
RZ Lyr	54612.7341	26268	–0.0046	HAV	0.0015
RZ Lyr	54977.7601	26982	–0.0056	MZK	0.0010
AV Peg	52525.8082	22377	0.0775	SAH	0.0011
AV Peg	53354.5862	24500	0.0900	SAH	0.0011
AV Peg	53712.5689	25417	0.0992	SAH	0.0011
AV Peg	54261.8359	26824	0.1089	BIZ	0.0011
AV Peg	55093.7405	28955	0.1251	SAH	0.0009
AV Peg	55147.6120	29093	0.1249	SAH	0.0017
RU Scl	52640.6474	43617	–0.1492	SAH	0.0014
RU Scl	53259.8076	44872	–0.1291	SAH	0.0014
RU Scl	53353.5512	45062	–0.1199	SAH	0.0012
RU Scl	54046.7107	46467	–0.1014	PRX	0.0017
RU Scl	54090.6208	46556	–0.0984	SAH	0.0015
RU Scl	54419.6875	47223	–0.0887	BIZ	0.0012
RU Scl	54423.6329	47231	–0.0900	PRX	0.0015
RU Scl	54832.6251	48060	–0.0757	SAH	0.0012
RU Scl	55123.7021	48650	–0.0685	SAH	0.0013
RV UMa	53610.6798	18235	0.0947	HES	0.0016
RV UMa	53837.6993	18720	0.1051	PRX	0.0012
RV UMa	54188.7485	19470	0.1093	BIZ	0.0017
RV UMa	54637.6224	20429	0.1137	MZK	0.0018
RV UMa	54909.5696	21010	0.1180	SAH	0.0015
RV UMa	54914.7179	21021	0.1176	PRX	0.0016
RV UMa	54920.8047	21034	0.1197	SAH	0.0012
RV UMa	54929.6974	21053	0.1192	SAH	0.0008
RV UMa	54944.6723	21085	0.1162	SAH	0.0010
RV UMa	54957.7762	21113	0.1144	SAH	0.0014

Table continued on following pages

Table 1. Recent times of maxima of stars in the AAVSO RR Lyrae program, cont.

Star	*JD (max) Hel. 2400000+*	*Cycle*	*O-C*	*Observer**	*Error*
RV UMa	54980.7113	21162	0.1146	SAH	0.0017
RV UMa	55008.7970	21222	0.1167	SAH	0.0018
AE UMa	54079.7666	214788	–0.0026	SAH	0.0007
AE UMa	54079.8580	214789	0.0028	SAH	0.0014
AE UMa	54079.9437	214790	0.0025	SAH	0.0007
AE UMa	54102.6471	215054	–0.0026	SAH	0.0006
AE UMa	54102.7365	215055	0.0007	SAH	0.0015
AE UMa	54102.8254	215056	0.0036	SAH	0.0009
AE UMa	54103.6849	215066	0.0029	SAH	0.0009
AE UMa	54103.7677	215067	–0.0003	SAH	0.0012
AE UMa	54104.7117	215078	–0.0025	SAH	0.0009
AE UMa	54107.6358	215112	–0.0029	SAH	0.0005
AE UMa	54107.7251	215113	0.0003	SAH	0.0009
AE UMa	54107.8138	215114	0.0030	SAH	0.0010
AE UMa	54107.8944	215115	–0.0024	SAH	0.0007
AE UMa	54110.7388	215148	0.0035	SAH	0.0011
AE UMa	54110.8207	215149	–0.0007	SAH	0.0006
AE UMa	54110.9051	215150	–0.0023	SAH	0.0007
AE UMa	54110.9977	215151	0.0043	SAH	0.0007
AE UMa	54125.7056	215322	0.0033	SAH	0.0010
AE UMa	54125.7883	215323	0.0000	SAH	0.0011
AE UMa	54125.8716	215324	–0.0028	SAH	0.0008
AE UMa	54125.9649	215325	0.0045	SAH	0.0014
AE UMa	54131.5550	215390	0.0035	SAH	0.0013
AE UMa	54131.6392	215391	0.0017	SAH	0.0008
AE UMa	54131.7212	215392	–0.0023	SAH	0.0006
AE UMa	54131.8106	215393	0.0011	SAH	0.0011
AE UMa	54131.8989	215394	0.0034	SAH	0.0006
AE UMa	54136.5446	215448	0.0041	SAH	0.0011
AE UMa	54136.6275	215449	0.0010	SAH	0.0006
AE UMa	54136.7104	215450	–0.0021	SAH	0.0008
AE UMa	54136.7998	215451	0.0013	SAH	0.0009
AE UMa	54136.8882	215452	0.0037	SAH	0.0007
AE UMa	54136.9697	215453	–0.0009	SAH	0.0012
AE UMa	54137.6581	215461	–0.0006	SAH	0.0013
AE UMa	54137.7491	215462	0.0044	SAH	0.0014
AE UMa	54137.8311	215463	0.0004	SAH	0.0009
AE UMa	54139.7226	215485	–0.0005	SAH	0.0009

Table continued on following pages

Table 1. Recent times of maxima of stars in the AAVSO RR Lyrae program, cont.

Star	*JD (max) Hel. 2400000+*	*Cycle*	*O-C*	*Observer**	*Error*
AE UMa	54139.8124	215486	0.0033	SAH	0.0008
AE UMa	54139.8942	215487	–0.0009	SAH	0.0005
AE UMa	54141.7876	215509	0.0001	SAH	0.0010
AE UMa	54141.8768	215510	0.0033	SAH	0.0007
AE UMa	54141.9575	215511	–0.0020	SAH	0.0009
AE UMa	54152.6241	215635	–0.0016	SAH	0.0011
AE UMa	54153.5746	215646	0.0028	SAH	0.0010
AE UMa	54154.6883	215659	–0.0018	SAH	0.0010
AE UMa	54154.7800	215660	0.0039	SAH	0.0009
AE UMa	54154.8618	215661	–0.0003	SAH	0.0006
AE UMa	54414.8939	218684	0.0022	SAH	0.0008
AE UMa	54414.9804	218685	0.0027	SAH	0.0007
AE UMa	54417.7271	218717	–0.0031	SAH	0.0006
AE UMa	54417.9058	218719	0.0035	SAH	0.0006
AE UMa	54417.9856	218720	–0.0027	SAH	0.0005
AE UMa	54440.6958	218984	–0.0010	SAH	0.0010
AE UMa	54442.7619	219008	0.0007	SAH	0.0009
AE UMa	54442.8516	219009	0.0044	SAH	0.0011
AE UMa	54442.9342	219010	0.0010	SAH	0.0013
AE UMa	54451.6243	219111	0.0034	SAH	0.0012
AE UMa	54460.6513	219216	–0.0014	SAH	0.0008
AE UMa	54460.7433	219217	0.0046	SAH	0.0007
AE UMa	54460.8247	219218	–0.0001	SAH	0.0005
AE UMa	54460.9089	219219	–0.0019	SAH	0.0006
AE UMa	54467.7955	219299	0.0034	SAH	0.0006
AE UMa	54468.7392	219310	0.0009	SAH	0.0006
AE UMa	54468.8220	219311	–0.0023	SAH	0.0007
AE UMa	54468.9120	219312	0.0016	SAH	0.0009
AE UMa	54469.6815	219321	–0.0030	SAH	0.0006
AE UMa	54469.7701	219322	–0.0004	SAH	0.0008
AE UMa	54469.8603	219323	0.0037	SAH	0.0006
AE UMa	54469.9414	219324	–0.0012	SAH	0.0006
AE UMa	54769.8859	222811	0.0019	SAH	0.0010
AE UMa	54770.8336	222822	0.0034	SAH	0.0005
AE UMa	54770.9152	222823	–0.0010	SAH	0.0005
AE UMa	54781.8384	222950	–0.0020	SAH	0.0007
AE UMa	54781.9301	222951	0.0037	SAH	0.0010
AE UMa	54788.8080	223031	0.0002	SAH	0.0006

Table continued on following pages

Table 1. Recent times of maxima of stars in the AAVSO RR Lyrae program, cont.

Star	*JD (max) Hel. 2400000+*	*Cycle*	*O-C*	*Observer**	*Error*
AE UMa	54788.8912	223032	–0.0026	SAH	0.0006
AE UMa	54788.9833	223033	0.0035	SAH	0.0012
AE UMa	54791.7333	223065	0.0009	SAH	0.0006
AE UMa	54791.8157	223066	–0.0027	SAH	0.0005
AE UMa	54791.9080	223067	0.0036	SAH	0.0011
AE UMa	54791.9938	223068	0.0034	SAH	0.0005
AE UMa	54807.8222	223252	0.0046	SAH	0.0006
AE UMa	54807.9032	223253	–0.0004	SAH	0.0005
AE UMa	54807.9866	223254	–0.0030	SAH	0.0007
AE UMa	54816.6793	223355	0.0020	SAH	0.0006
AE UMa	54816.7612	223356	–0.0021	SAH	0.0006
AE UMa	54816.8501	223357	0.0007	SAH	0.0012
AE UMa	54816.9399	223358	0.0045	SAH	0.0009
AE UMa	54837.6637	223599	–0.0018	SAH	0.0009
AE UMa	54837.7565	223600	0.0050	SAH	0.0009
AE UMa	54843.6886	223669	0.0019	SAH	0.0007
AE UMa	54843.7704	223670	–0.0023	SAH	0.0008
AE UMa	54843.8567	223671	–0.0020	SAH	0.0009
AE UMa	54843.9494	223672	0.0047	SAH	0.0010
AE UMa	54846.6137	223703	0.0024	SAH	0.0008
AE UMa	54846.6960	223704	–0.0013	SAH	0.0007
AE UMa	54847.7336	223716	0.0041	SAH	0.0008
AE UMa	54847.8164	223717	0.0009	SAH	0.0007
AE UMa	54847.8988	223718	–0.0027	SAH	0.0006
AE UMa	54855.6469	223808	0.0039	SAH	0.0010
AE UMa	54855.7316	223809	0.0025	SAH	0.0010
AE UMa	54855.8119	223810	–0.0032	SAH	0.0006
AE UMa	54855.9023	223811	0.0012	SAH	0.0010
AE UMa	54864.5873	223912	–0.0015	SAH	0.0005
AE UMa	54864.6724	223913	–0.0024	SAH	0.0007
AE UMa	54864.7649	223914	0.0040	SAH	0.0009
AE UMa	54864.8477	223915	0.0008	SAH	0.0006
AE UMa	54864.9296	223916	–0.0033	SAH	0.0006
AE UMa	54868.6346	223959	0.0030	SAH	0.0008
AE UMa	54868.7166	223960	–0.0010	SAH	0.0008
AE UMa	54868.8033	223961	–0.0004	SAH	0.0014
AE UMa	54868.8941	223962	0.0044	SAH	0.0009
AE UMa	54878.6935	224076	–0.0021	SAH	0.0006

Table continued on following page

Table 1. Recent times of maxima of stars in the AAVSO RR Lyrae program, cont.

Star	*JD (max) Hel. 2400000+*	*Cycle*	*O-C*	*Observer**	*Error*
AE UMa	54878.7811	224077	–0.0005	SAH	0.0008
AE UMa	54878.8721	224078	0.0044	SAH	0.0009

**Observers: BM, M. Baldwin; BIZ, J. Bialozynski; BKS, S. Brady; GHS, H. Gerner; HAV, R. Harvan; HES, C. Hesseltine; MKE, R. Manske; MZK, K. Menzies; NMI, M. Nicholas; PRX, R. Poklar; SRIC, R. Sabo; SAH, G. Samolyk; SNE, N. Simmons; VJA, J. Virtanen.*

Photometry of the Dwarf Nova SDSS J094002.56+274942.0 in Outburst

Tom Krajci
Astrokolkhoz Observatory, P.O. Box 1351, Cloudcroft, New Mexico 88317; tom_krajci@tularosa.net

Patrick Wils
Vereniging Voor Sterrenkunde, Aarschotsebaan 31, Hever, B-3191, Belgium; patrickwils@yahoo.com

Received December 14, 2009; revised January 4, 2010; accepted January 4, 2010

Abstract Data from the first observed outburst of the dwarf nova SDSS J094002.56+274942.0 show cyclical variations increasing in amplitude when the object fades. These variations are likely due to the ellipsoidal shape of the red dwarf and possibly also eclipses of the accretion disk. An orbital period of 3.92 hours is derived.

1. Introduction

The cataclysmic variable (CV) SDSS J094002.56+274942.0 was discovered by Szkody *et al.* (2007) in spectra from the Fifth Data Release of the Sloan Digital Sky Survey (SDSS; Adelman-McCarthy *et al.* 2007). It was observed only once by SDSS at magnitude $g = 19.10 \pm 0.01$. No further details were provided by Szkody *et al.* (2007).

With $E(B - V) = 0.018$ (Schlegel *et al.* 1998), Galactic extinction is almost negligible in the direction of SDSS J094002.56+274942.0. The SDSS colors $u - g = 0.54 \pm 0.04$ and $g - r = 0.78 \pm 0.01$ therefore make it a fairly red CV, indicating that there is a substantial contribution of the red dwarf to the total light. In this case the orbital period should be fairly large, i.e., above the period gap. This conclusion is further strengthened by the 2MASS colors (Skrutskie *et al.* 2006): $J = 16.1 \pm 0.1$, $J - H = 0.5 \pm 0.2$ and $J - K_s = 0.7 \pm 0.2$ (note that the signal to noise ratio of the 2MASS detections in the H and K_s bands are fairly low). However, there is no immediate evidence for the red dwarf in the SDSS spectrum. The Galaxy Evolution Explorer (GALEX; Martin *et al.* 2005) observed the object twice at $nuv = 19.7 \pm 0.1$, $fuv - nuv = 0.8 \pm 0.3$, and $nuv = 19.3 \pm 0.1$, $fuv - nuv = 0.4 \pm 0.2$, apparently both at quiescence. The spectral energy distribution of SDSS J094002.56+274942.0 is given in Figure 1.

2. Observations

Like many other CVs, SDSS J094002.56+274942.0 is being monitored by the Catalina Real-time Transient Survey (CRTS; Drake *et al.* 2009). Normally

it has an unfiltered magnitude around 18. On 18 November 2009, an outburst to magnitude 14.6 was detected by CRTS (http://nesssi.cacr.caltech.edu/catalina/20010319/103191260474100307p.html), and follow-up observations were promptly started at the Astrokolkhoz Observatory.

For the observations a C14 Schmidt-Cassegrain was used, equipped with an ST-10 CCD camera and a Cousins *R* filter (for the first four nights), and a clear filter afterwards (last four nights). The comparison star used was GSC 1965-146, and GSC 1965-893 and GSC 1965-1064 were used as check stars. Using the transformation formulae from Lupton (http://www.sdss.org/dr7/algorithms/sdssUBVRITransform.html#Lupton2005), a magnitude $R = 13.8$ was calculated for GSC 1965-146. The same magnitude was adopted for the unfiltered observations. On each night, except for the short run on the seventh night, standard deviations on the magnitude of the check star were better than 0.01 magnitude. Median standard deviations on five-point averages of the variable gradually deteriorated from 0.013 on the first night to 0.049 on the last night.

The overall light curve of the outburst is given in Figure 2. On 26 November the object was only half a magnitude above its normal brightness, and on 28 November it had effectively returned to its quiescence magnitude.

Near outburst maximum the light curve was fairly featureless. After a couple of days, a double wave became visible with a period of 0.16352 day and growing in amplitude. With the object at quiescence this double wave had an amplitude of around 0.3 magnitude and was clearly visible in the light curve. We interpret these periodic variations at the later stages of the outburst and at quiescence as due to the changing aspect angle of the ellipsoidal shape of the red dwarf, for which the contribution to the total light is increasing when the system fades. These variations can be seen when the inclination of the orbit is high enough. The period of 0.16352 day (3.92 hours) is then the orbital period of the system. Further proof of this scenario can be obtained by observing variations in the color of the object during all stages of an outburst. A phased light curve is given in Figure 3. The dwarf nova HS 0218+3229 shows similar variations due to the ellipsoidal shape of the secondary (Rodríguez-Gil *et al.* 2009), although in that case the orbital period is much longer (7.13 hours).

During the brightest stages of the outburst of SDSS J094002.56+274942.0, there is a small dip corresponding to the phase of one of the minima of the ellipsoidal variations. This may be due to the red dwarf (partially) eclipsing the accretion disk or hot spot. Unfortunately, the phase coverage was not complete on the first nights, missing the time at which the eclipse was expected. It would be especially worthwhile to observe a full orbital cycle close to maximum to verify the possible eclipse at that stage. The minimum at phase zero is sometimes fairly sharp, even near quiescence, so that it actually may be the result of an eclipse as well.

The SDSS spectrum published by Szkody *et al.* (2007) is fairly flat in the near-infrared, with no sign of TiO bands. As most CVs with an orbital period

near 4 hours have M4-5 type secondaries, the lack of TiO bands in the spectrum would indicate that the contribution of the red dwarf to the total light is small. However, this seems to be in contradiction with the observed colors and rules out that the observed 0.3-magnitude variations are due to the secondary. Another possibility is that the red dwarf has an early M-type spectrum with little TiO present. A detailed spectral analysis and a radial velocity study is needed to settle the case.

3. Outburst frequency

After the recent outburst archival images of the dwarf nova were investigated, and a further outburst was found on images of the Near Earth Asteroid Tracking survey (NEAT) (http://skyview.gsfc.nasa.gov/skymorph/skymorph.html) in November 2002. The unfiltered magnitude of the object was 14.57 ± 0.02 on 22 November and 14.72 ± 0.03 on 23 November, again adopting magnitude 13.8 for GSC 1965-146.

Following Southworth *et al.* (2009), an estimate can be made of the outburst frequency of SDSS J094002.56+274942.0, based on the dates at which the object was observed by NEAT (three images on one night in December 1997 and forty-one images from sixteen nights between June 2001 and February 2003) and CRTS (282 observations on seventy-two nights between January 2005 and November 2009). Because the latest CRTS observation prior to the outburst detection dates from October 2009, it is not possible to fix the exact start of the outburst. From our data it follows that the outburst lasted at least eight days. A duration of eight days agrees with the empirical relation derived by (Ak *et al.* 2002) for a dwarf nova with the orbital period of SDSS J094002.56+274942.0. In the following an outburst duration of eight days will therefore be assumed. Using Monte Carlo simulations, the efficiency to detect an outburst during the observation interval can be estimated to be 5% for NEAT (or 16% for an outburst between June 2001 and February 2003) and 30% for CRTS.

Further assuming periodic outbursts, the number of observed outbursts in the given observing interval can be calculated. On average a single outburst will have been detected by NEAT if the outburst cycle is around 100 days, and by CRTS if it is around 500 days. If the outburst cycle would be less than 250 days, CRTS would have detected two outbursts or more on average. These discrepant values are of course a result of small number statistics, but an outburst cycle of about one year or longer can be assumed. Southworth *et al.* (2009) found a similar value for SDSS J100658.40+233724.4, another dwarf nova with a 4-hour orbital period. This outburst cycle is much longer than the average cycle found by Ak *et al.* (2002) for historically known and frequently observed dwarf novae with a similar orbital period. This suggests that the sample of previously known dwarf novae, mostly detected because of their variability, was biased towards objects with a high outburst frequency.

4. Conclusion

SDSS J094002.56+274942.0 has been found to be a dwarf nova with an orbital period of 3.92 hours, with a 0.3-magnitude variability at quiescence due to the ellipsoidal shape of the secondary. Possibly also eclipses of the accretion disk may be observed. Unlike the majority of CVs discovered through SDSS spectroscopy (Gänsicke *et al.* 2009), it has an orbital period above the period gap. The outburst frequency is estimated to be about once per year or less, but this has to be confirmed by further observations.

5. Acknowledgements

This study made use of NASA's Astrophysics Data System, and the SIMBAD and VIZIER databases operated at the Centre de Données Astronomiques (Strasbourg) in France.

References

Adelman-McCarthy, J. K., *et al.* 2007, *Astrophys. J., Suppl. Ser.*, **172**, 634.
Ak, T., Ozkan, M. T., and Mattei, J. A. 2002, *Astron. Astrophys.*, **389**, 478.
Drake, A. J., *et al.* 2009, *Astrophys. J.*, **696**, 870.
Gänsicke, B. T., *et al.* 2009, *Mon. Not. Roy. Astron. Soc.*, **397**, 2170.
Martin, D. C., *et al.*, 2005, *Astrophys. J., Lett. Ed.*, **619**, L1.
Rodríguez-Gil, P., Torres, M. A. P., Gänsicke, B. T., Muñoz-Darias, T., Steeghs, D., Schwarz, R., Rau, A., and Hagen, H.-J. 2009, *Astron. Astrophys.*, **496**, 805.
Schlegel, D. J., Finkbeiner, D. P., and Davis, M. 1998, *Astrophys. J.*, **500**, 525.
Skrutskie, M. F., *et al.* 2006, *Astron. J.*, **131**, 1163.
Southworth, J., Hickman, R. D. G., Marsh, T. R., Rebassa-Mansergas, A., Gänsicke, B. T., Copperwheat, C. M., and Rodríguez-Gil, P. 2009, *Astron. Astrophys.*, **507**, 929.
Szkody, P., *et al.* 2007, *Astron. J.*, **134**, 185.

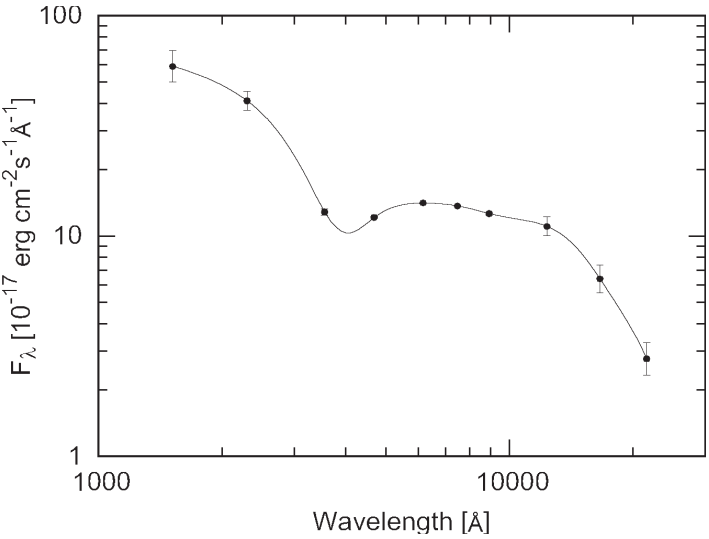

Figure 1. Spectral energy distribution of SDSS J094002.56+274942.0, based on photometry from GALEX, SDSS, and 2MASS. Both axes have logarithmic scales.

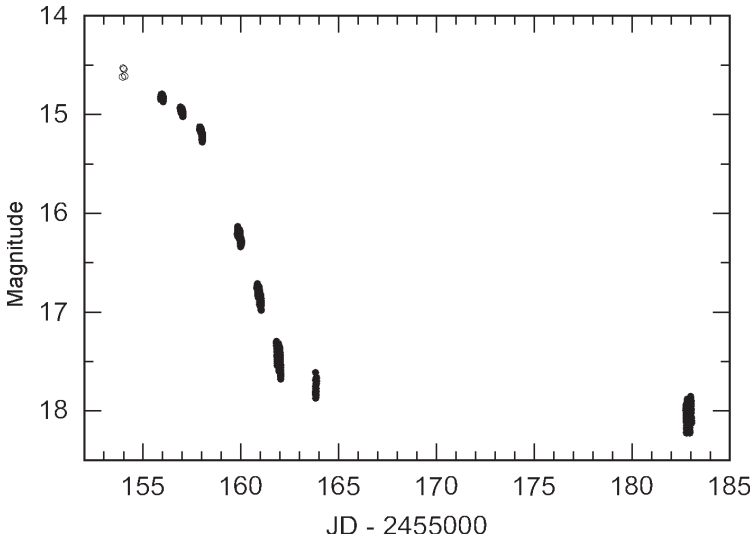

Figure 2. Light curve of the November 2009 outburst of SDSS J094002.56+274942.0. Open circles represent unfiltered CRTS data, filled circles represent *R* and (for the last four nights) unfiltered data from Astrokolkhoz Observatory.

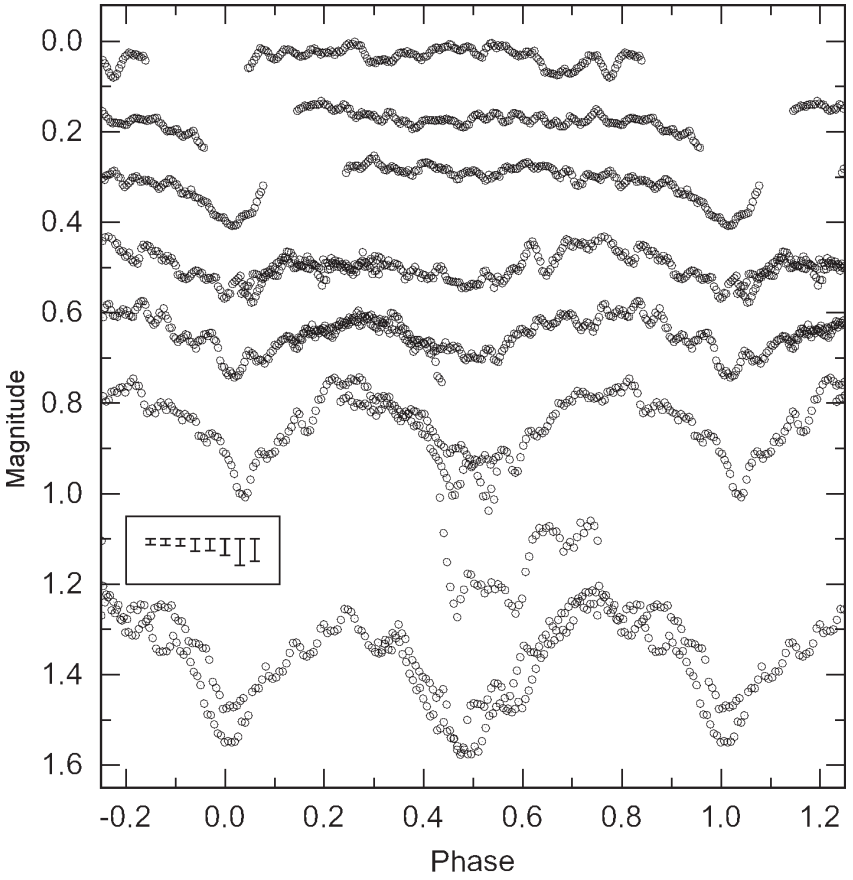

Figure 3. Light curve of five-point moving averages of Astrokolkhoz Observatory data for SDSS J094002.56+274942.0, phased with a period of 0.16352 day. The magnitudes have been arbitrarily shifted for clarity, with the night the object was brightest on top. For the fourth, fifth, and sixth nights a linear fading trend was subtracted from the data. JD = 2455156.06 was taken for the zeropoint of the phase. The vertical lines at bottom left indicate the median standard deviation on the five-point averages for each of the nights.

The 2009 July Superoutburst of IL Vulpeculae

David Boyd
5 Silver Lane, West Challow, Wantage, OX12 9TX, UK; drsboyd@dsl.pipex.com

Tut Campbell
7021 Whispering Pine, Harrison, AR 72601; jmontecamp@yahoo.com

George Roberts
2007 Cedarmont Drive, Franklin, TN 37067; georgeroberts@comcast.net

Received September 28, 2009; revised October 19, 2009; accepted October 19, 2009

Abstract IL Vulpeculae experienced its first recognized superoutburst in 2009 July, thereby identifying itself as a UGSU-type dwarf nova. We measured the superhump period and amplitude as 0.071(1) day and 0.12 magnitude, respectively, and estimate its orbital period to be 0.069(1) day.

1. Background

The first reported outburst of IL Vul was in *IBVS* No. 80 by Hoffmeister (1965) using the name S9068 Vul. He observed it on 1964 August 14.98 UT at magnitude 15 on plates taken at the Karl-Schwarzschild Observatory. He reported its normal magnitude as being in the range 19–20. In the same paper he also reports two "rather certain" observations, on 1930 August 20 at magnitude 15.5 and 1955 September 22 at magnitude 15.0, found during a search of plate archives from 1928 to 1964. No outburst brighter than magnitude 15 was found.

Bruch *et al.* (1987) listed IL Vul as an identified dwarf nova, noting it is extremely faint on POSS blue prints. They reported five observations of it during 1981 with one outburst detected on 1981 September 5.91 but they did not give a magnitude. Liu *et al.* (1999) reported a spectroscopic observation on 1997 August 8.71 UT with *V* magnitude 17.8, and they related its spectrum as that of a dwarf nova after outburst. On the available evidence, the *General Catalogue of Variable Stars* (GCVS; Kholopov *et al.* 1985) classified IL Vul as a UG-type dwarf nova with unknown orbital period. At the time of writing, its classification in VSX (Watson *et al.* 2007) is the same.

A further outburst was reported on 2005 July 3.388 at magnitude 15.5CR by Schmeer (2005). Observing the following day, Krajci (2005) saw the star fading steadily at magnitude 16.8 with no sign of superhumps. This was probably a normal outburst. A search of the AAVSO International Database revealed several positive observations between 2005 July and 2008 July in the magnitude range 16.7 to 18.4, which may be normal outbursts, but nothing brighter until the present outburst.

2. Observations

The 2009 outburst of IL Vul was first reported to several variable star newsgroups by Muyllaert (2009). He observed it unfiltered with the Bradford Robotic Telescope and measured its magnitude on July 09.144 UT as 15.69 using a preliminary USNO-derived sequence.

DB obtained unfiltered time-series observations on July 9.931–10.080 UT while TC and GR obtained further unfiltered data on July 10.282–10.406 UT. Both sites were operating under poor conditions. Bad weather persisted, with DB being able to obtain only short runs on July 14.922–14.979 UT and July 19.947–19.951 UT.

Astrometry using images taken on July 9 gives a mean position for IL Vul of R.A. $20^h\ 38^m\ 32.72(1)^s$, Dec. +22° 42' 17.0(1)" (J2000). Figure 1 shows an image of the field taken on July 9.984 UT.

V magnitudes of possible comparison stars around IL Vul were derived from r' magnitudes in the CMC14 catalogue (Univ. of Cambridge 2005) and *J* and *K* magnitudes in the 2MASS catalogue (Skrutskie *et al.* 2006) using the formula in Dymock and Miles (2009). Comparison stars were selected which were as blue as possible to minimize their color difference from the dwarf nova.

3. Analysis

All images were dark-subtracted and flat-fielded and instrumental magnitudes obtained by aperture photometry. Absolute magnitudes were then calculated by reference to the comparison stars. Heliocentric corrections were applied to the times of observation. The resulting light curve is shown in Figure 2. The downward slope indicates we observed the outburst during its later stages. Figure 3 expands the data from July 9 and 10. These show the first recorded superhumps in IL Vul and confirm that this is a UGSU-type dwarf nova.

A Discrete Fourier Transform (DFT; Vanmunster 2007) power spectrum of the data from July 9 and 10 is shown in Figure 4 and reveals two prominent signals at periods of 0.071(1) day and 0.088(2) day with more power at the shorter period. The distribution of alias signals is as expected from a spectral window analysis of the data and there are harmonic repeats of this pattern with decreasing power.

To decide which of these is the superhump period, we measured the times of maximum of the four superhumps recorded on July 9 and 10 by fitting a quadratic to the light curve around each maximum. We then fitted a linear ephemeris to these times of maximum to determine the superhump period. Depending on the assignment of cycle number to each maximum, we find the superhump period to be either 0.0712(3) day with χ^2 of 3.0 or 0.0890(4) day with χ^2 of 85.2. We therefore adopt the shorter period as the correct superhump period. Taking the more conservative estimate of its uncertainty, we report the superhump period

as 0.071(1) day. The phase diagram obtained by folding the data on this period is shown in Figure 5. The superhump amplitude is 0.12 magnitude.

As we observed the later stages of the outburst, during what Kato *et al.* (2009) refer to as stage C, we use their relationship between the superhump period and the orbital period in this regime to estimate an orbital period for IL Vul of 0.069(1) day (1.65 hours).

4. Conclusions

We have detected superhumps during the outburst of IL Vul in 2009 July, confirming this is a UGSU-type dwarf nova. Although our observations were limited, we were able to measure its superhump period and amplitude to be 0.071(1) day and magnitude 0.12, respectively. We estimate empirically that its orbital period is 0.069(1) day.

5. Acknowledgements

We acknowledge with thanks the variable star observations from the AAVSO International Database contributed by observers worldwide and used in this research, the NASA Astrophysics Data System, and the SIMBAD and VIZIER services operated by CDS Strasbourg.

References

Bruch, A., *et al.* 1987, *Astron. Astrophys., Suppl. Ser.*, **70**, 481.

Dymock, R., and Miles, R. 2009, *J. Brit. Astron. Assoc.*, **119**, 149.

Hoffmeister, C. 1965, *Inf. Bull. Var. Stars*, No. 80.

Kato, T., *et al.* 2009, *Publ. Astron. Soc. Japan*, **61**, 395.

Kholopov, P. N., *et al.* 1985, *General Catalogue of Variable Stars*, 4th ed., Moscow.

Krajci, T. 2005, cvnet-outburst 422, http://tech.groups.yahoo.com/group/cvnet-outburst/message/422

Liu, W., *et al.* 1999, *Astrophys. J., Suppl. Ser.*, **122**, 243.

Muyllaert, E. 2009, baavss-alert 1995, http://tech.groups.yahoo.com/group/baavss-alert/message/1995

Schmeer, P. 2005, vsnet-alert 8524, http://ooruri.kusastro.kyoto-u.ac.jp/pipermail/vsnet-alert/2005- July/000143.html

Skrutskie, M. F., *et al.* 2006, *Astron. J.,* **131**, 1163.

University of Cambridge, Institute for Astronomy 2005, *Carlsberg Meridian Catalogue 14* (CMC14), http://www.ast.cam.ac.uk/~dwe/SRF/cmc14.html

Vanmunster, T. 2007, PERANSO period analysis software, http://www.peranso.com

Watson, C. L., Henden, A. A., and Price, A. 2007, International Variable Star Index (VSX), http://www.aavso.org/vsx/*, J. Amer. Assoc. Var. Star Obs.*, **35**, 414.

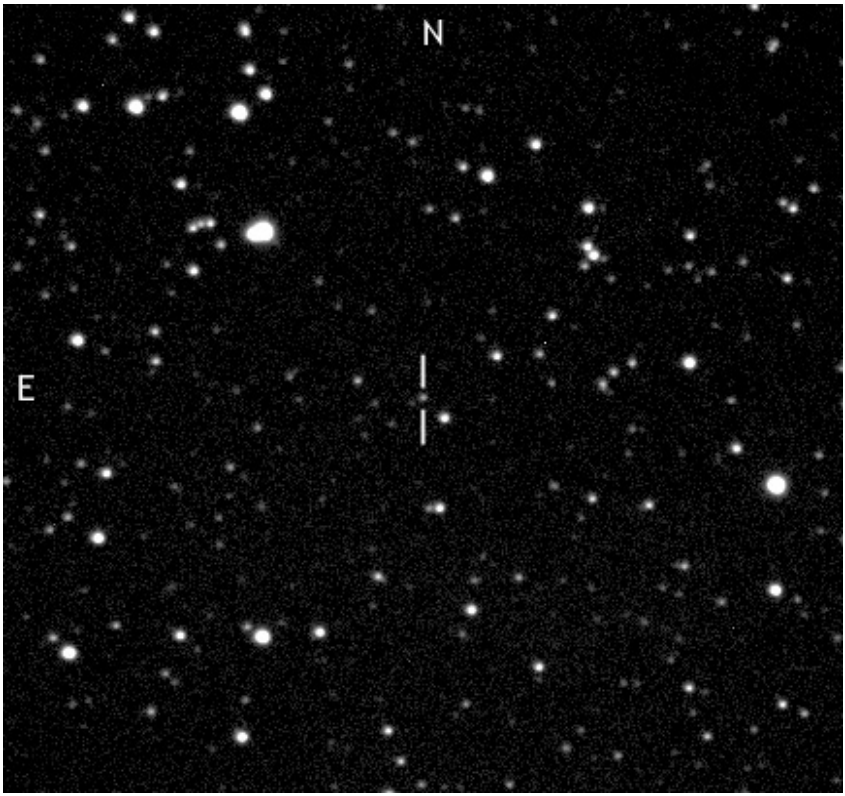

Figure 1. Image of the field around IL Vul taken on 2009 July 9.984 UT—10 × 10 arcmin.

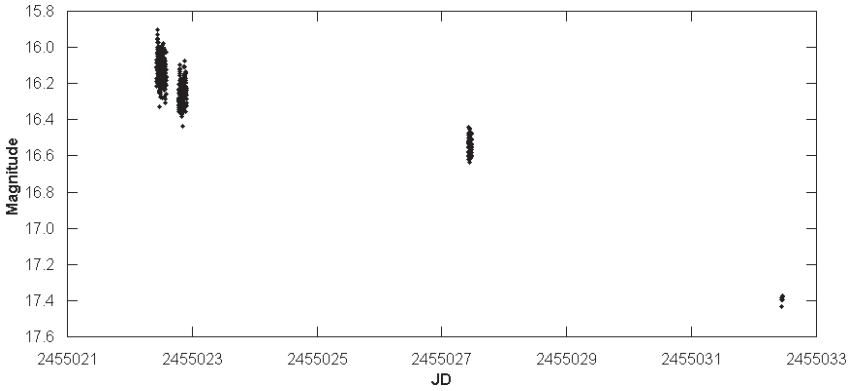

Figure 2. Light curve of the 2009 July superoutburst of IL Vul.

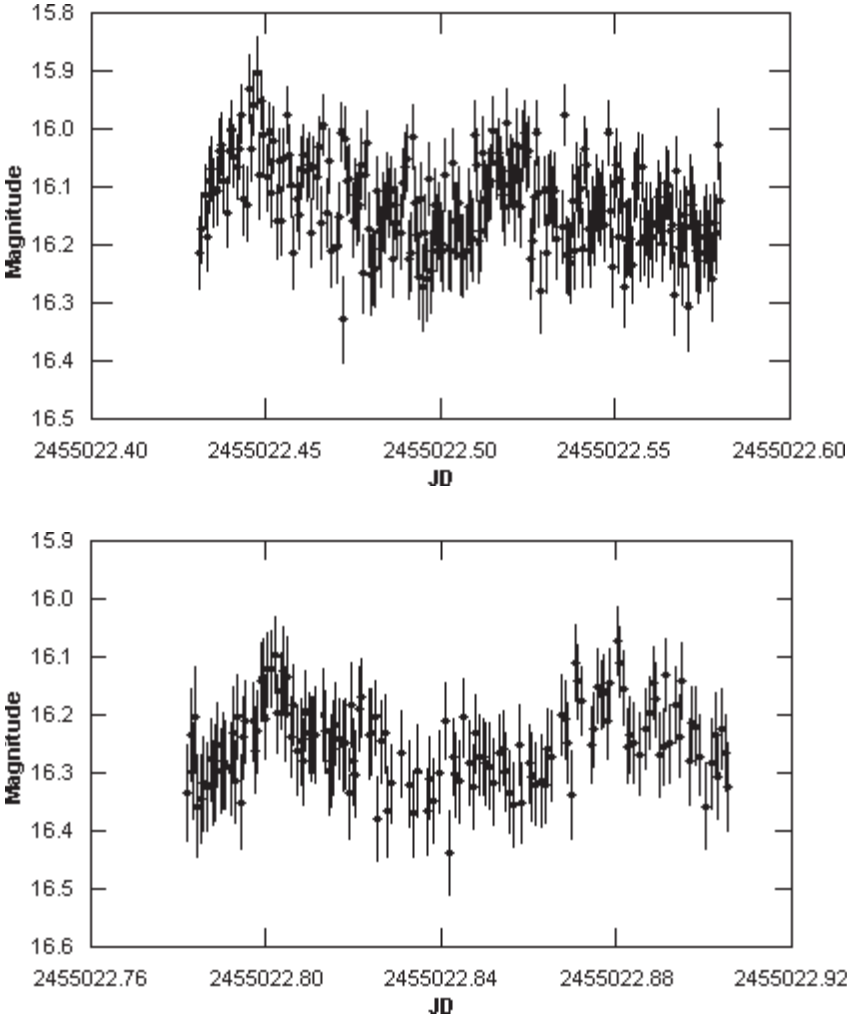

Figure 3. Superhumps recorded on 2009 July 9 (top) and 10 (bottom).

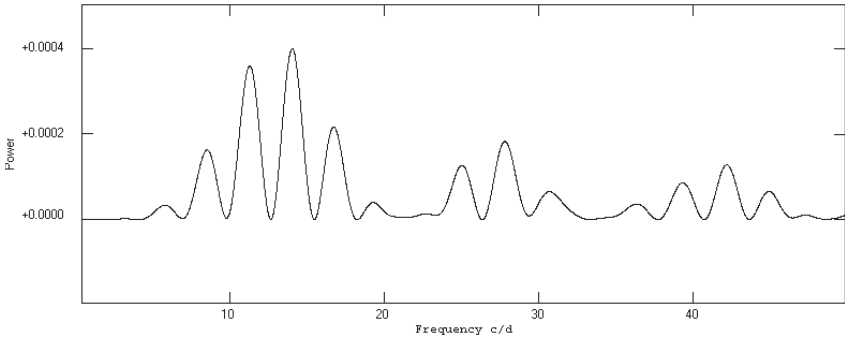

Figure 4. Discrete Fourier Transform power spectrum of data from 2009 July 9 and 10.

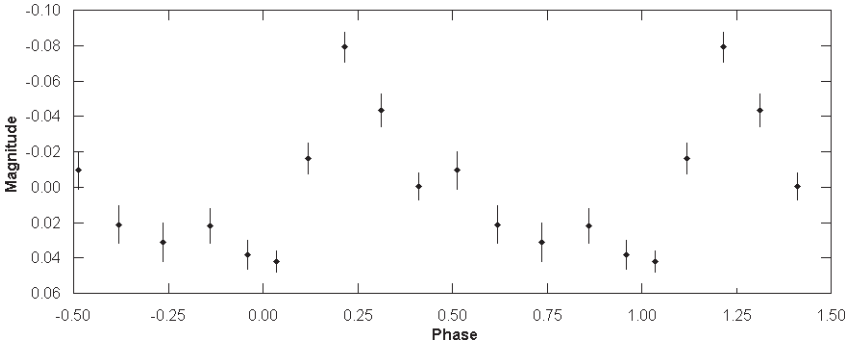

Figure 5. Phase plot for a period of 0.071 day.

NSV 19431 and YY Centauri—Two Mira Variables

Peter F. Williams
3 McAuley Close, Heathcote NSW 2233, Australia; pfwilliams@onaustralia.com.au

Received September 28, 2009; revised February 22, 2010; accepted February 22, 2010

Abstract Visual observations of NSV 19431 and YY Cen spanning the twenty-eight years 1980 through 2007 are discussed. These show NSV 19431 is a Mira star of mean period of 298.1 days and visual brightness range of 10.8 to fainter than 15.0. Elements for determining the dates of maximum brightness are JD 2447700 ± 298.1 days (±10 days). The O–C diagram shows what appear to be random cycle-to-cycle fluctuations with a current mean cycle of 298.1 days, evident from the maximum of JD 2447700 (1989).

YY Cen is a Mira star of mean period 371.3 days and brightness range 10.6 to fainter than 15.0. On at least three occasions during this twenty-eight years YY Cen has experienced individual cycles that are significantly longer or shorter than the 371.3-day mean period. Subsequent cycles remain close to the mean period but there is a resulting clear shift in the O–C values. Elements for predicting the dates of maximum brightness are JD2446897 ± 371.3 days (±10 days), but they should be treated with some caution due to the random instances of long/short cycles observed thus far and which may prove to be a long term characteristic of YY Cen.

1. Introduction

During the course of determining the *V*-magnitude comparison star sequence for the Mira star YY Cen at the Auckland Observatory, a new large amplitude variable star was discovered (Bateson *et al.* 1979). This new variable was plotted on Chart 449 of the Variable Star Section, Royal Astronomical Society of New Zealand (VSS RASNZ; Bateson *et al.* 1979). It was referred to as YYA Cen within the database of the VSS RASNZ and as 1230–54B (Var SE) in the AAVSO database. It subsequently received the designation NSV 19431 (Samus 2010) and listed as a possible Mira star of maximum *V*-magnitude 12.7 and position as $23^h\ 36^m\ 20.7^s$ –54° 36' 38" (J2000). Chart 449 of the VSS RASNZ with the *V*-magnitudes shown thereon has been used for these observations.

YY Cen appears in the *General Catalogue of Variable Stars* (GCVS; Kholopov *et al.* 1985; Samus 2010) as a probable Mira variable of photographic range 12.5 to fainter than 14.3 but no period is indicated. It is located at $12^h\ 35^m\ 41.8^s$ –54° 34' 52" (J2000).

NSV 19431 and YY Cen are both conveniently located within the same telescopic field of view. Each has been observed on a regular basis by the author during the twenty-eight year interval 1980 through 2007.

The normal observing season is February through August with less frequent observation outside these months when the field is only accessible in the morning sky. A seasonal gap is therefore present in both sets of data.

Observations for each star were plotted on large scale light curves with a scale typically near 1mm equal to 4.7 days and the dates of maximum brightness measured directly from the curve at the mid-point between the rise and fall branches of the curve, typically one magnitude below the maximum of the smoothed curve. A symmetrical shape to the light curve was assumed; it appeared appropriate in the case of both YY Cen and NSV 19431. This procedure also eliminated the necessity for a high density of data points around the time of maximum, providing for an internally consistent set of dates. Where an individual cycle had insufficient observations, a mean light curve was overlaid on the available observations as a "best fit" and the date of maximum measured from this. For both stars the errors in the derived dates are believed to be of the order of ±3 days, based on the scale of the light curves from which the dates were measured.

The observed characteristics of NSV 19431 and YY Cen are discussed below.

2. Discussion

2.1. NSV 19431

As described below, a mean period of 298.1 days has been determined with individual cycles ranging from 254 to 327 days. At maximum brightness NSV 19431 ranges between magnitude 10.8 and 12.8 and falls to fainter than 15.0 at minimum.

Details of the observed maxima are shown in Table 1. Where column 1 lists the cycle number relative to the well observed maximum of JD 2447700, column 2 the date of maximum, and column 3 the reliability of this date, weighted 1 = good for well observed cycles, to 3 = poor where only the rise or fall, or part of each, was recorded and the determined date of maximum is based largely on overlay of the mean light curve (and takes into account the upper limits where the variable was invisible, and which placed constraints on the derived dates). Column 4 lists the interval to the following maximum, with values shown in brackets where one or more cycle has passed unobserved. Column 5 is the maximum magnitude, column 6 the calculated date of maximum relative to the epoch of JD 2447700, and column 7 the O–C value based on the derived mean period of 298.1 days.

A number of O–C diagrams were constructed for various periods between 296 and 302 days but none of these was considered truly reliable over the full 33 observed cycles. Mean periods were then determined over four portions of the overall interval. Here, cycles –11 to 0(E) gave a mean of 302.0 days, cycles 1 to 11 gave 298.5 days, cycles 12 to 18 gave 299.7 days, and the overlapping cycles 16 to 22 gave 296.5 days.

This merely demonstrates the instability of pulsations in NSV 19431, a well-known feature of the Mira-type stars. Here, the changing slope of the O–C

curve may simply represent random cycle-to-cycle fluctuations in the observed period, as first described by Eddington and Plakidis (1929) and further discussed by Percy and Colivas (1999) and Templeton *et al.* (2005). It is unfortunate that NSV 19431 had not been noted earlier and under observation over a longer time span to allow for better study of this feature.

The O–C diagram shown in Figure 1 is based on the period 298.1 days, representing the mean period of cycles 0 through 22; the earlier cycles are clearly of longer mean length.

The variations in the O–C data suggest NSV 19421 may be an interesting star for ongoing study, and observers are therefore encouraged to obtain brightness measurements on a regular basis.

Nothing can be said about the behavior of NSV 19431 when at minimum but the shape of the light curve suggests it falls well below the threshold magnitude 15 of the telescopes used. The observed upper limits, where the variable star was invisible and typically fainter than visual magnitude 14 to 15, do, however, exclude a cycle length shorter than the value derived here.

Elements for determining the dates of maximum brightness are currently satisfied by JD 2447700 ± 298.1 days (±10 days).

2.2. YY Centauri

YY Cen is found to be a Mira variable of mean period 371.3 days over the 27 observed cycles spanning 10,024 days, with maximum visual brightness ranging between 10.5 and 12.0. During the twenty-eight years 1980 through 2007 individual cycles ranged between 345 and 397 days, with unusually short or long cycles resulting in a marked shift in the O–C dates of subsequent maxima.

Details of the 28 observed cycles are listed in Table 2 in the same format as given for NSV 19431.

The resulting O–C diagram is shown as Figure 2. Here, the cycles of markedly longer or shorter period are marked and clearly indicate turning points in the O–C curve, as would be expected. As is the case with NSV 19431, it is unfortunate that the available observations do not cover a much longer time span to allow for a better understanding of this star's behavior. Observers are therefore encouraged to monitor YY Cen on a regular basis.

For the purposes of determining the dates of maximum brightness the elements are JD 2446987 ± 371.3 days (±10 days). This is, however, subject to some uncertainty due to the demonstrated behavior of this star which may result in substantial shift in the O–C values.

No information is available regarding minimum brightness as YY Cen falls below the limiting magnitude of the telescopes used. The upper limits when the variable is invisible do exclude a period shorter than that derived here.

3. Conclusion

Both NSV 19431 and YY Cen are shown to be typical Mira type variables. Elements for determining the dates of maximum brightness of NSV 19431 are JD 2447700 ± 298.1 days (±10 days). At maximum it ranges between visual magnitude 10.8 and 12.8 and falls fainter than 15.0 at minimum.

The dates of maximum brightness for YY Cen are determined by the elements JD 2446987 ± 371.3 days (±10 days). It has a maximum visual brightness ranging between 10.5 and 12.0 and falls below magnitude 15 at minimum.

Both NSV 19431 and YY Cen have shown changes in their O–C values that appear to be random cycle-to-cycle variations and both stars may be interesting objects for ongoing study.

References

Bateson, F. M., Morel, M., and Winnett, R. 1979, *Charts for Southern Variables, Series 10*, Astronomical Research, Ltd, Tauranga, New Zealand.

Eddington, A. S., and Plakidis, S. 1929, *Mon. Not. Roy. Astron. Soc.*, **90**, 65.

Kholopov, P. N., *et al.* 1985, *General Catalogue of Variable Stars*, 4th ed., Moscow.

Percy, J. R., and Colivas, T. 1999, *Publ. Astron. Soc. Pacific*, **111**, 94.

Samus, N. N. 2010, *General Catalogue of Variable Stars*, http://www.sai.msu.su/groups/cluster/gcvs/gcvs/

Templeton, M. R., Mattei, J. A., and Willson, L. A. 2005, *Astron. J.*, **130**, 776.

Table 1. Details of observed cycles for NSV 19431, 1980 through 2007.

Cycle	*JD 2400000+*	*Weight*	*Interval*	*Mag.*	*C (298.1) 2400000+*	*O–C*
–11	44378	1	239	11.4	44420.9	–42.9
–10	44667	1	306	12.0	44719.0	–52.0
–9	44973	2	(593)	11.5	45017.1	–44.1
–7	45566	1	327	12.8	45613.3	–47.3
–6	45893	1	292	11.3	45911.4	–18.1
–5	46185	2	(593)	11.6	46209.5	–24.5
–3	46778	2	(625)	11.6	46805.7	–27.7
–1	47403	1	297	11.4	47401.9	–1.1
0	47700	1	296	11.6	E	E
1	47996	1	284	11.5	47998.1	–2.1
2	48280	3	(943)	11.5	48296.2	–16.2
5	48223	1	275	11.6	49190.5	+32.5
6	49498	1	306	11.6	49488.6	+9.4
7	49804	3	(1179)	10.8	49786.7	+17.3
11	50983	1	306	11.6	50979.1	+3.9
12	51289	1	298	11.6	51277.2	+11.8
13	51587	2	(638)	11.9	51575.3	+11.7
15	52225	1	254	11.5	52171.5	+53.5
16	52479	1	298	11.4	52469.6	+9.4
17	52777	1	304	11.4	52767.7	+9.3
18	53081	3	(881)	13.0	53065.8	+15.2
21	53962	1	296	11.3	53960.1	+1.9
22	54258	1	—	12.1	54258.2	–0.2

(Weight 1 = best, 3 = worst)

Table 2. Details of observed cycles for YY Cen, 1980 through 2007.

Cycle	*JD 2400000+*	*Weight*	*Interval*	*Mag.*	*C (371.3) 2400000+*	*O–C*
–7	44304	2	374	10.6	44297.9	+6.1
–6	44678	1	379	11.6	44669.2	+8.8
–5	45057	1	379	10.8	45040.5	+16.5
–4	45436	2	359	12.0	45411.8	+24.2
–3	45795	1	369	10.8	45783.1	+11.9
–2	46164	1	388	11.4	46154.4	+9.6
–1	46552	1	345	11.0	46525.7	+26.3
0	46897	1	379	11.5	E	E
1	47276	1	379	11.0	47268.3	+7.7
2	47655	2	354	10.7	48639.6	+15.4
3	48009	1	369	11.4	48010.9	–1.9
4	48378	1	367	11.0	48382.2	–4.2
5	48745	1	364	10.8	48753.5	–8.5
6	49109	1	364	10.6	49124.8	–15.8
7	49473	1	372	10.8	49496.1	–23.1
8	49845	2	362	10.7	49867.4	–22.4
9	50207	1	364	12.0	50238.7	–31.7
10	50571	2	384	10.6	50610.0	–39.0
11	50955	1	371	10.8	50981.3	–26.3
12	51326	1	367	10.7	51352.6	–26.6
13	51693	1	378	10.6	51723.9	–30.9
14	52071	1	374	11.3	52095.2	–24.4
15	52445	1	369	10.6	52466.5	–21.5
16	52814	1	379	10.8	52837.8	–23.8
17	53193	1	397	11.0	53209.1	–16.1
18	53590	1	367	11.3	53580.4	+9.6
19	53957	1	371	11.2	53951.7	+5.3
20	54328	2	—	10.8	54323.0	+5.0

(Weight 1 = best, 3 = worst)

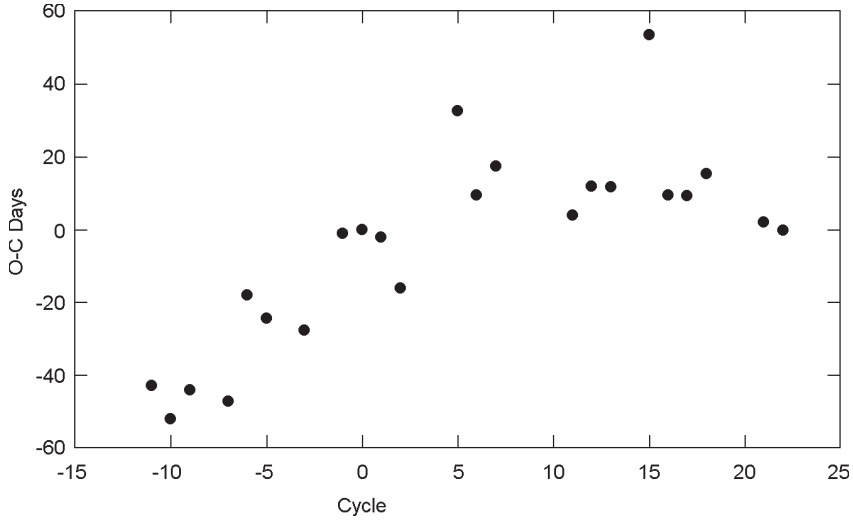

Figure 1. O–C diagram for NSV 19431, period 298.1 days.

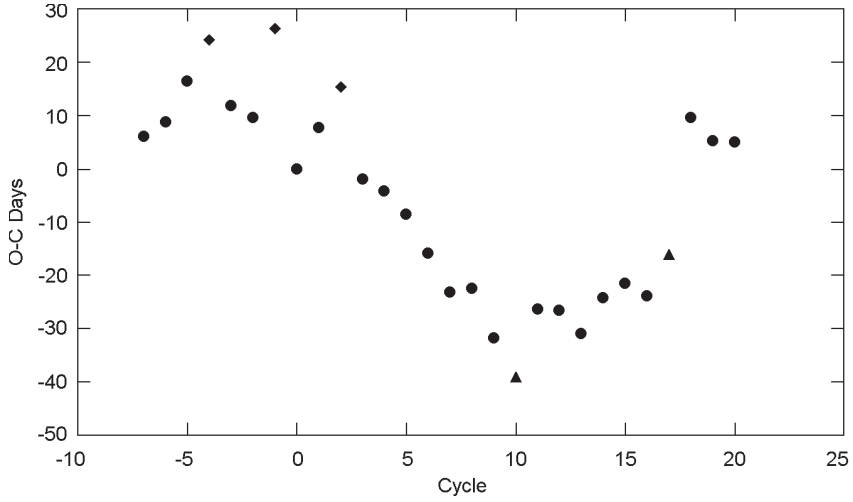

Figure 2. O–C diagram for YY Cen, period 371.3 days. Circles, near average cycle; diamonds, short cycle; triangles, long cycle.

Two New Eclipsing Binary Systems: GSC 1393-1461 and GSC 2449-0654, and One New Flare Star: GSC 5604-0255

P. V. Sada
Departamento de Física y Matemáticas, Universidad de Monterrey, Av. I. Morones Prieto 4500 Pte., San Pedro Garza García, N.L. 66238, México; pvaldes@udem.edu.mx

Received October 29, 2009; revised December 15, 2009, Accepted December 23, 2009

Abstract We introduce three new variable stars discovered during asteroid photometry. This includes two new eclipsing binary stars, GSC 1393-1461 (P = 0.311145d) and GSC 2449-0654 (P = 0.343802d), and one new flare star: GSC 5604-0255, which had a 35% ± 2% intensity increase with a decay half-life of 20 ± 1 minutes. This paper presents light curves along with basic models and analysis of the data.

1. Introduction

The Universidad de Monterrey Observatory (MPC 720) in Mexico has been making photometric observations of asteroids since 2000 in order to derive the rotation periods from their light curves. At times variable stars have been detected in the asteroid field-of-view in the process of selecting suitable comparison stars for differential photometry. Some of these have been previously unknown variables and were targeted for follow-up studies. Short period variable stars are particularly suited for discovery using this method, since each field is observed over the span of only one night as part of the asteroid program. The current paper presents observations and analysis of three rapid variables discovered in this way, including two short period variable stars and one flare star. The short period variables are the stars GSC 1393-1461 and GSC 2449-0654, and the flare star is GSC 5604-0255.

2. Observations

The Universidad de Monterrey Observatory uses an SBIG STL-1301E/LE CCD camera attached to a 36-cm SCT inside a 2-m automated dome. The discovery observations were made unfiltered as this is our normal mode for asteroid photometry. The flare star was discovered in unfiltered images on one night only, hence the images are unfiltered. Follow-up observations of the two short period variable stars were made in the V and R_c bandpasses using filters according to the Bessell prescription for the Johnson Cousins system (Persha 1999 and references therein). All images were acquired in 2×2 binning mode, giving an image scale of ~1 arcsec/pixel over a 21.1×16.9 arcmin field of view.

Exposures ranged from 120 to 240 seconds, depending on the particular filter used. Typical 1-sigma uncertainties for observations of ~14th magnitude stars, like the ones presented here, are ~0.007 magnitude for unfiltered exposures and ~0.011 magnitude for filtered ones.

Table 1 lists a log of observations which includes basic information for the stars and observing details such as filter and number of photometric measurements obtained. P_{mag} is the photographic magnitude, *JD* is the date of the observation, *Filters* are the bandpasses used during the observing session, and N_{obs} the number of photometric measurements obtained per night. *R.A., Dec.,* and P_{mag} are taken from the GSC-ACT star catalog. The filter labeled "clear" indicates that no filter was used; hence the effective wavelength is that of the CCD response, about 645 nm, which is similar to the effective wavelength of the R_c filter. Photometric measurements were made using differential photometry against other stars in the same image. The same comparison stars were used in each frame, hence only small residual corrections were needed to combine the light curves obtained from observations made on different nights. All photometry was done using custom applications written in IDL.

3. Analysis

3.1. GSC 1393-1461 and GSC 2449-0654

3.1.1. Period analysis

For the eclipsing binary stars the best-fit period was obtained by computing the power spectrum of the time series of data (Scargle 1982; Horne and Baliunas 1986). The linear ephemeris equations were determined to be:

GSC 1393-1461 Min I (hel.) = 2454473.9731 + 0.311145 E
$\pm 0.0015 \pm 0.000001$

GSC 2449-0654 Min I (hel.) = 2454478.7207 + 0.343802 E
$\pm 0.0015 \pm 0.000001$

3.1.2. Light Curve Analysis

Light curves for the two eclipsing binary stars are presented in Figure 1. The individual observations are represented by dots and the smooth curves show preliminary model fits to the data. These models were constructed by varying the main parameters in the commercially available program BINARY MAKER 3.0 (Bradstreet 2005). This java-based program employs Roche geometry to accurately compute light and radial velocity curves and is widely used by professionals and amateurs for solving eclipsing binary light curves. The resulting model parameters are presented in Table 2. Starspots were excluded from the solution because including them in the model did not significantly change the resulting essential model parameters and only slightly improved the light curve fits. From the shape of their light curves it is clear that both are ordinary over-contact eclipsing binary systems. GSC 2449-0654 in particular was best modeled by a

system of two stars of equal mass, while GSC 1393-1416 required a mass ratio of 1.80 ± 0.10 to produce the best fitting model.

3.2. GSC 5604-0255

We were fortunate to register a full flare episode for this star during our five-hour observing period. The star increased in brightness by 35% ± 2% in the time span of three two-minute exposures (~7 minutes including download time) beginning at JDH 2454617.717, and then proceeded to decrease in brightness with a decay half-life of 20 ± 1 minutes. Figure 2 shows the flare star observations (symbols) and the model fit (curve). Note that the brightness of the star did not decrease to its pre-flare state until an additional small drop occurred at JD 2454617.815, which was ~140 minutes after outburst. The increased scatter near the beginning and end of the data results from high airmass at both ends of the observational timeline. We used a least squares technique to fit the light curve using a simple exponential function in which the peak intensity and decay rate were the parameters of the fit. The best solution was found for both parameters simultaneously since fitting the peak intensity first and then the decay rate yielded a poorer fit to the data. Points between JD 2454617.760 and JD 2454617.815 were subjectively excluded because modeling this "residual afterglow" also yielded a poorer fit to the data, and the modeling of a higher order function would have been required.

4. Conclusions

The asteroid light curve observing program at the Universidad de Monterrey Observatory has been successful in identifying previously unknown short-period variable stars. In this paper we presented a preliminary analysis of three such objects. The flare star GSC 5604-0255 was observed through a complete flare event, including pre-flare baseline observations. In addition, GSC 1393-1461 and GSC 2449-0654 were discovered to be short period over-contact binary systems. Follow-up observations allowed determination of the fundamental characteristics of both systems. Additional observations are necessary to better constrain the initial system parameters derived in this paper.

5. Acknowledgements

The author greatly appreciates the critical review, corrections, and suggestions from the referee that made the manuscript much clearer and easier to read.

References

Bradstreet, D. H. 2005, BINARY MAKER 3.0, Contact Software, Norristown, PA.
Horne, J. H., and Baliunas, S. L. 1986, *Astrophys. J.*, **302**, 757.

Persha, G. 1999, "Cousins/Bessell vs. Johnson Filter Standards", URL: http://www.company7.com/library/optec/filtermono.html.
Scargle, J. D. 1982, *Astrophys. J.*, **263**, 835.

Table 1. Basic data and observing log for the stars studied herein.

Star	*R.A. (2000)* *h m s*	*Dec. (2000)* ° ′ ″	*Pmag*	*JD*	*Filters*	*Nobs*
GSC1393-1461	08 26 16.26	+20 57 08.9	14.7	2454472	clear	115
				2454473	clear	214
				2454524	V, R_c	41, 42
				2454528	V, R_c	41, 42
				2454886	clear	151
GSC2449-0654	06 56 48.52	+36 06 50.9	13.6	2454478	clear	220
				2454503	V, R_c	50, 50
				2454522	V, R_c	38, 38
				2454523	V, R_c	36, 36
				2454885	clear	176
GSC5604-0255	15 39 28.65	–12 33 40.9	14.7	2454617	clear	124

Table 2. Model Parameters for the eclipsing binary stars.

	GSC1393-1461	*GSC2449-0654*
i	67° ± 1°	58° ± 1°
T_1	5000K (assumed)	5050K (assumed)
T_2	5600K ± 40K	5050K ± 50K
q_0 (m_1/m_2)	1.80 ± 0.10	1.00 ± 0.05
$g_1 = g_2$	0.32 (assumed)	0.32 (assumed)
fill-out–*f*	0.15 ± 0.10	0.15 ± 0.05
HJD_0	2454473.9731 (15)	2454478.7207 (15)
P	0.311145 (1) day	0.343802 (1) day

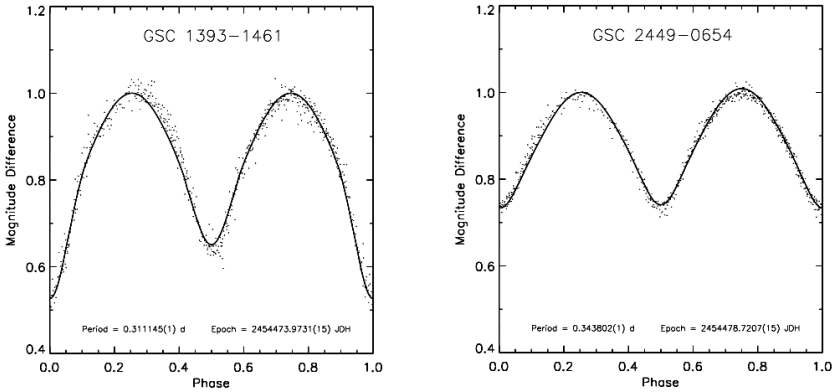

Figure 1. Light curves of the eclipsing binary stars. Data are represented by the points and the curve represents the basic models parameters from Table 2.

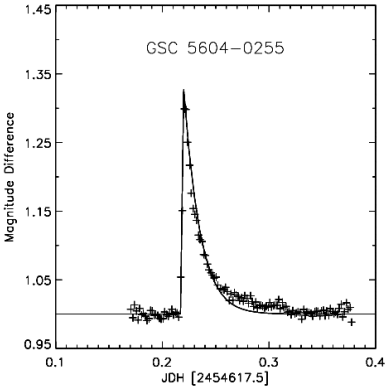

Figure 2. Registered flare for GSC5604-0255. Symbols represent data and the curve is the model described in the text.

A Unified Roche-Model Light Curve Solution for the W UMa Binary AC Bootis

Kevin B. Alton
UnderOak Observatory, 70 Summit Avenue, Cedar Knolls, NJ 07927; kbalton@optonline.net

Received June 8, 2009; revised October 8, 2009; accepted October 8, 2009

Abstract Over forty years of photoelectric light curves published by five different investigators and CCD data more recently (2006) collected in *V*- and *R*-bands were analyzed using a Roche-type geometry as implemented by the Wilson-Devinney code. This has not only resulted in a revised ephemeris and orbital period for AC Boo, but has lead to a unified light curve solution. Based upon moments of minima residual analysis, AC Boo has experienced a continual increase in orbital period for the past forty-eight years or longer, thereby suggesting an ongoing exchange of mass. Fourier analysis also revealed possible periodicity in O–C residuals which is heavily influenced by a putative sinusoidal-like wave most apparent over the past twenty years. The weight of evidence, nonetheless, points to a W-subtype W UMa system that does not necessarily vary as the result of an unseen companion (third light) but rather by spot formation on either stellar component. A series of spotted solutions, based upon a nearly symmetrical light curve collected in 1962, has provided a theoretical fit of all published photoelectric data that largely accounts for the observed peak asymmetry, unequal successive maxima, and varying depths of minima.

1. Introduction

The variability of AC Bootis was first discovered in 1955 (Geyer) and since then studied by a number investigators, including Binnendijk (1965), Mauder (1964), Mancuso *et al.* (1977, 1978), Schieven *et al.* (1983), Robb (1985), Linnell *et al.* (1990), and Hrivnak (1993). This binary system completes mutual eclipses in a little more than eight hours (0.35245 day). Typical of the W UMa class of overcontact binaries, many light curves exhibit peak asymmetry visible as unequal heights of successive maxima, which has been referred to as the O'Connell effect. AC Boo belongs to the W-type subclass of W UMa binaries, since the less massive but hotter star is occulted by the more massive but cooler component during primary minimum (Tsesevich 1956, 1959). The spectral type of the primary component is listed as F8Vn (Bilir *et al.* 2005). Our view of this system is nearly edge-on (orbital inclination ~84°), so the eclipses are total/annular.

Historically, model fits to photometric data on individual W UMa variables like AC Boo have varied significantly across investigations with respect to orbital

inclination (i), Roche potential (Ω), T_{eff}, and mass ratio (q). Since fundamental changes to these physical elements likely transpire over millennia, rather than measured in human lifetimes, the expectation is that these parameters should have remained fairly constant over just fifty-plus years of recorded photometric data. If a reference set of values can be established for i, Ω, T_1, T_2, and q, epochal variations in light curve morphology could potentially be modeled by the addition of putative spot(s) or by the presence of additional orbital mass within the gravitational influence of the binary system (also known as "third light"). Although the inspiration for this exercise with AC Boo pre-dates a recent public challenge (Ruciński *et al.* 2009) to combine light curve data extant for individual systems, the rationale is self-evident. Given the wide range of reported values for fundamental physical properties of binary star systems, there have been improbably small uncertainties established for each parameter. Public access to software applications like PHOEBE (PHysics Of Eclipsing BinariEs; Prša and Zwitter 2005), PERIOD04 (Lenz and Breger 2005), MINIMA (Nelson 2005b), and WDWINT (Nelson 2005c), has expanded the repertoire of user-friendly light curve modeling tools to amateur astronomers. For those so inclined, this greatly facilitates the retrospective analysis of published data which is the main focus of this paper. Having said that, with the advances made in affordable optics and CCD cameras, the modern amateur astronomer can also generate new research-quality light curves for variable star systems that had in the past only been within the domain of the professional community. In this regard, AC Boo is well suited for study, since this relatively bright variable (Vmag ~10) is easily within the detection limits of a consumer-grade CCD camera coupled with a telescope of modest aperture. During the late spring months, this system passes near zenith for mid-latitude observers in the Northern Hemisphere.

2. Observations and data reduction

2.1. Astrometry

Images of AC Boo were matched against the standard star fields provided in MPO CANOPUS (Minor Planet Observer 1996–2008) as described previously for SW Lac (Alton and Terrell 2006).

2.2. Photometry

CCD photometric observations of AC Boo began on 29 April 2006 with the intent of generating light curves which could be used to: 1) potentially refine the orbital period, 2) calculate an updated ephemeris, and 3) further investigate the light curve asymmetry regularly observed for this system. Equipment included a 0.2-meter catadioptric (f/6.4) reflector with an SBIG ST-402ME CCD camera mounted at primary focus. V- or R-band imaging was carried out during separate sessions through Schüler photometric filters (1.25-inch) based upon the Johnson-Cousins Bessell prescription. A more detailed description and performance characteristics of this photometric system has been described elsewhere by Alton

(2006) and Alton and Terrell (2006). Each unbinned exposure was captured over a fifteen-second period with thermoelectric cooling regulated to maintain the CCD chip 20°C below the initial ambient temperature. A typical session lasted from two to four hours, with images taken every sixty seconds. PC clock time was updated via the Internet Time Server immediately prior to each session. Image acquisition (raw lights, darks, and flats) was performed using SBIG CCDSOFT 5 while calibration and registration were accomplished with AIP4WIN (Berry and Burnell 2000). Photometric reduction with MPO CANOPUS used at least three non-varying comparison stars. Instrumental readings were not reduced to standard magnitudes before generating light curves to calculate ephemerides and orbital period. Phased differential magnitude photometric data in all passbands published by Binnendijk (1965), Mauder (1964), Mancuso *et al.* (1977, 1978), Robb (1985), and Schieven *et al.* (1983) were converted to flux ($F = 10^{-0.4*\Delta m}$) and then normalized.

2.3. Light curve analyses

Light curve modeling was performed using PHOEBE (Prša and Zwitter 2005) and WDWINT (Nelson 2005c), both of which employ the Wilson-Devinney (W-D) code (Wilson and Devinney 1971; Wilson 1979). PHOEBE is a well-designed execution of the W-D code which provides a convenient user interface. Each model fit incorporated individual observations and was not binned to normal points. SIGMA was assigned according to the standard deviation measured from the average difference in instrumental magnitude (C_{avg}) for each comparison star. For the *V* and *R* passbands, variability was typically ±0.03 magnitude. Three-dimensional representations showing the location of putative starspot(s) were rendered by BINARY MAKER 3.0 (Bradstreet and Steelman 2002).

3. Results and discussion

3.1. Astrometry

The position determined for AC Boo (Table 1) based upon the reference coordinates in the *MPO Star Catalog* (Minor Planet Observer 2008) agreed within 0.441 arcsec of right ascension or declination reported on the SIMBAD website (ICRS 2000 coordinates).

Table 1. Positions and magnitudes of AC Boo and comparison stars.

Star Identification	*R.A.* *h m s*	*Dec.* ° ′ ″	V_T *mag*	B_T *mag*
AC Boo	14 56 28.33	+46 21 44.1	10.294	10.849
TYC3474-00966-1	14 56 26.31	+46 26 51.0	9.434	9.817
TYC3474-00714-1	14 56 19.60	+46 19 08.8	12.394	12.943
TYC3474-00835-1	14 56 07.82	+46 21 26.6	11.242	11.841

3.2. Ensemble photometry

Every attempt was made to ensure that comparison stars were themselves not variable, at least over the observation time span. This was verified prior to accepting data from each session. On any night, no less than three stars from the *Tycho2 Catalogue* (Høg *et al.* 2000) were used for differential measurements. The airmass for all observations over the entire campaign ranged from 1.048 to 1.792. Plotting the difference in magnitude over time for AC Boo against the averaged magnitude for all comparisons (C_{avg}) yielded a narrow range of values with no obvious trend (Figure 1). Collectively, C_{avg} for the comparison stars did not exhibit a pattern that would otherwise suggest variability beyond experimental error (< 0.03 magnitude) in both passbands.

3.3. Folded light curve and ephemerides

Photometric readings in *V* (942) and *R* (890) passbands produced seven times of minima (ToM) which were captured during eight viewing sessions between 29 April 2006 and 17 July 2006. The Fourier analysis routine (Harris *et al.* 1989) in MPO CANOPUS provided a period solution. A ToM for the latest primary epoch was estimated by CANOPUS using the Hertzsprung method as detailed by Henden and Kaitchuck (1990). As such the linear ephemeris equation (1) was initially determined to be:

$$\text{Min I (hel.)} = 2453932.5819 + 0.352457(69)\text{E} \quad (1)$$

This orbital period based upon a limited dataset compares favorably with values reported by Binnendijk (1965), Mancuso *et al.* (1977, 1978), Schieven *et al.* (1983), Robb (1985), Linnell *et al.* (1990), and Demircan *et al.* (2003). Periodograms produced using PERANSO (Vanmunster 2005) by applying periodic orthogonals (Schwarzenberg-Czerny 1996) to fit observations and analysis-of-variance to evaluate fit quality also confirmed the period determination. ToM values for all epochs were then separately estimated by MINIMA (Nelson 2005b) using the simple mean from a suite of six different methods including parabolic fit, tracing paper, bisecting chords, Kwee and van Woerden (1956), Fourier fit, and sliding integrations (Ghedini 1981). These seven new minima along with additional published CCD observations (*IBVS* and *Var. Star Bull.* as provided in the reference list) were entered into a MICROSOFT EXCEL spreadsheet adapted from the "Eclipsing Binary O–C" files developed by Nelson (2005a). Using the following reference epoch from Kreiner (2004):

$$\text{Min I (hel.)} = 2452500.3020\ (9) + 0.3524485\ (1)\ \text{E} \quad (2)$$

new ephemerides were established for AC Boo (Table 1). Due to the complex curvilinear nature of the O–C residuals observed for at least forty-eight years (Figure 2), two separate regression analyses were performed. A revised ephemeris equation (3) based upon a linear least squares fit (Figure 3) of near term $(O–C)_1$ data from 16 Feb 2006 to 07 May 2009 was calculated:

$$\text{Min I (hel.)} = 2452499.9500\,(9) + 0.3524484\,(2)\,E \quad (3)$$

As a result of the parabolic O–C vs time relationship, updated linear elements for AC Boo may only be valid for a short time after 2009. Expanding the analysis to include O–C data starting from 18 Jan 1961 revealed a parabolic relationship (Figure 2) between daily residuals $(O–C)_1$ and time (cycle number) that could be fit by a quadratic expression (4):

$$O–C = a + bE + cE^2 \quad (4)$$

where:

$a = –0.33910 \quad \pm 0.0008$
$b = –4.6351 \times 10^{-6} \quad \pm 0.1090 \times 10^{-6}$
$c = 2.3003 \times 10^{-10} \quad \pm 0.03789 \times 10^{-10}$

This solution which is defined by an upwards parabola ($c > 0$) suggests that the period is increasing linearly with time and leads to the following quadratic ephemeris (5):

$$\text{Min I (hel.)} = 2452499.9629\,(8) + 0.3524439\,(1)\,E + 2.300\,(38) \times 10^{-10}\,E^2 \quad (5)$$

Since 1961 the orbital period rate of increase can be defined by the equation (6) below:

$$dP/dt = 2 \times (2.300 \times 10^{-10})\,(1/0.3524439)\,(86400)\,(365.25) = 0.0412\ \text{sec/yr} \quad (6)$$

Commonly observed in W UMa binary systems, orbital period increases may be associated with material transfer from the secondary to the more massive primary component. Recalculated quadratic residuals, $(O–C)_Q$, are shown in the bottom panel of Figure 2. There is a visual suggestion of a sinusoidal-like wave particularly over the past twenty years that was further examined using PERANSO Lomb-Scargle periodogram analysis (Vanmunster 2005) and discrete Fourier analysis as implemented in PERIOD04 (Lenz and Breger 2005). Both mathematical approaches are particularly effective at least squares fitting of sine waves with unevenly sampled data. The highest peak (c/d) in each power spectrum corresponded to periods ranging between $7,225 \pm 1,091$ days (PERANSO) and $7,553 \pm 658$ days (PERIOD04); peak amplitude was estimated to be ~0.009 day. Two other statistical algorithms within PERANSO yielded similar values with equal or higher error estimates. These included date compensated discrete Fourier Transform DCDFT (Ferraz-Mello 1981) and CLEANEST (Foster 1995). The sinusoidal-like fit (Figure 4) of quadratic O–C residuals between 18 Jan 1961 and 07 May 2009 is strongly influenced by Time of Minimum (ToM) values collected over the past twenty years. Given the scatter in residuals prior to cycle –14,000, it will probably require at least twenty years of additional data to confirm this putative periodicity with statistical certainty. Whether this behavior is real, associated with a third body, or some other cyclic phenomena such as the "Applegate mechanism" (Applegate 1992), remains to be determined. Applegate

proposed that a late-type short-period binary system consisting of at least one star with a convective envelope would exhibit a magnetic activity cycle analogous to the eleven-year solar sunspot cycle. Variable tidal effects (physical distortion) would be observed as changes in the orbital period of the binary system which may be regular but not exactly periodic. The presence of a third body has been proposed by Hrivnak (1993) and Linnell (1991), based on radial velocity data collected around cycle –13,000 (est. 1989). Collectively, however, despite the putative presence of a sinusoidal-like feature over the past twenty years, there still is not enough evidence from the analysis of O–C vs time plots to argue unequivocally for persistent periodicity, a prerequisite for third light effects. In addition, it should be noted that no improvement in any light curve model fit using W-D code (Wilson and Devinney 1971; Wilson 1979) could be obtained with a non-zero value for third light (l_3); differential corrections including l_3 as a variable did not lead to a statistically significant non-zero solution.

With regard to the 2006 photometric readings, folded light curves incorporating all observations (Figure 5) in *V*- and *R*-passbands show that both minima are separated by 0.5 phase, an observation consistent with a circular orbit. Although the light curve in *R* has a gap at Max I due to poor weather, asymmetry in maximum light (Max I > Max II) is clearly seen in *V*-band. Both passbands exhibit unequal depths at minima (Min I < Min II). With the exception of the 1962 light curves (*B* and *V*) reported by Binnendijk (1965) which have near equal maximum light and matching minima, all others produced since then have had asymmetric maxima along with near equal minima (Mancuso *et al.* 1977; Schieven *et al.* 1983), or unequal minima (Binnendijk 1965; Mauder 1964; Robb 1985; and the present paper).

A plausible explanation for this variability attributed to the O'Connell effect might involve the changing presence of starspot(s) on one or more binary components and is explored in more detail below. A recent publication by Wilsey and Beaky (2009) provides an excellent overview of the O'Connell effect in eclipsing binary systems. Therein a number of theoretical models which could explain the diagnostic out-of-eclipse asymmetry at maximum light are discussed. The most thoroughly published approach to model this effect has been to invoke the presence of starspot(s). Analogous to differential rotation on the Sun, localized magnetic disturbances on W UMa binaries can block convective motion towards the surface and result in cool starspots which may survive for a protracted period of time (Berdyugina 2005). Alternatively, hot spots akin to solar flares may also appear but can be expected to evolve in a more transient manner. Both phenomena disturb luminous homogeneity and can produce asymmetric features on a light curve. The W-D code has been designed to accommodate the introduction of idealized circular starspots to improve the model fit, a software feature not implemented for any of the alternative theories which account for light curve asymmetry. Not unexpectedly, this limitation which fails to address other sources of light curve variability has perhaps led to overuse of starspot modeling. As mentioned earlier, a parabolic relationship (Figure 2) between daily residuals and time is often

attributed to conservative mass transfer. This sets the stage for an alternative theory in which a superluminous spot is produced by the impact of a streaming flow of gaseous matter through L1, the inner Lagrangian point. If the hotspot is offset from the central axis (not at 90° co-latitude, 0° longitude in W-D parlance), then a difference in luminosity can be observed during Max I or Max II. Taking a sneak look ahead, this scenario is suggested by the spotted W-D model fit of the 2006 light curve (Figure 15). Another less conventional explanation for the O'Connell effect involves a variation on the gas-stream impact theory in which the two components sweep through and capture matter in cloud of circumstellar material, thereby converting kinetic energy into a thermal glow on each leading hemisphere (Liu and Yang 2003). It remains to be seen whether this explanation will be supported by spectroscopic evidence, since an increased incidence of emission lines is expected along with a difference in spectra captured at Min I and Min II. Still another theory invokes the presence of an asymmetrically dense circumbinary cloud of gas and/or dust which directly attenuates light at different orbital phases (Lehmann and Mkrtichian 2004). Finally Zhou and Leung (1990) proposed that the asymmetric deflection of an incoming stream of matter due to Coriolis forces can account for unequal light curve maxima in an over-contact binary. To date, no one of these alternative theories has accumulated sufficient experimental evidence to completely supplant the presence of starspot(s) as the most viable explanation for the O'Connell effect.

3.4. Roche modeling and light curve analyses

Model fits to photometric data from individual W UMa variables like AC Boo vary significantly in the literature with respect to orbital inclination (i), Roche potential (Ω), T_{eff}, and mass ratio (q). Since these basic physical elements likely change over millennia, their individual reported uncertainties are unrealistically small. Being nearly symmetrical, the 1962 light curves from Binnendijk (1965) offer an opportunity to create a reference set of values for i, Ω, T_1, T_2, and q. Thereafter, epochal variations in light curve morphology could potentially be explained by additional orbital mass within the gravitational influence of the binary system (also known as "third light") or the presence of putative spot(s).

For overcontact binary systems of the W UMa type, W-D light curve solutions generally employ "mode 3" (a documented feature of the W-D code) with synchronous rotation and circular orbits. In this case, however, the "overcontact binary but not in thermal contact" option in PHOEBE yielded the best model fits. Since AC Boo has a convective envelope ($T_{eff} < 7500$ K), values for bolometric albedo (0.5) and gravity darkening exponents (0.32) were based on theoretical considerations described by Ruciński (1969) and Lucy (1967), respectively. Logarithmic limb darkening coefficients for both stars were interpolated within PHOEBE according to van Hamme (1993) with any change in temperature. AC Boo conforms to the W-subtype where the less massive but hotter star is eclipsed at primary minimum. Although the secondary and less-massive star has the higher

surface temperature, it nonetheless contributes less to the overall luminosity of this binary system due to its smaller size. Therefore, T_{eff} for the primary (T_1) was set equal to 6252 K, based on tabulated values (de Jager and Nieuwenhuijzen 1987) for an F8 main sequence dwarf star. Initial attempts to obtain a light curve fit involved adjustment of parameters for the mean effective temperature of the secondary (T_2), orbital inclination (i), mass ratio (q), bandpass-specific luminosity of the primary (L_1), and common envelope surface potential ($\Omega_1 = \Omega_2$). Once an approximate fit was obtained, differential corrections (DC) were applied simultaneously to photometric data in all filters. To alleviate strong correlations, the method of multiple subsets (Wilson and Biermann 1976) was used only when necessary to reach convergence.

3.4.1. Binnendijk 1962 light curves (*B* and *V*)

Although a spectroscopic mass ratio ($q = 0.41$) for AC Boo was determined by Hrivnak (1993), this value ultimately led to unrealistically complex fits when all light curves were considered. Fortunately, AC Boo exhibits total/annular eclipses, a pre-condition to obtaining a robust value for q by photometric means (Wilson 1994; Terrell and Wilson 2005). A new search for q was initiated by allowing this physical element to vary freely also with i, Ω, and T_2 during DC iterations. Simultaneously in both passbands, an excellent fit quickly converged at $q \sim 0.31$, so this parameter was investigated further under more controlled conditions. Mass ratio (q) was fixed over a range of 0.21 to 0.5 and the free model parameters (i, Ω, and T_2) allowed to converge. The response curve generated by plotting χ^2 as a function of the putative mass ratio showed a minimum between 0.30 and 0.32 (Figure 6). This value was further refined ($q = 0.306$) and thereafter used as the de facto mass ratio for modeling AC Boo. It should be noted that a very similar estimate for q had been previously reported by Mancuso *et al.* (1978) and Schieven *et al.* (1983). A comparison of light curves (Figure 7) from 0.28 to 0.41q reveals the sensitivity to mass ratio in achieving good model prediction during each eclipse. All that remained for this idealized light curve was to determine i, Ω, and T_2 by DC with fixed values for q and T_1. Final physical and geometrical elements from modeling the 1962 light curves for AC Boo are summarized in Table 2; synthetic light curves are illustrated in Figure 8.

3.4.2. Binnendijk 1963 light curves (*B* and *V*)

Not unexpectedly, the exact light curve solution for the 1962 data discussed above did not provide a best fit for AC Boo light curves produced before and thereafter. While trying to explain perturbations in radial velocity data, Hrivnak (1993) points to the possibility of a third body in the AC Boo system. In an earlier study reported by Linnell (1991), light curve data (which were not available for further analysis) required the introduction of 8% third light to obtain an accurate Roche model fit. Contrary to these assumptions, O–C residuals calculated from time-of-minima data which stretch back over forty-eight years do not exhibit the strict sinusoidal periodicity that one would expect from an orbiting third body

(Budding and Demircan 2007). Therefore, a strategy to build a Roche model was based on the premise that asymmetric maxima and/or unequal minima observed for AC Boo arise from starspot(s) on either component. BINARYMAKER 3 enabled visualization of spot placement so that combinations of A_S, Θ, ϕ, and r_S could be tested prior to final optimization with PHOEBE and WDWINT. Concerns regarding the use of starspots to minimize residuals during light curve synthesis have been well documented (Berdyugina 2005). Consequently, every effort was made to minimize the number of spots used to best fit each light curve. In some cases, due to the significant variability associated with each epoch two spots were required; the 1963 photometric readings from AC Boo were no exception in this regard. Results from modeling these light curves are summarized in Table 2 and illustrated in Figure 9. As can also be seen in subsequent light curve fits from four other epochs, a cool spot on the more massive star (Figure 15) which is exposed during primary eclipse serves to deepen Min I. In a similar, but opposing fashion, a hot spot located on the smaller companion body slightly brightened Min II during transit in the 1963 dataset.

3.4.3. Mauder 1961 light curves (*B* and *V*)

Light curves from Mauder (1964) were only available in graphical form, so photometric data (Δ mag) in *B*- and *V*-passbands were extracted using Dexter (Demleitner *et al.* 2001), a JAVA applet which allows the user to digitize a plot by creating an x-y coordinate system and then positioning a marker on each datum point. This utility is available on the NASA Astrophysics Data System website (http://adswww.harvard.edu/index.html) and can be directly invoked with GIF scanned articles. Physical and geometrical elements garnered from modeling these 1961 light curves for AC Boo are summarized in Table 2. Starspot locations (co-latitude and longitude) which improved the Roche model fit for these 1961 light curves from Mauder (1964) were very similar to those employed for the 1963 data acquired by Binnendijk (1965). With some exceptions discussed later, there was a tendency for maximum light after the secondary minimum to exhibit greater variability with transient excursions suggestive of flare activity (Figure 10).

3.4.4. Mancuso 1972 and 1973 light curves (*V*)

The results from modeling these photoelectrically derived light curves for AC Boo are summarized in Table 2 and plotted in Figure 11. As with previous light curves covering consecutive years (1961–1963), considerable differences were observed between 1972 and 1973. Most notably in 1973, maximum light appeared in the first quadrature, a feature shared only with the 1984 and 2006 light curves. In both Mancuso light curves the model supported placement of a subluminous spot on the more massive star (longitude = 180°) which served to deepen the primary minimum. Mancuso *et al.* (1978) reported for the first time geometric and physical elements for AC Boo estimated from a Roche-based model (Wilson and Devinney 1971). Given the assumptions and model limitations at that time, direct comparisons reveal values for *i* (85.47°), T_1 (5830–6017 K),

T_2 (6100 K), and q (0.28) that are reasonably close to those calculated herein (Table 2) using PHOEBE.

3.4.5. Schieven 1982 light curves (*U*, *B*, and *V*)

Arguably, upon first inspection (Figure 12), a case can be made that the light curves produced with *B* and *V* filters are equivalent from a standpoint of symmetry, maximum light, and depth of minima when compared to those generated in 1962 (Figure 8) by Binnendijk (1965). It should be pointed out that each plotted value represents the mean of four determinations, so that unlike in 1962, some of the variability has been smoothed out in the 1982 light curves. Successive minima appear nearly equal in depth across all passbands. However, without a hot starspot (Figure 15) positioned on the secondary star, a less than optimal fit to the Roche model was obtained in *B*- and *U*-passbands. This was particularly evident in the first quadrature following primary minimum. Schieven *et al.* (1983) only provided a partial list of physical elements determined from light curve synthesis. Notably, values for q (0.28–0.31) and i (82.6°–84.0°) are very consistent with findings reported herein (Table 2).

3.4.6. Robb 1984 light curves (*U*, *B*, and *V*)

As with Mauder (1964), AC Boo light curves produced by Robb (1985) were only available in a figure from a scanned copy of their publication. Photoelectric data (Δ mag) in *U*-, *B*-, and *V*-passbands were extracted on-line as described earlier using Dexter (Demleitner *et al.* 2001) and then converted to flux. The results from modeling these data are summarized in Table 2 and shown in Figure 13. Due to significant variability and frequent gaps in the data, an acceptable model fit for these light curves proved to be a challenge. Nonetheless, a reasonable fit was found by positioning a cool spot on the primary constituent (Figure 15).

3.4.7. Light curves (*V* and *R*) from 2006 study

Physical and geometric elements used and estimated in modeling these CCD observations are summarized in Table 2. Unequal minima, very apparent at visible wavelengths (Figure 14), were closer in depth as compared to those measured in *R*-passband. Due to uncooperative weather, a gap around maximum light still remained in the *R*-filtered dataset after the seasonal campaign on this star system was terminated. As mentioned earlier, maximum light which appeared in first quadrature was a feature common with the 1973 and 1984 light curves. In this case a hot spot positioned in the neck region (Figure 15) was effective in improving the model fit to the observed data near first quadrature.

4. Conclusions

Recent *V*- and *R*-filtered CCD-based observations have led to the construction of light curves which were used to: 1) revise the orbital period for AC Boo, 2) calculate updated ephemerides and, 3) further investigate the peak asymmetries

regularly observed for this system. A parabolic relationship between O–C residuals and cycle number has been derived which suggests continual period increases over nearly five decades. Fourier analysis of the associated quadratic residuals provided a hint, but not compelling evidence for strict sinusoidal periodicity occurring approximately every twenty-one years. Despite reports to the contrary, and until which time sufficient moments-of-minima data are collected from AC Boo, it would be premature to corroborate the gravitational influence of another body on this binary system. Using PHOEBE, analysis of photometric data covering the past forty-eight years and published by several investigators has produced a uniform solution of all light curves using Roche-based modeling. Epochal variability such as peak asymmetry, unequal successive maxima, and dissimilar minima was addressed by incorporating starspot(s) on one or both binary constituents. This has provided synthetic fits of light curve data that largely account for the observed differences.

5. Acknowledgements

The insightful comments from an anonymous referee, and the helpfulness and thorough work of the *JAAVSO* editorial and production staff are much appreciated and greatly improved the overall quality of this manuscript. The NASA Astrophysics Data System hosted by the Computation Facility at the Harvard-Smithsonian Center for Astrophysics is gratefully acknowledged. This investigation also made use of the SIMBAD database, operated at Centre de Données Astronomiques de Strasbourg (CDS), Strasbourg, France. Finally, special thanks is due to Dr. Andrej Prša for his personal assistance in using PHOEBE.

References

Agerer, F., and Hübscher, J. 1996, *Inf. Bull. Var. Stars*, No. 4382.
Agerer, F., and Hübscher, J. 1997, *Inf. Bull. Var. Stars*, No. 4472.
Agerer, F., and Hübscher, J. 1998, *Inf. Bull. Var. Stars*, No. 4606.
Agerer, F., and Hübscher, J. 2002, *Inf. Bull. Var. Stars*, No. 5296.
Agerer, F., and Hübscher, J. 2003, *Inf. Bull. Var. Stars*, No. 5484.
Aksu, O., *et al.* 2005, *Inf. Bull. Var. Stars*, No. 5588.
Alton, K. 2006, *Open Eur. J. Var. Stars*, **39**, 1.
Alton, K. B., and Terrell, D. 2006, *J. Amer. Assoc. Var. Star Obs.*, **34**, 188.
Applegate, J. H. 1992, *Astrophys. J.*, **385**, 621.
Bakis, V., Bakis, H., Erdem, A., Çiçek, C., Demircan, O., and Budding, E. 2003, *Inf. Bull. Var. Stars*, No. 5464.
Bakis, V., Dogru, S. S., Bakis, H., Dogru, D., Erdem, A., Çiçek, C., and Demircan, O. 2005, *Inf. Bull. Var. Stars*, No. 5662.
Berdyugina, S. V. 2005, *Living Rev. Sol. Phys.*, **2**, 8.
Berry, R., and Burnell, J. 2000–2006, "Astronomical Image Processing Software,"

version 2.1.10, provided with *The Handbook of Astronomical Image Processing*, Willmann-Bell, Richmond.
Bilir, S., Karataş, Y., Demircan, O., and Eker, Z. 2005, *Mon. Not. Roy. Astron. Soc.*, **357**, 2, 497.
Binnendijk, L. 1965, *Astron. J.*, **70**, 201.
Bradstreet, D. H., and Steelman, D. P. 2002, *Bull. Amer. Astron. Soc.*, **34**, 1224.
Budding, E., and Demircan, O. 2007, *Introduction to Astronomical Photometry*, Cambridge Univ. Press, Cambridge, UK.
de Jager, C., and Nieuwenhuijzen, H. 1987, *Astron. Astrophys.*, **177**, 217.
Demircan, O., *et al.* 2003, *Inf. Bull. Var. Stars*, No. 5364.
Demleitner, M., Accomazzi, A., Eichhorn, G., Grant, C. S., Kurtz, M. J., and Murray, S. S. 2001, in *Astronomical Data Analysis Software and Systems X*, eds. F. R. Harnden, Jr., F. A. Primini, and H. E. Payne, Astron. Soc. Pacific Conf. Ser., 238, Astron. Soc. Pacific, San Francisco, 321.
Diethelm, R. 2005, *Inf. Bull. Var. Stars*, No. 5653.
Diethelm, R. 2006, *Inf. Bull. Var. Stars*, No. 5713.
Diethelm, R. 2009, *Inf. Bull. Var. Stars*, No. 5894.
Dogru, S. S., Dogru, D., Erdem, A., Çiçek, C., and Demircan, O. 2006, *Inf. Bull. Var. Stars*, No. 5707.
Dvorak, S.W. 2006, *Inf. Bull. Var. Stars*, No. 5677.
Dvorak, S.W. 2008, *Inf. Bull. Var. Stars*, No. 5814.
Ferraz-Mello, S. 1981, *Astron. J.*, **86**, 619.
Foster, G. 1995, *Astron. J.*, **109**, 1889.
Geyer, E. 1955, *Bamberg Kleine Veröff. der Remeis-Sternwarte*, **9**, 4.
Ghedini, S. 1981, *Mem. Soc. Astron. Italia*, **52**, 633.
Harris, A. W., *et al.* 1989, *Icarus*, **77**, 171.
Henden, A. A., and Kaitchuck, R. H. 1990, *Astronomical Photometry: A Text and Handbook for the Advanced Amateur and Professional Astronomer*, Willmann-Bell, Richmond.
Høg, E., *et al.*, 2000, *The Tycho-2 Catalogue of the 2.5 Million Brightest Stars, Astron. Astrophys.*, **355**, L27.
Hrivnak, B. J. 1993, in *New frontiers in binary star research: a colloquium sponsored by the U.S. National Science Foundation and the Korean Science and Engineering Foundation, Seoul and Taejon, Korea, November 5-13, 1990,* eds. K-C. Leung and I-S. Nha, Astron. Soc. Pacific Conf. Ser. 38, Astron. Soc. Pacific, San Francisco, 269.
Hübscher, J. 2005, *Inf. Bull. Var. Stars*, No. 5643.
Hübscher, J. 2007, *Inf. Bull. Var. Stars*, No. 5802.
Hübscher, J., Paschke, A., and Walter, F. 2005, *Inf. Bull. Var. Stars*, No. 5657.
Hübscher, J., Paschke, A., and Walter, F. 2006, *Inf. Bull. Var. Stars*, No. 5731.
Hübscher, J., Steinbach, H-M., and Walter, F. 2008, *Inf. Bull. Var. Stars*, No. 5830.
Hübscher, J., Steinbach, H-M., and Walter, F. 2009, *Inf. Bull. Var. Stars*, No. 5874.
Hübscher, J., Steinbach, H-M., and Walter, F. 2009, *Inf. Bull. Var. Stars*, No. 5889.
Hübscher, J., and Walter, F. 2007, *Inf. Bull. Var. Stars*, No. 5761.

Kiliçoglu, T., *et al.* 2007, *Inf. Bull. Var. Stars*, No. 5801.
Kim, C-H., Lee, C-U., Yoon, Y-N., Park, S-S., Kim, D-H., Cha, S-M., and Won, J-H. 2006, *Inf. Bull. Var. Stars*, No. 5694.
Kreiner, J. M. 2004, *Acta Astron.*, **54**, 207.
Kwee, K. K., and van Woerden, H. 1956, *Bull. Astron. Inst. Netherlands*, **12**, 327.
Lehmann, H., and Mkrtichian, D. E. 2004, *Astron. Astrophys.*, **413**, 293.
Lenz, P., and Breger, M. 2005, PERIOD04 v1.1.1 software, *Commun. Asteroseismology*, **146**, 53.
Linnell, A. P. 1991, in *The Sun and Cool Stars. Activity, Magnetism, Dynamos*, eds. I. Tuominen, D. Moss, and G. Rudiger, Proc. IAU Colloq. 130, Helsinki, July 17–20, 1990, Springer-Verlag, Berlin, 376.
Linnell, A. P., Hrivnak, B., and Olson, E. C. 1990, *Bull. Amer. Astron. Soc.*, **22**, 1291.
Liu, Q., and Yang, Y. 2003, *Chinese J. Astron. Astrophys.*, **3**, 142.
Lucy, L. B. 1967, *Z. Astrophys.*, **65**, 89.
Maciejewski, G., and Karska, A. 2004, *Inf. Bull. Var. Stars*, No. 5494.
Mancuso, S., Milano, L., and Russo, G. 1977, *Astron. Astrophys. Suppl.*, **29**, 57.
Mancuso, S., Milano, L., and Russo, G. 1978, *Astron. Astrophys., Suppl. Ser.*, **63**, 193.
Mauder, H. 1964, *Z. Astrophys.*, **60**, 222.
Minor Planet Observer 1996–2008, MPO CANOPUS (version 9.5.0.3), and *PhotoRed Installation Guide and Reference Manual*, BDW Publishing, Colorado Springs (http://www.minorplanetobserver.com).
Nagai, K. 2003, *Var. Star Bull.*, **40**, 1.
Nagai, K. 2004, *Var. Star Bull.*, **42**, 2.
Nagai, K. 2005, *Var. Star Bull.*, **43**, 1.
Nagai, K. 2006, *Var. Star Bull.*, **44**, 2.
Nelson, R. 2001, *Inf. Bull. Var. Stars*, No. 5040.
Nelson, R. 2004, *Inf. Bull. Var. Stars*, No. 5493.
Nelson, R. 2005a, "Eclipsing Binary O–C," (http://www.aavso.org/observing/programs/eclipser/omc/).
Nelson, R. 2005b, MINIMA (version 24d) astronomy software, http://members.shaw.ca/bob.nelson/software1.htm
Nelson, R. 2005c, WDWINT (version 5.4e) astronomy software, http://members.shaw.ca/bob.nelson/software1.htm
Nelson, R. 2008, *Inf. Bull. Var. Stars*, No. 5820.
Parimucha, S., Dubovsky, P., Baludansky, D., Pribulla, T., Hambálek, L., Vanko, M., and Ogloza, W. 2009, *Inf. Bull. Var. Stars*, No. 5898.
Pejcha, O. 2005, *Inf. Bull. Var. Stars*, No. 5645.
Prša, A., and Zwitter, T. 2005, *Astrophys. J.*, **628**, 1, 426.
Robb, R. M. 1985, *Inf. Bull. Var. Stars*, No. 2764.
Ruciński, S. M. 1969, *Acta Astron.*, **19**, 245.
Ruciński, S. M., *et al.* 2009, "Commission 42, Triennial Report 2006–2009," to appear in *Trans. IAU, Reports on Astronomy*, **27A**, ed. K. A. van der Hucht, Cambridge, Univ. Press, Cambridge.

Safár, J., and Zejda, M. 2002, *Inf. Bull. Var. Stars*, No. 5263.
Schieven, G., Morton, J. C., McLean, B. J., and Hughes, V. A. 1983, *Astron. Astrophys., Suppl. Ser.*, **52**, 463.
Schwarzenberg-Czerny, A. 1996, *Astrophys. J., Lett.*, **460**, L107.
Senavci, H. V., *et al.* 2007, *Inf. Bull. Var. Stars*, No. 5754.
Terrell, D., and Wilson, R. E. 2005, *Astrophys. Space Sci.*, **296**, 221.
Tsesevich, V. P. 1956, *Astron. Tsirk.*, **171**, 20.
Tsesevich, V. P. 1959, *Astron. Tsirk.*, **173**, 14.
van Hamme, W. 1993, *Astron. J.*, **106**, 2096.
Vanmunster, T. 2005, PERANSO period analysis software (version 2.1), www.peranso.com
Wilsey, N. J., and Beaky, M. M. 2009, in *The Society for Astronomical Sciences 28th Annual Symposium on Telescope Science*, held May 19–21, 2009, Big Bear Lake, CA, Soc. Astron. Sci., Rancho Cucamonga, CA, 107.
Wilson, R. E. 1994, *Publ. Astron. Soc. Pacific*, **106**, 921.
Wilson, R. E. 1979, *Astrophys. J.*, **234**, 1054.
Wilson, R. E., and Biermann, P. 1976, *Astron. Astrophys.,* **48**, 349.
Wilson, R. E., and Devinney, E. J. 1971, *Astrophys. J.*, **166**, 605.
Yilmaz, M., *et al.* 2009, *Inf. Bull. Var. Stars*, No. 5887.
Zejda, M. 2002, *Inf. Bull. Var. Stars*, No. 5287.
Zejda, M. 2004, *Inf. Bull. Var. Stars*, No. 5583.
Zhou, D.-Q., and Leung, K.-C. 1990, *Astrophys. J.*, **355**, 271.

Table 1. AC Bootis recalculated residuals $(O–C)_L$ following linear least squares fit of $(O–C)_1$ and cycle number between 16 Feb 2006 and 07 May 2009.

Time of Minimum	*Type Number*	*Cycle*	*$(O–C)_1$*	*$(O–C)_L$*	*Reference*
53782.5082	I	3639	–0.35389150	–0.001386	IBVS 5754
53798.5466	II	3684.5	–0.35189825	0.000614	IBVS 5754
53817.4000	I	3738	–0.35449300	–0.001973	IBVS 5761
53855.6428	II	3846.5	–0.35235525	0.000181	Present study
53859.5211	II	3857.5	–0.35098875	0.001549	IBVS 5713
53860.4008	I	3860	–0.35241000	0.000128	IBVS 5802
53862.5157	I	3866	–0.35220100	0.000338	IBVS 5707
53862.6921	II	3866.5	–0.35202525	0.000514	Present study
53884.7194	I	3929	–0.35275650	–0.000208	Present study
53895.4705	II	3959.5	–0.35133575	0.001217	IBVS 5731
53897.7599	I	3966	–0.35290100	–0.000347	Present study
53898.4647	I	3968	–0.35294800	–0.000394	IBVS 5731
53901.4619	II	3976.5	0.35156025	0.000995	IBVS 5731
53903.7514	I	3983	0.35301550	0.000459	Present study
53904.4553	I	3985	0.35397250	0.001416	IBVS 5761
53904.4562	I	3985	0.35307250	0.000516	IBVS 5754
53919.4375	II	4027.5	0.35083375	0.001729	IBVS 5761
53923.6644	II	4039.5	0.35331575	0.000751	Present study
53932.4785	II	4064.5	0.35042825	0.002140	IBVS 5761
53932.6518	I	4065	0.35334250	0.000774	Present study
53934.4142	I	4070	0.35319500	0.000626	IBVS 5761
53935.4711	I	4073	0.35364050	0.001071	IBVS 5761
54131.9628	II	4630.5	0.35197925	0.000672	IBVS 5820
54170.5550	I	4740	0.35289000	0.000222	IBVS 5802
54189.4124	II	4793.5	0.35148475	0.001191	IBVS 5801
54192.4074	I	4802	0.35229700	0.000380	IBVS 5898
54197.8699	II	4817.5	0.35274875	0.000070	IBVS 5814
54204.3908	I	4836	0.35214600	0.000536	IBVS 5889
54210.3819	I	4853	0.35267050	0.000014	IBVS 5802
54213.3783	II	4861.5	0.35208275	0.000603	IBVS 5874
54218.4880	I	4876	0.35288600	0.000198	IBVS 5802
54220.4258	II	4881.5	0.35355275	0.000864	IBVS 5802
54313.4732	II	5145.5	0.35255675	0.000171	IBVS 5830
54491.6398	I	5651	0.34867350	0.004129	IBVS 5887
54531.6382	II	5764.5	0.35317825	0.000359	IBVS 5898
54533.4012	II	5769.5	0.35242075	0.000399	IBVS 5898
54572.3454	I	5880	0.35378000	0.000944	IBVS 5897

Table 1 continued on following page

Table 1. AC Bootis recalculated residuals $(O–C)_L$ following linear least squares fit of $(O–C)_1$ and cycle number between 16 Feb 2006 and 07 May 2009, continued.

Time of Minimum	*Type*	*Number*	*Cycle*	*$(O–C)_1$*	*$(O–C)_L$*	*Reference*
54572.5224	II	5880.5	–0.35300425	–0.000168	IBVS 5697
54595.4321	II	5945.5	–0.35245675	0.000389	IBVS 5889
54597.5459	II	5951.5	–0.35334775	–0.000501	IBVS 5889
54598.4267	I	5954	–0.35366900	–0.000822	IBVS 5889
54600.5411	I	5960	–0.35396000	–0.001112	IBVS 5889
54637.5482	I	6065	–0.35395250	–0.001089	IBVS 5889
54639.4887	II	6070.5	–0.35191925	0.000945	IBVS 5889
54643.3642	II	6081.5	–0.35335275	–0.000487	IBVS 5887
54648.4743	I	6096	–0.35375600	–0.000888	IBVS 5889
54671.3810	I	6161	–0.35620850	–0.003331	IBVS 5887
54672.4404	I	6164	–0.35415400	–0.001276	IBVS 5889
54942.4166	I	6930	–0.35350500	–0.000514	IBVS 5898
54958.8099	II	6976.5	–0.34906025	0.003938	IBVS 5894

Table 2. Comparison of selected geometrical and physical elements for AC Boo following Roche model light curve fitting.

Parameter[a]	*Mauder (1964) 1961*	*Binnendijk (1965) 1962*
T_1 (K)	6252	6252
T_2 (K)	6349 (6)	6349 (6)
q (m_2/m_1)	0.306 (0.002)	0.306 (0.002)
$A_{1,2}$	0.5	0.5
$g_{1,2}$	0.32	0.32
x_{1V}, y_{1V}	0.726, 0.269	0.726, 0.269
x_{2V}, y_{2V}	0.720, 0.272	0.720, 0.272
x_{1B}, y_{1B}	0.816, 0.212	0.816, 0.212
x_{2B}, y_{2B}	0.812, 0.221	0.812, 0.221
x_{1U}, y_{1U}	—	—
x_{2U}, y_{2U}	—	—
x_{1R}, y_{1R}	—	—
x_{2R}, y_{2R}	—	—
$\Omega_1 = \Omega_2$	2.4303 (0.005)	2.4303 (0.005)
i	84.03 (0.43)	84.03 (0.43)
r_1 pole	0.4645 (0.0013)	0.4645 (0.0007)
r_1 side	0.5020 (0.0018)	0.5020 (0.0010)
r_1 back	0.5308 (0.0020)	0.5308 (0.0011)
r_2 pole	0.2736 (0.0044)	0.2736 (0.0022)
r_2 side	0.2865 (0.0054)	0.2865 (0.0027)
r_2 back	0.3286 (0.0107)	0.3286 (0.0054)
$M_1/M_\odot$	1.688	1.688
$M_2/M_\odot$	0.517	0.517
$R_1/R_\odot$	1.367	1.367
$R_2/R_\odot$	0.813	0.813
$\Sigma (O–C)^2$	0.1111	0.0641
$A_{S1} = T_S/T$	0.75 (0.09)	—
Θ_{S1} (spot co-latitude)	90	—
ϕ_{S1} (spot longitude)	180	—
r_{S1} (angular radius)	10.0 (0.3)	—
$A_{S2} = T_S/T$	1.19 (0.04)	—
Θ_{S2} (spot co-latitude)	90	—
ϕ_{S2} (spot longitude)	210	—
r_{S2} (angular radius)	9.03 (0.38)	—

a: errors in parenthesis from WDWINT *v5.4e.*

Table 2 continued on following pages

Table 2. Comparison of selected geometrical and physical elements for AC Boo following Roche model light curve fitting, continued.

Parameter[a]	*Binnendijk (1965) 1963*	*Mancuso (1976) 1972*
T_1 (K)	6252	6252
T_2 (K)	6349 (6)	6349 (6)
q (m_2/m_1)	0.306 (0.002)	0.306 (0.002)
$A_{1,2}$	0.5	0.5
$g_{1,2}$	0.32	0.32
x_{1V}, y_{1V}	0.726, 0.269	0.726, 0.269
x_{2V}, y_{2V}	0.720, 0.272	0.720, 0.272
x_{1B}, y_{1B}	0.816, 0.212	—
x_{2B}, y_{2B}	0.812, 0.221	—
x_{1U}, y_{1U}	—	—
x_{2U}, y_{2U}	—	—
x_{1R}, y_{1R}	—	—
x_{2R}, y_{2R}	—	—
$\Omega_1 = \Omega_2$	2.4303 (0.005)	2.4303 (0.005)
i	84.03 (0.43)	84.03 (0.43)
r_1 pole	0.4645 (0.0006)	0.4645 (0.0013)
r_1 side	0.5020 (0.0008)	0.5020 (0.0018)
r_1 back	0.5308 (0.0009)	0.5308 (0.0019)
r_2 pole	0.2736 (0.0019)	0.2736 (0.0050)
r_2 side	0.2865 (0.0024)	0.2865 (0.0062)
r_2 back	0.3286 (0.0046)	0.3286 (0.0122)
$M_1/M_\odot$	1.688	1.688
$M_2/M_\odot$	0.517	0.517
$R_1/R_\odot$	1.367	1.367
$R_2/R_\odot$	0.813	0.813
$\Sigma (O–C)^2$	0.0787	0.1613
$A_{S1} = T_S/T$	0.75 (0.02)	0.85 (0.03)
Θ_{S1} (spot co-latitude)	90	90
ϕ_{S1} (spot longitude)	180	180
r_{S1} (angular radius)	10.7 (0.1)	8.06 (0.43)
$A_{S2} = T_S/T$	11.22 (0.01)	—
Θ_{S2} (spot co-latitude)	90	—
ϕ_{S2} (spot longitude)	200	—
r_{S2} (angular radius)	913.75 (0.18)	—

a: errors in parenthesis from wdwint v5.4e.

Table 2 continued on following pages

Table 2. Comparison of selected geometrical and physical elements for AC Boo following Roche model light curve fitting, continued.

Parameter[a]	*Mancuso (1976) 1973*	*Schieven (1983) 1982*
T_1 (K)	6252	6252
T_2 (K)	6349 (6)	6349 (6)
q (m_2/m_1)	0.306 (0.002)	0.306 (0.002)
$A_{1,2}$	0.5	0.5
$g_{1,2}$	0.32	0.32
x_{1V}, y_{1V}	0.726, 0.269	0.726, 0.269
x_{2V}, y_{2V}	0.720, 0.272	0.720, 0.272
x_{1B}, y_{1B}	—	0.816, 0.212
x_{2B}, y_{2B}	—	0.812, 0.221
x_{1U}, y_{1U}	—	0.858, 0.188
x_{2U}, y_{2U}	—	0.852, 0.213
x_{1R}, y_{1R}	—	—
x_{2R}, y_{2R}	—	—
$\Omega_1 = \Omega_2$	2.4303 (0.005)	2.4303 (0.005)
i	84.03 (0.43)	84.03 (0.43)
r_1 pole	0.4645 (0.0013)	0.4645 (0.0008)
r_1 side	0.5020 (0.0017)	0.5020 (0.0011)
r_1 back	0.5308 (0.0010)	0.5308 (0.0013)
r_2 pole	0.2736 (0.0048)	0.2736 (0.0026)
r_2 side	0.2865 (0.0059)	0.2865 (0.0032)
r_2 back	0.3286 (0.0117)	0.3286 (0.0063)
$M_1/M_\odot$	1.688	1.688
$M_2/M_\odot$	0.517	0.517
$R_1/R_\odot$	1.367	1.367
$R_2/R_\odot$	0.813	0.813
$\Sigma (O–C)^2$	0.0843	0.0435
$A_{S1} = T_S/T$	0.78 (0.03)	—
Θ_{S1} (spot co-latitude)	90	—
ϕ_{S1} (spot longitude)	180	—
r_{S1} (angular radius)	10.5 (0.4)	—
$A_{S2} = T_S/T$	—	1.15 (0.01)
Θ_{S2} (spot co-latitude)	—	90
ϕ_{S2} (spot longitude)	—	140
r_{S2} (angular radius)	—	10.60 (0.22)

a: errors in parenthesis from wdwint v5.4e.

Table 2 continued on following page

Table 2. Comparison of selected geometrical and physical elements for AC Boo following Roche model light curve fitting, continued.

Parameter[a]	*Robb (1985) 1984*	*Present 2006*
T_1 (K)	6252	6252
T_2 (K)	6349 (6)	6349 (6)
q (m_2/m_1)	0.306 (0.002)	0.306 (0.002)
$A_{1,2}$	0.5	0.5
$g_{1,2}$	0.32	0.32
x_{1V}, y_{1V}	0.726, 0.269	0.726, 0.269
x_{2V}, y_{2V}	0.720, 0.272	0.720, 0.272
x_{1B}, y_{1B}	0.816, 0.212	—
x_{2B}, y_{2B}	0.812, 0.221	—
x_{1U}, y_{1U}	0.858, 0.188	—
x_{2U}, y_{2U}	0.852, 0.213	—
x_{1R}, y_{1R}	—	0.634, 0.276
x_{2R}, y_{2R}	—	0.627, 0.279
$\Omega_1 = \Omega_2$	2.4303 (0.005)	2.4303 (0.005)
i	84.03 (0.43)	84.03 (0.43)
r_1 pole	0.4645 (0.0018)	0.4645 (0.0006)
r_1 side	0.5020 (0.0024)	0.5020 (0.0007)
r_1 back	0.5308 (0.0027)	0.5308 (0.0008)
r_2 pole	0.2736 (0.0056)	0.2736 (0.0018)
r_2 side	0.2865 (0.0068)	0.2865 (0.0022)
r_2 back	0.3286 (0.0134)	0.3286 (0.0043)
$M_1/M_\odot$	1.688	1.688
$M_2/M_\odot$	0.517	0.517
$R_1/R_\odot$	1.367	1.367
$R_2/R_\odot$	0.813	0.813
$\Sigma (O–C)^2$	0.0782	0.0157
$A_{S1} = T_S/T$	—	1.20 (0.01)
Θ_{S1} (spot co-latitude)	—	35
ϕ_{S1} (spot longitude)	—	10
r_{S1} (angular radius)	—	14.8 (0.2)
$A_{S2} = T_S/T$	0.96 (0.01)	1.20 (0.01)
Θ_{S2} (spot co-latitude)	90	90
ϕ_{S2} (spot longitude)	180	340
r_{S2} (angular radius)	15.3 (1.1)	18.5 (0.5)

a: errors in parenthesis from wdwint v5.4e.

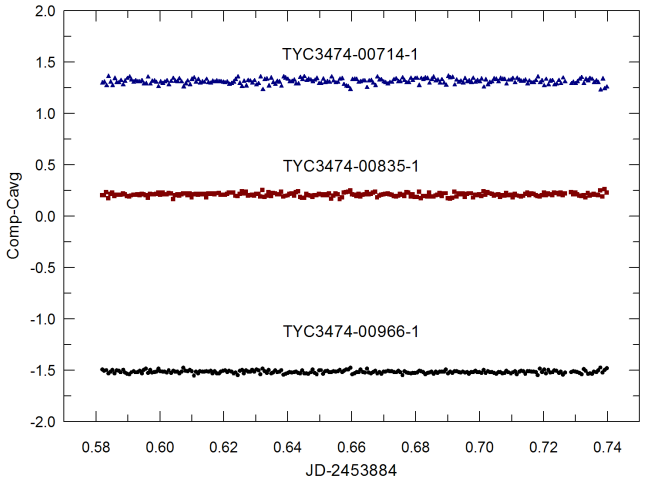

Figure 1. Constant relative magnitude (*V*-band) exhibited by comparison stars during a typical AC Boo photometric session (29 May 2006).

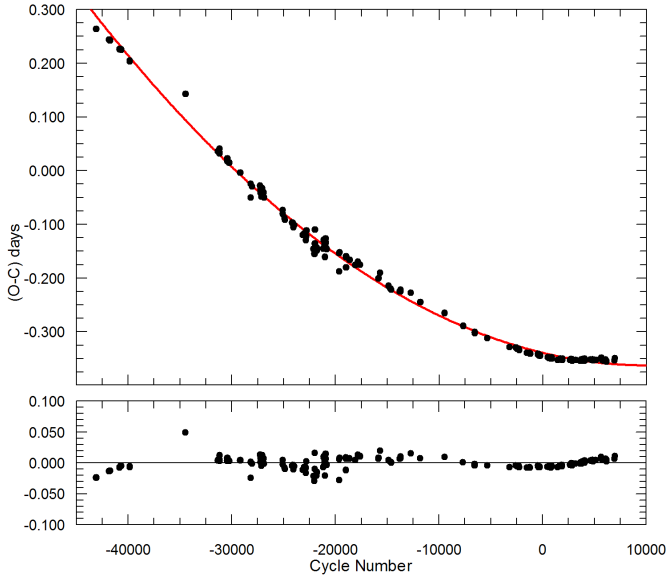

Figure 2. Quadratic least square fit of residuals $(O–C)_1$ as a function of cycle number for AC Boo observed between 18 Jan 1961 and 07 May 2009 (top panel). Quadratic residuals $(O–C)_Q$ are shown in the bottom panel.

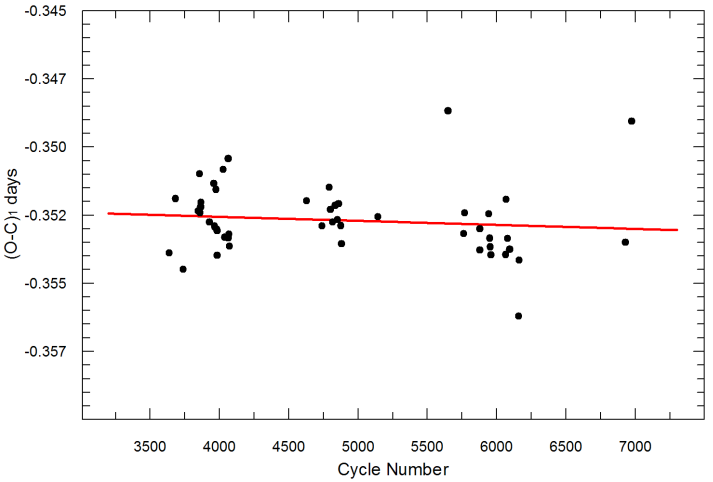

Figure 3. Near term simple least squares fit of residuals $(O–C)_1$ as a function of cycle number for AC Boo observed between 16 Feb 2006 and 07 May 2009.

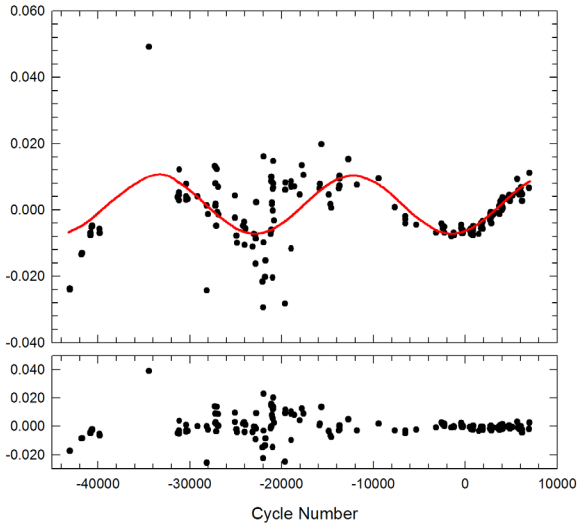

Figure 4. Fourier transform of quadratic residuals $(O–C)_Q$ calculated for AC Boo between 18 Jan 1961 and 07 May 2009 (top panel). The sinusoidal-like periodicity (P~21 years) is strongly influenced by the fit of data over the past two decades (cycle –14000 to 6977). Corresponding residuals (O–C)S are plotted in the bottom panel.

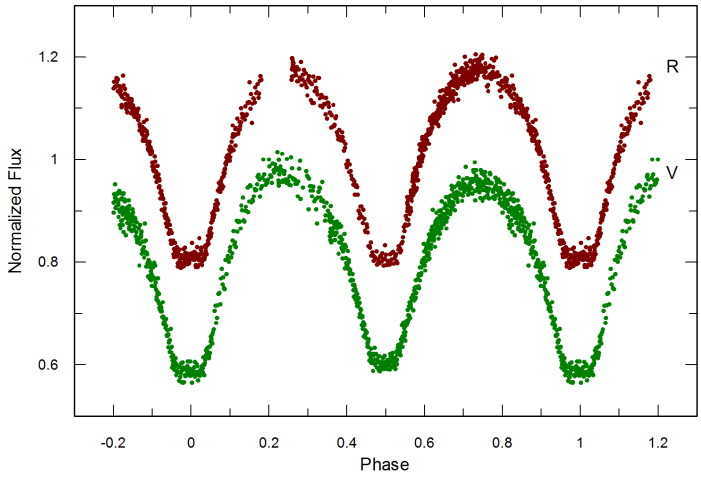

Figure 5. Folded CCD-derived light curves for AC Boo captured in *V*- (April–July 2006) and *R*-band (June–July 2006). Curves in each passband are offset for clarity.

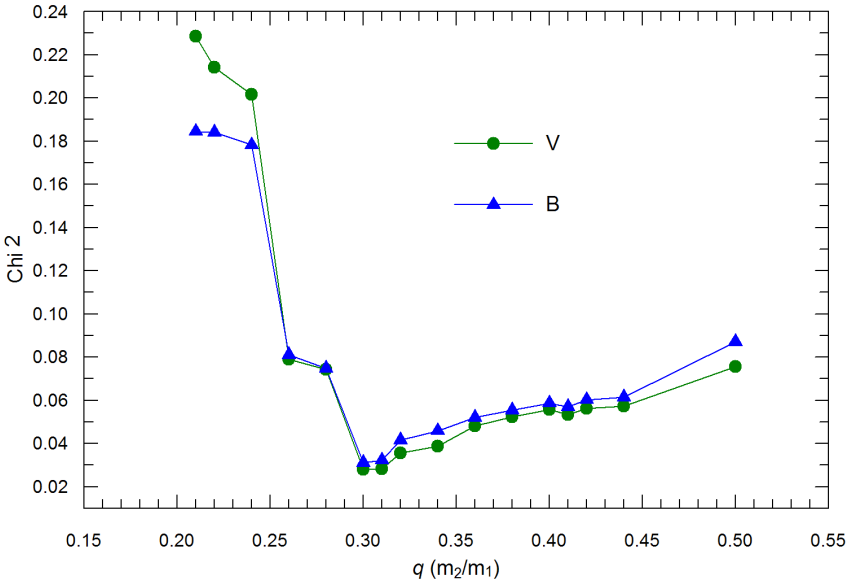

Figure 6. Photometric search for AC Boo mass ratio (m_2/m_1) using Roche modeling of 1962 light curves from Binnendijk (1965).

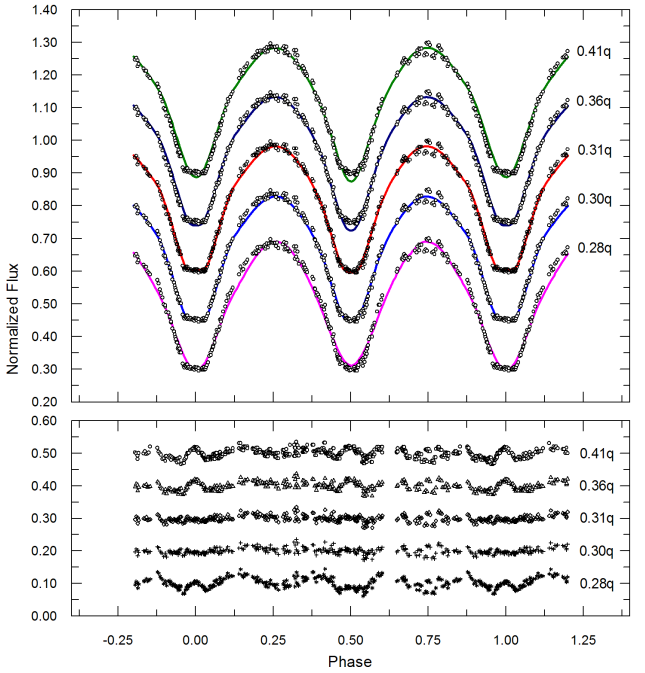

Figure 7. Series of Roche model predictions using varying values for *q* with the 1962 light curve (*V*-band) reported by Binnendijk (1965).

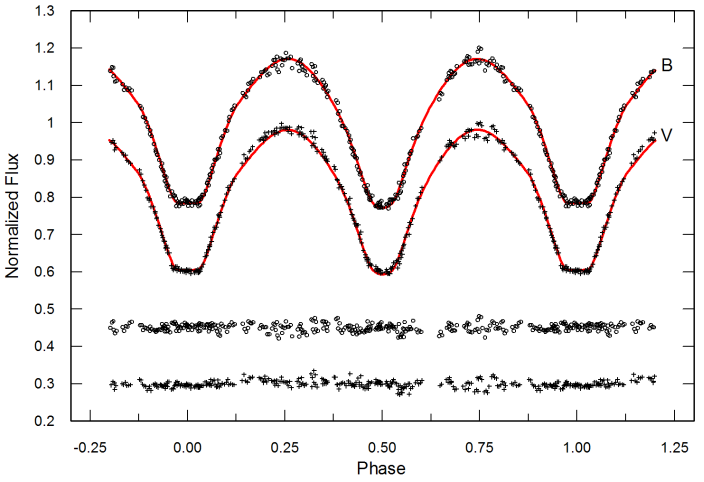

Figure 8. *V*- and *B*-band light curves for AC Boo captured in 1962 by Binnendijk (1965). Solid line represents the best theoretical fit using the Roche model without invoking spots. Light curves (top) and model fit residuals (bottom) in each passband are offset for clarity.

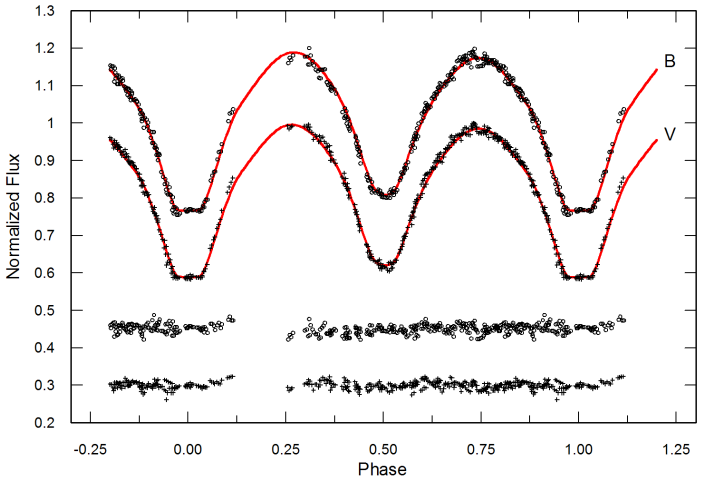

Figure 9. *V*- and *B*-band photoelectric light curves for AC Boo captured in 1963 by Binnendijk (1965). Solid line is the best theoretical fit using the Roche model with a single hot (secondary) and cool (primary) spot on each star. Light curves (top) and model fit residuals (bottom) are offset for clarity.

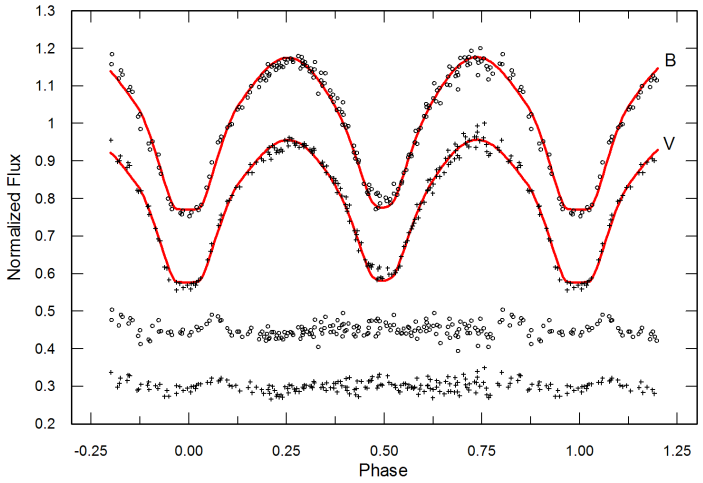

Figure 10. *V*- and *B*-band photoelectric light curves for AC Boo captured in 1961 by Mauder (1964). Solid line represents the best theoretical fit using the Roche model with a single hot (secondary) and cool (primary) spot on each star. Light curves (top) and model fit residuals (bottom) are offset for clarity.

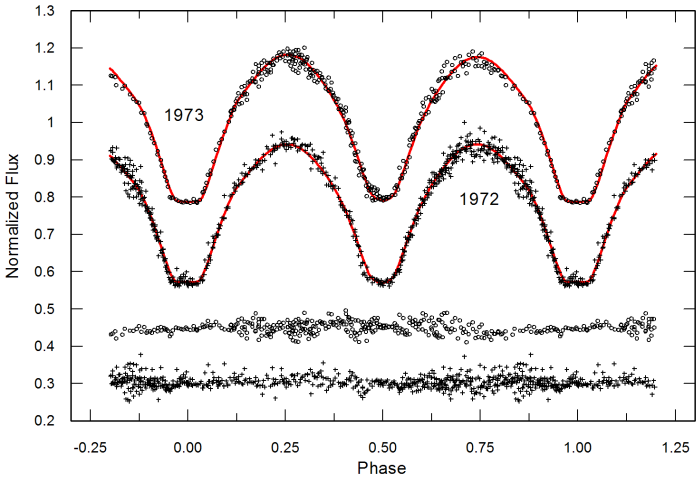

Figure 11. *V*-band photoelectric light curves for AC Boo acquired in 1972 (bottom) and 1973 (top) by Mancuso *et al.* (1976). Solid line is the best theoretical fit using the Roche model with a single cool spot on the primary. Light curves (top) and model fit residuals (bottom) for each year are offset for clarity.

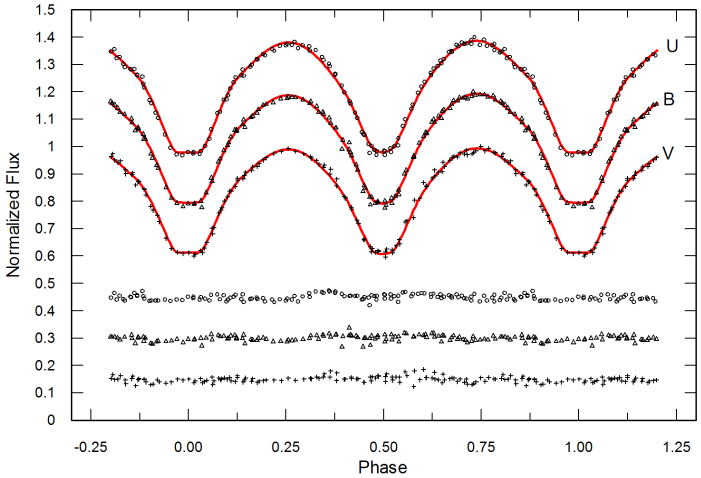

Figure 12. *U*-, *B*- and *V*-band photoelectric light curves for AC Boo captured in 1982 by Schieven *et al.* (1983). Solid line represents the best theoretical fit using the Roche model with a hot spot on the less massive star. Light curves (top) and model fit residuals (bottom) in each passband are offset for clarity.

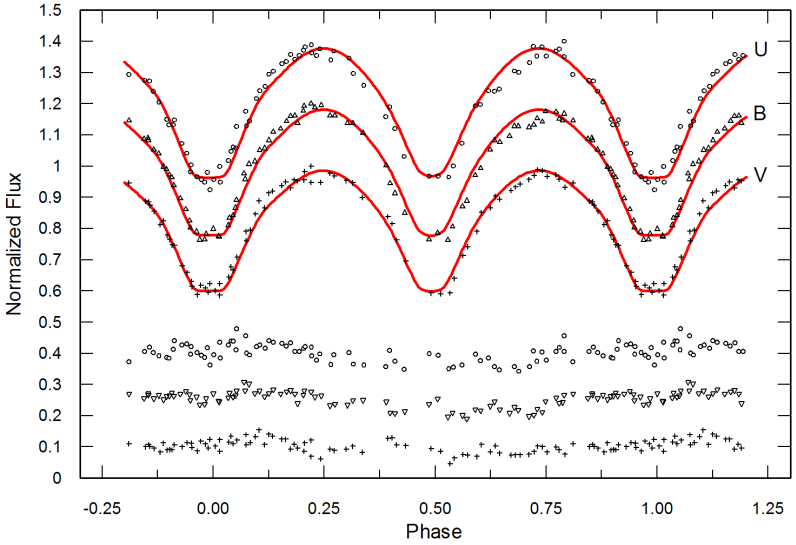

Figure 13. *U*-, *B*- and *V*-band photoelectric light curves for AC Boo acquired in 1984 by Robb (1985). Solid line represents the best theoretical fit using the Roche model with a cool spot on the more massive star. Light curves (top) and model fit residuals (bottom) in each passband are offset for clarity.

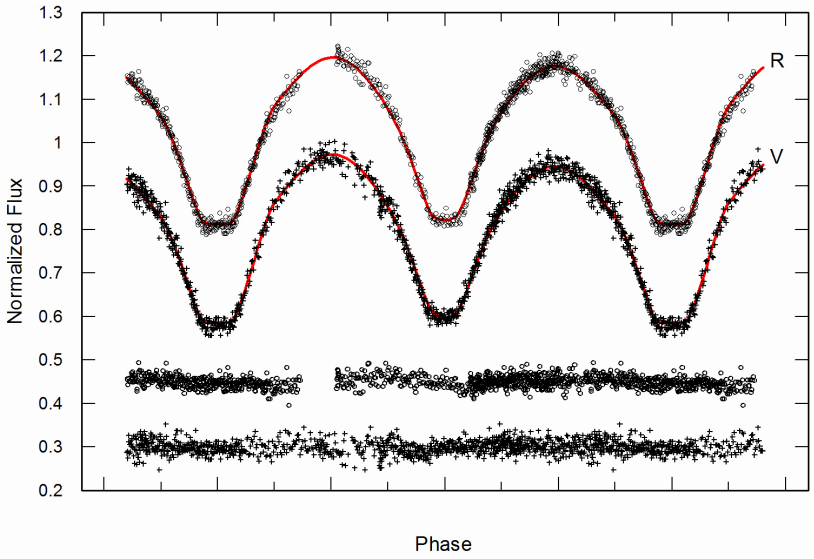

Figure 14. *R*- and *V*-band CCD light curves for AC Boo captured in 2006 (present study). Solid line represents the best theoretical fit using the Roche model with a hot spot on each star. Light curves (top) and model fit residuals (bottom) for each passband are offset for clarity.

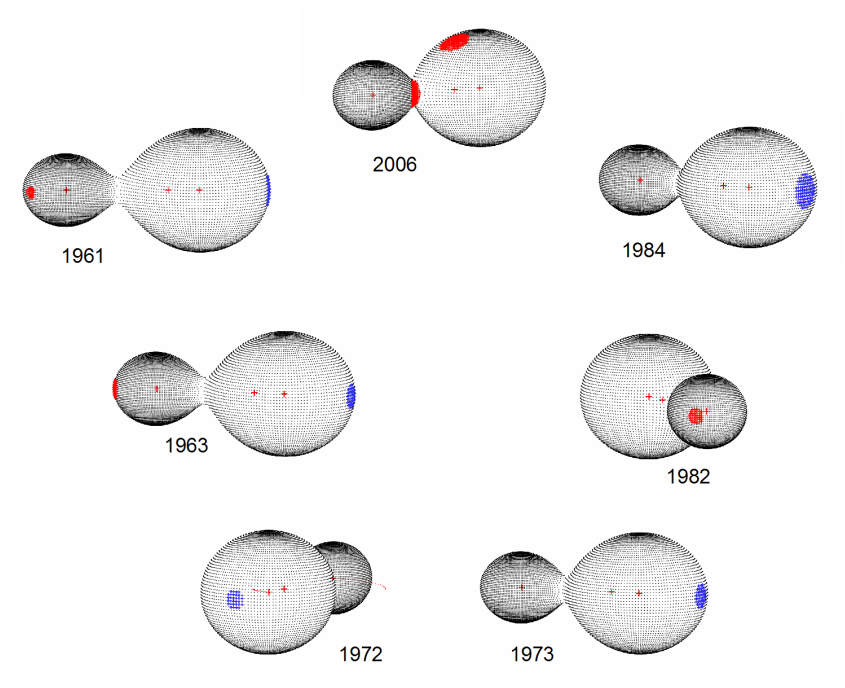

Figure 15. Three-dimensional renderings of Roche lobe geometry for the W-type W UMa overcontact binary AC Boo showing starspot locations from 1961 to 2006. Images were produced using BINARYMAKER 3.

Recent Minima of 161 Eclipsing Binary Stars

Gerard Samolyk
P.O. Box 20677; Greenfield, WI 53220; gsamolyk@wi.rr.com

Received September 23, 2009; accepted September 25, 2009

Abstract This paper continues the publication of times of minima for eclipsing binary stars from observations reported to the AAVSO Eclipsing Binary Section. Times of minima from observations made from March 2009 through August 2009, along with a few unpublished times of minima from older data, are presented.

1. Recent observations

The accompanying list contains times of minima calculated from recent CCD observations made by participants in the AAVSO's eclipsing binary program. This list will be web-archived and made available through the AAVSO ftp site at ftp://ftp.aavso.org/public/datasets/jsamoj381.txt. This list, along with eclipsing binary data from earlier AAVSO publications, is also included in the Lichtenknecker database administrated by the Bundesdeutsche Arbeitsgemeinschaft für Veränderliche Sterne e.V. (BAV) at http://www.bav-astro.de/LkDB/index.pho?lang=en. These observations were reduced by the observers or the writer using the method of Kwee and Van Woerden (1956). The standard error is included when available.

The linear elements in the *General Catalogue of Variable Stars* (GCVS, Kholopov *et al.* 1985) were used to compute the O–C values for most stars. For a few exceptions where the GCVS elements are missing or are in significant error, light elements from another source are used: CD Cam (Baldwin and Samolyk 2007), CW Cas (Samolyk 1992a), DV Cep (Frank and Lichtenknecker 1987), DF Hya (Samolyk 1992b), EF Ori (Baldwin and Samolyk 2005), and GU Ori (Samolyk 1985). O–C values listed in this paper can be directly compared with values published in recent numbers of the AAVSO *Observed Minima Timings of Eclipsing Binaries* series.

The number of observations used for determination of each time of minimum is given under *N* when available.

References

Baldwin, M. E., and Samolyk, G. 2005, *Observed Minima Timings of Eclipsing Binaries No. 10*, AAVSO, Cambridge, MA.

Baldwin, M. E., and Samolyk, G. 2007, *Observed Minima Timings of Eclipsing Binaries No. 12*, AAVSO, Cambridge, MA.

Frank, P., and Lichtenknecker, D. 1987, *BAV Mitt.*, No. 47.

Kholopov, P. N., *et al.* 1985, *General Catalogue of Variable Stars*, 4th ed., Moscow.

Kwee, K. K., and Van Woerden, H. 1956, *Bull. Astron. Inst. Netherlands*, **12**, 327.
Samolyk, G. 1985, *J. Amer. Assoc. Var. Star Obs.*, **14**, 12.
Samolyk, G. 1992a, *J. Amer. Assoc. Var. Star Obs.*, **21**, 34.
Samolyk, G. 1992b, *J. Amer. Assoc. Var. Star Obs.*, **21**, 111.

Table 1. Recent times of minima of stars in the AAVSO eclipsing binary program.

Star	*HJD(min) 2400000+*	*Cycle*	*O–C*	*N*	*Type*	*Observer**	*Standard Error*
RT And	55058.8316	22128	–0.0097	90	CCD	SAH	0.0001
UU And	55056.8102	9020	0.0803	72	CCD	SAH	0.0001
WZ And	54788.2731	20004	0.0485	110	CCD	OYE	0.0001
AB And	55050.8067	57070.5	–0.0235	168	CCD	MZK	0.0001
BD And	55058.8557	43414	0.0152	82	CCD	SAH	0.0001
BX And	55062.8103	30378	–0.0512	80	CCD	SAH	0.0004
OO Aql	55011.6746	32357.5	0.0442	84	CCD	SAH	0.0001
OO Aql	55060.5795	32454	0.0440	132	CCD	MZK	0.0001
V346 Aql	55058.6473	11877	–0.0101	83	CCD	SAH	0.0001
V417 Aql	55056.3893	32529	0.0656		CCD	OYE	0.0001
WW Aur	54905.6327	8697	0.0012	128	CCD	SAH	0.0002
HL Aur	54892.2435	47074	–0.0215	94	CCD	OYE	0.0001
TU Boo	54939.7427	67451	–0.1302	66	CCD	SAH	0.0002
TY Boo	54933.8403	64491.5	0.0844	61	CCD	SAH	0.0003
TY Boo	54939.7067	64510	0.0836	63	CCD	PRX	0.0002
TY Boo	54983.3093	64647.5	0.0784	94	CCD	OYE	0.0001
TY Boo	54983.4673	64648	0.0778	62	CCD	OYE	0.0001
TY Boo	54994.4101	64682.5	0.0790	137	CCD	OYE	0.0002
TY Boo	55005.6731	64718	0.0833	72	CCD	SAH	0.0001
TZ Boo	54938.6886	51506.5	0.0722	58	CCD	SAH	0.0004
TZ Boo	55005.7001	51732	0.0737	84	CCD	SAH	0.0003
TZ Boo	55007.3298	51737.5	0.0690	152	CCD	OYE	0.0001
VW Boo	54894.8426	69295.5	–0.1662	55	CCD	MZK	0.0002
VW Boo	54938.6590	69423.5	–0.1675	81	CCD	SAH	0.0003
VW Boo	54945.6780	69444	–0.1661	62	CCD	PRX	0.0004
VW Boo	54982.6468	69552	–0.1685	85	CCD	SAH	0.0003
VW Boo	55000.2712	69603.5	–0.1738	142	CCD	OYE	0.0001
AC Boo	55011.3202	82952	0.1631	148	CCD	OYE	0.0001
AD Boo	54939.6199	13056	0.0272	89	CCD	SAH	0.0002
EF Boo	54970.3321	5874	0.0025	57	CCD	OYE	0.0002
SV Cam	54905.6112	20758	0.0500	126	CCD	SAH	0.0002
AL Cam	54893.6144	21442	–0.0323	102	CCD	SAH	0.0001
AN Cam	54955.6932	1378.5	5.6531	157	CCD	SAH	0.0007
CD Cam	54933.7449	2841	–0.0010	178	CCD	SAH	0.0006

Table 1 continued on following pages

Table 1. Recent times of minima of stars in the AAVSO eclipsing binary program, cont.

Star	*HJD(min) 2400000+*	*Cycle*	*O–C*	*N*	*Type*	*Observer**	*Standard Error*
UU CMa	54895.6039	4753	–0.1075	82	CCD	SAH	0.0003
RW CMi	54889.4443	392	0.0065	122	CCD	CLZ	0.0001
TX CMi	54890.4652	47023	–0.0928	110	CCD	CLZ	0.0001
TY Cap	55043.7825	7201	0.0685	117	CCD	SAH	0.0002
TV Cas	55055.6686	5767	–0.0236	106	CCD	SAH	0.0007
AB Cas	54781.3221	8828	0.0975	67	CCD	OYE	0.0002
CW Cas	55056.6313	42101	–0.0512	74	CCD	SAH	0.0001
CW Cas	55066.6755	42132.5	–0.0512	91	CCD	SAH	0.0002
DZ Cas	55058.6882	33921	–0.1758	101	CCD	SAH	0.0004
IR Cas	55018.6854	18591	0.0091	115	CCD	SAH	0.0001
IR Cas	55058.8457	18650	0.0090	64	CCD	SAH	0.0001
PV Cas	55074.8554	8482	–0.0344	160	CCD	MZK	0.0001
V364 Cas	55056.6785	13430	–0.0227	96	CCD	SAH	0.0004
V375 Cas	55045.8217	13848	0.1408	65	CCD	MZK	0.0005
V375 Cas	55045.8247	13848	0.1438	84	CCD	SAH	0.0003
U Cep	54937.7766	4170	0.1654	181	CCD	SAH	0.0002
SU Cep	55055.8268	31873	0.0045	81	CCD	SAH	0.0002
WZ Cep	54986.6771	64550	–0.0892	77	CCD	SAH	0.0003
DK Cep	54987.7220	21703	0.0324	111	CCD	SAH	0.0002
DK Cep	55062.6516	21779	0.0331	89	CCD	SAH	0.0001
DV Cep	54986.6449	7077	–0.0038	73	CCD	SAH	0.0002
EG Cep	54912.6532	22618	0.0141	99	CCD	SAH	0.0001
EG Cep	54980.7311	22743	0.0143	84	CCD	SAH	0.0001
EK Cep	55066.7656	3628	0.0100	142	CCD	SAH	0.0001
IO Cep	55073.4594	19699	0.0114		CCD	OYE	0.0001
RW Com	54912.7687	62737	–0.0173	102	CCD	SAH	0.0002
RW Com	54916.6844	62753.5	–0.0178	68	CCD	PRX	0.0001
RW Com	54933.6551	62825	–0.0174	80	CCD	SAH	0.0002
RW Com	54964.2664	62954	–0.0237	80	CCD	OYE	0.0001
RZ Com	54933.7184	59367.5	0.0413	78	CCD	SAH	0.0001
SS Com	54930.8131	72500.5	0.6840	112	CCD	SAH	0.0004
SS Com	54959.7104	72570.5	0.6858	72	CCD	PRX	0.0003
CC Com	54913.6353	69692	–0.0159	30	CCD	MZK	0.0001
CC Com	54930.6285	69769	–0.0156	109	CCD	SAH	0.0001
CC Com	54946.6278	69841.5	–0.0160	40	CCD	SAH	0.0001
CC Com	54956.6703	69887	–0.0148	42	CCD	PRX	0.0003
U CrB	54939.7975	11063	0.1224	88	CCD	SAH	0.0004
RW CrB	54951.6187	19548	–0.0015	197	CCD	MZK	0.0001
RW CrB	54996.6565	19610	–0.0013	117	CCD	SAH	0.0002

Table 1 continued on following pages

Table 1. Recent times of minima of stars in the AAVSO eclipsing binary program, cont.

Star	HJD(min) 2400000+	Cycle	O–C	N	Type	Observer*	Standard Error
TW CrB	54911.5452	28891	0.0395	201	CCD	VJA	0.0001
W Crv	54891.7955	39280.5	0.0205	72	CCD	SAH	0.0002
W Crv	54912.7508	39334.5	0.0194	41	CCD	HES	0.0003
W Crv	54952.7236	39437.5	0.0199	81	CCD	PRX	0.0002
RV Crv	54905.7815	18570	–0.0740	56	CCD	SAH	0.0004
RV Crv	54938.6581	18614	–0.0765	94	CCD	SAH	0.0005
V Crt	54939.6060	19290	–0.0027	71	CCD	SAH	0.0002
SW Cyg	55074.7252	2888	–0.3034	149	CCD	SAH	0.0001
WW Cyg	55055.7773	4424	0.0812	111	CCD	SAH	0.0001
ZZ Cyg	55043.7086	15977	–0.0533	109	CCD	MZK	0.0001
ZZ Cyg	55043.7088	15977	–0.0531	126	CCD	SAH	0.0002
AE Cyg	54980.7565	10725	–0.0050	92	CCD	SAH	0.0003
AE Cyg	55047.6320	10794	–0.0034	74	CCD	MZK	0.0002
BR Cyg	54987.7031	10092	0.0003	150	CCD	SAH	0.0001
CG Cyg	54989.7525	24661	0.0622	119	CCD	MZK	0.0001
DK Cyg	54980.7713	36077	0.0845	110	CCD	SAH	0.0003
DK Cyg	55062.6703	36251	0.0834	78	CCD	SAH	0.0001
KR Cyg	55018.7782	30660	0.0141	146	CCD	SAH	0.0001
KV Cyg	54976.7977	8985	0.0512	127	CCD	MZK	0.0003
KV Cyg	54996.6722	8992	0.0527	120	CCD	SAH	0.0003
V346 Cyg	55018.7984	7047	0.1401	130	CCD	SAH	0.0002
V387 Cyg	55009.6803	42186	0.0196	67	CCD	SAH	0.0002
V388 Cyg	55022.6435	15214	–0.0858	167	CCD	MZK	0.0001
V388 Cyg	55030.3727	15223	–0.0879	153	CCD	OYE	0.0001
V456 Cyg	54949.7867	11264	0.0448	79	CCD	MZK	0.0001
V466 Cyg	55011.6815	18854.5	0.0059	127	CCD	SAH	0.0001
V466 Cyg	55059.6905	18889	0.0058	138	CCD	MZK	0.0001
V477 Cyg	54987.7441	4601	–0.0236	116	CCD	SAH	0.0001
V477 Cyg	55074.5823	4638	–0.0240	443	CCD	MZK	0.0001
V499 Cyg	55058.3477	35009	0.0462	—	CCD	OYE	0.0001
V548 Cyg	55011.7105	5847	0.0173	99	CCD	SAH	0.0002
V704 Cyg	55009.7667	29911	0.0304	63	CCD	SAH	0.0002
V704 Cyg	55045.7197	29974	0.0290	81	CCD	MZK	0.0002
V841 Cyg	52418.7078	23372	0.0082	40	CCD	DKS	0.0003
V841 Cyg	55042.3394	26819	0.0035	165	CCD	OYE	0.0002
V1034 Cyg	54996.7148	12343	–0.0035	115	CCD	SAH	0.0005
V1034 Cyg	54999.6466	12346	–0.0025	118	CCD	MZK	0.0004
W Del	55074.6869	2444	0.0290	148	CCD	SAH	0.0002
TY Del	55044.6723	10146	0.0539	69	CCD	SAH	0.0001

Table 1 continued on following pages

Table 1. Recent times of minima of stars in the AAVSO eclipsing binary program, cont.

Star	*HJD(min) 2400000+*	*Cycle*	*O–C*	*N*	*Type*	*Observer**	*Standard Error*
TY Del	55069.6861	10167	0.0540	141	CCD	MZK	0.0001
YY Del	55055.7648	15252	0.0106	88	CCD	SAH	0.0002
FZ Del	55058.7646	30304	–0.0390	84	CCD	SAH	0.0001
RZ Dra	55045.7930	19729	0.0483	88	CCD	SAH	0.0002
TW Dra	54925.8446	3844	0.0297	139	CCD	SAH	0.0001
TW Dra	55043.7303	3886	0.0279	163	CCD	SAH	0.0001
UZ Dra	54954.6709	4104	0.0029	143	CCD	SAH	0.0001
AR Dra	52332.6721	14003	0.0082	24	CCD	DKS	0.0001
AR Dra	54912.3465	17820	0.0108	91	CCD	OYE	0.0001
CM Dra	54970.2679	9521	–0.0025	35	CCD	OYE	0.0001
QW Gem	54544.3743	5708	–0.0010	250	CCD	SFV	0.0001
Z Her	55018.7701	10502	–0.0309	136	CCD	SAH	0.0003
SZ Her	54942.4034	15986	–0.0209	157	CCD	VJA	0.0001
SZ Her	55008.6693	16067	–0.0209	72	CCD	SAH	0.0001
SZ Her	55062.6636	16133	–0.0211	79	CCD	SAH	0.0001
TT Her	54913.8512	16356	0.0370	182	CCD	MZK	0.0002
TT Her	54987.7285	16437	0.0362	98	CCD	SAH	0.0002
TU Her	54933.8055	4796	–0.1909	105	CCD	SAH	0.0001
TU Her	54983.6776	4818	–0.1928	156	CCD	MZK	0.0001
UX Her	54996.7584	9894	0.0788	125	CCD	SAH	0.0003
CC Her	54986.7347	8834	0.1855	103	CCD	SAH	0.0001
CC Her	55059.5650	8876	0.1875	72	CCD	MZK	0.0001
CT Her	55009.6965	6990	0.0046	122	CCD	SAH	0.0003
LT Her	54945.7970	13090	–0.1219	202	CCD	MZK	0.0002
WY Hya	54932.6618	20058	0.0279	76	CCD	SAH	0.0004
WY Hya	54946.6225	20077.5	0.0265	44	CCD	SAH	0.0003
DF Hya	54904.7758	36651	–0.0128	84	CCD	SAH	0.0001
DF Hya	54939.6540	36756.5	–0.0134	81	CCD	SAH	0.0002
SW Lac	55043.7617	30458	–0.1032	140	CCD	SAH	0.0001
CM Lac	55066.6948	17474	–0.0022	140	CCD	SAH	0.0001
CM Lac	55074.7168	17479	–0.0037	522	CCD	MZK	0.0001
Y Leo	54905.5831	5616	–0.0167	112	CCD	GHS	0.0001
Y Leo	54915.6988	5622	–0.0176	61	CCD	PRX	0.0003
UV Leo	54904.6844	27436	0.0320	123	CCD	SAH	0.0001
WZ Leo	54905.7266	16894	–2.4730	97	CCD	SAH	0.0002
XY Leo	54908.4031	34614.5	0.0404	43	CCD	CLZ	0.0003
AP Leo	50538.602	25565	–0.032	1	CCD	CK	—
AP Leo	51610.619	28056	–0.036	1	CCD	CK	—
AP Leo	52644.7667	30459	–0.0374	38	CCD	DKS	0.0002

Table 1 continued on following pages

Table 1. Recent times of minima of stars in the AAVSO eclipsing binary program, cont.

Star	HJD(min) 2400000+	Cycle	O–C	N	Type	Observer*	Standard Error
AP Leo	54940.2878	35793	–0.0438	80	CCD	OYE	0.0001
CE Leo	54977.2843	32725.5	–0.0139	75	CCD	OYE	0.0001
RT LMi	52351.5523	19602	–0.0050	47	CCD	DKS	0.0001
RT LMi	52354.5517	19610	–0.0050	31	CCD	DKS	0.0002
RT LMi	52403.6660	19741	–0.0049	18	CCD	DKS	0.0001
RT LMi	52689.7270	20504	–0.0064	34	CCD	DKS	0.0010
RT LMi	52964.9170	21238	–0.0062	34	CCD	DKS	0.0001
RT LMi	54912.4204	26432.5	–0.0143	110	CCD	OYE	0.0001
SS Lib	54980.7001	9614	0.1244	86	CCD	SAH	0.0002
RY Lyn	54912.5950	8380	–0.0474	99	CCD	SAH	0.0002
UZ Lyr	54982.7043	5971	–0.0265	103	CCD	HES	0.0002
EW Lyr	54933.7527	14591	0.2384	113	CCD	HES	0.0001
EW Lyr	55011.7016	14631	0.2384	96	CCD	SAH	0.0001
EW Lyr	55050.6767	14651	0.2390	51	CCD	MZK	0.0001
FL Lyr	55045.6128	7724	–0.0043	382	CCD	MZK	0.0002
FL Lyr	55058.6838	7730	–0.0022	116	CCD	SAH	0.0002
AT Mon	54932.6277	13960	0.0085	50	CCD	SAH	0.0004
EP Mon	54905.7105	19177	0.0342	150	CCD	GHS	0.0006
V508 Oph	54987.7142	28728	–0.0171	155	CCD	SAH	0.0001
V508 Oph	55013.3950	28802.5	–0.0233	83	CCD	OYE	0.0001
V508 Oph	55030.2914	28851.5	–0.0217	55	CCD	OYE	0.0001
V508 Oph	55074.6009	28980	–0.0180	62	CCD	SAH	0.0001
V839 Oph	54982.7072	35536	0.2366	106	CCD	SAH	0.0002
V1010 Oph	55005.6669	24293	–0.1271	75	CCD	SAH	0.0003
EF Ori	54887.4659	1566.5	0.0095	130	CCD	CLZ	0.0009
FL Ori	54904.5815	6162	0.0342	67	CCD	SAH	0.0001
FL Ori	54904.5818	6162	0.0345	87	CCD	GHS	0.0001
FZ Ori	54891.6364	27169	–0.0578	75	CCD	GHS	0.0003
FZ Ori	54912.6342	27221.5	–0.0593	81	CCD	SAH	0.0003
GU Ori	54905.6039	25146	–0.0435	98	CCD	SAH	0.0002
U Peg	54786.2599	48761	–0.1261	47	CCD	OYE	0.0001
U Peg	54792.2558	48777	–0.1267	140	CCD	OYE	0.0001
U Peg	54803.3116	48806.5	–0.1269	52	CCD	OYE	0.0003
BB Peg	55022.7710	31143.5	–0.0031	115	CCD	MZK	0.0001
BB Peg	55044.8219	31204.5	–0.0038	48	CCD	SAH	0.0004
GP Peg	55062.7882	14170	–0.0454	77	CCD	SAH	0.0002
IK Per	54880.2727	40653	–0.1694	175	CCD	OYE	0.0001
IU Per	54895.5985	10833	0.0096	50	CCD	SAH	0.0005
AV Pup	54901.6674	42642	0.1330	67	CCD	PRX	0.0002

Table 1 continued on following pages

Table 1. Recent times of minima of stars in the AAVSO eclipsing binary program, cont.

Star	*HJD(min) 2400000+*	*Cycle*	*O–C*	*N*	*Type*	*Observer**	*Standard Error*
U Sge	54996.7204	11201	–0.0081	126	CCD	SAH	0.0002
U Sge	55067.7131	11222	–0.0084	146	CCD	SAH	0.0001
V505 Sgr	55044.6829	8947	–0.0596	113	CCD	SAH	0.0002
V1968 Sgr	55008.7890	30516	–0.0139	82	CCD	SAH	0.0002
AO Ser	54939.6925	23661	–0.0115	104	CCD	SAH	0.0001
AO Ser	54968.7113	23694	–0.0112	97	CCD	HES	0.0001
AU Ser	52452.4111	20000	–0.0806	21	CCD	BAMA	0.0003
AU Ser	53078.9254	21621	–0.0842	38	CCD	DKS	0.0001
AU Ser	55013.3426	26626	–0.1038	138	CCD	OYE	0.0001
CC Ser	54933.8224	33820	0.9227	65	CCD	SAH	0.0004
CC Ser	55009.6808	33967	0.9282	96	CCD	SAH	0.0003
TY Tau	54895.5573	31283	0.2502	51	CCD	SAH	0.0004
WY Tau	54925.6374	25295	0.0557	107	CCD	HES	0.0002
WY Tau	54925.6380	25295	0.0563	68	CCD	SAH	0.0003
X Tri	55056.8244	12922	–0.0745	71	CCD	SAH	0.0001
W UMa	54903.6751	27389	–0.0606	207	CCD	MZK	0.0001
TY UMa	54903.7848	43355	0.2673	85	CCD	MZK	0.0001
TY UMa	54904.6719	43357.5	0.2681	71	CCD	PRX	0.0002
TY UMa	54938.7095	43453.5	0.2699	106	CCD	SAH	0.0002
UX UMa	54912.7689	88879	0.0018	47	CCD	SAH	0.0001
UX UMa	54933.6158	88985	0.0015	51	CCD	SAH	0.0001
UX UMa	54953.6762	89087	0.0015	52	CCD	SAH	0.0003
UX UMa	54970.3893	89172	–0.0025	25	CCD	OYE	0.0002
UX UMa	54975.3057	89197	–0.0029	82	CCD	OYE	0.0002
UX UMa	55004.4181	89345	0.0022	38	CCD	OYE	0.0001
VV UMa	54865.3333	13166	–0.0483	92	CCD	OYE	0.0001
VV UMa	54908.6375	13229	–0.0490	71	CCD	PRX	0.0002
VV UMa	54911.3795	13233	–0.0565	140	CCD	OYE	0.0001
VV UMa	54912.7628	13235	–0.0480	115	CCD	SAH	0.0002
XZ UMa	54912.8045	7154	–0.0988	89	CCD	SAH	0.0001
ZZ UMa	54945.6687	8261	–0.0022	86	CCD	MZK	0.0001
AF UMa	54982.6946	5361	0.5422	130	CCD	SAH	0.0004
BM UMa	54887.5962	64667	0.0092	100	CCD	CLZ	0.0001
BM UMa	54946.3095	64883.5	0.0032	55	CCD	OYE	0.0002
BM UMa	54964.3473	64950	0.0048	59	CCD	OYE	0.0002
KM UMa	54940.3492	6935	–0.0029	70	CCD	OYE	0.0001
KM UMa	54951.2574	6966	–0.0024	60	CCD	OYE	0.0001
W UMi	54895.5959	12470	–0.1624	66	CCD	SAH	0.0007
RU UMi	54912.6509	25368	–0.0129	124	CCD	HES	0.0001

Table 1 continued on following page

Table 1. Recent times of minima of stars in the AAVSO eclipsing binary program, cont.

Star	HJD(min) 2400000+	Cycle	O–C	N	Type	Observer*	Standard Error
RU UMi	54913.7005	25370	–0.0132	83	CCD	PRX	0.0002
RU UMi	54934.6974	25410	–0.0133	80	CCD	PRX	0.0001
VV Vir	54891.8051	53057	–0.0384	92	CCD	SAH	0.0001
AG Vir	54914.7267	14755	0.0003	271	CCD	MZK	0.0002
AG Vir	54934.6502	14786	0.0016	192	CCD	MZK	0.0003
AH Vir	54905.7824	22308.5	0.2152	91	CCD	SAH	0.0002
AH Vir	54939.8099	22392	0.2147	81	CCD	SAH	0.0004
AH Vir	54986.6748	22507	0.2147	65	CCD	SAH	0.0004
AK Vir	54933.6824	10353	–0.0467	95	CCD	SAH	0.0001
AW Vir	54938.6532	28011.5	0.0226	98	CCD	SAH	0.0001
AW Vir	54938.6532	28011.5	0.0226	98	CCD	PRX	0.0001
AW Vir	54977.5933	28121.5	0.0231	70	CCD	MZK	0.0001
AW Vir	54989.6294	28155.5	0.0233	74	CCD	MZK	0.0001
AW Vir	54998.2966	28180	0.0175	123	CCD	OYE	0.0001
AZ Vir	54904.7801	31253.5	–0.0184	66	CCD	SAH	0.0003
AZ Vir	54924.7101	31310.5	–0.0193	50	CCD	MZK	0.0002
AZ Vir	54924.7101	31310.5	–0.0193	—	CCD	PRX	0.0002
AZ Vir	54937.6478	31347.5	–0.0192	86	CCD	MZK	0.0002
BH Vir	54934.7379	14328	–0.0075	86	CCD	MZK	0.0001
BH Vir	54943.7225	14339	–0.0085	76	CCD	PRX	0.0002
Z Vul	54939.8200	4885	–0.0103	87	CCD	SAH	0.0004
AW Vul	55017.7063	10828	–0.0146	69	CCD	SAH	0.0003
AX Vul	55066.6453	5044	–0.0306	95	CCD	SAH	0.0002
AY Vul	55017.7260	5112	–0.0790	71	CCD	SAH	0.0003
BE Vul	55074.7077	9641	0.0705	108	CCD	SAH	0.0001
BO Vul	55062.8061	9802	–0.0328	75	CCD	SAH	0.0001
BS Vul	55005.6791	24653	–0.0235	93	CCD	SAH	0.0002
BT Vul	55005.7164	17178	0.0028	73	CCD	SAH	0.0003
BT Vul	55011.4193	17183	–0.0003	84	CCD	OYE	0.0001
BT Vul	55061.6364	17227	0.0040	121	CCD	MZK	0.0001
BU Vul	55058.7044	37830	0.0162	87	CCD	SAH	0.0001
CD Vul	55008.7330	12739	0.0004	100	CCD	SAH	0.0001
CD Vul	55069.5860	12828	0.0001	97	CCD	MZK	0.0001
GR Vul	55063.2953	16018	–0.0355	—	CCD	OYE	0.0002
HS Vul	55073.2919	55151	–0.0117	—	CCD	OYE	0.0001

**Observers: BAMA, L. Baldinelli and A. Maitan; CK , S. Cook; CLZ, L. Corp; DKS, S. Dvorak; GHS, H. Gerner; HES, C. Hesseltine; MZK, K. Menzies; OYE, Y. Ogmen; PRX, R. Poklar; SAH, G. Samolyk; SFV, F. Salvaggio; VJA, J. Virtanen.*

Photometry of V578 Monocerotis

Arnold M. Heiser
Dyer Observatory, Vanderbilt University, Brentwood, TN 37027

Received September 16, 2009; revised January 4, 2010; accepted January 4, 2010;
a.heiser@vanderbilt.edu

Abstract V578 Monocerotis (= HDE 259135), a member of the galactic cluster NGC 2244, is an eclipsing binary containing two early B-type stars with a period of 2.4048 days. From early photometric observations of V578 Mon obtained by the author, and from data by D. S. Hall's collaborators (Anon. 1995), both the orbital period, noted above, and an apsidal motion period of about 30.4 years was determined. The current study is a summary of all the *UBV* photometric data obtained by the author from 1962 through the 2005–2006 season. The purposes of this study were to obtain an improved orbital period of this eclipsing binary, to determine a better estimate of the apsidal motion period, and to search for any light curve changes over time.

1. Introduction

The photometric variations of HDE 259135 (= V578 Mon) were accidentally discovered during a *uvby*-β study of the galactic open cluster NGC 2244 (Hardie 1970; Heiser 1977). The star was noted, from only two radial velocity observations, as a possible variable by Hayford (1932). Morgan *et al.* (1965) in their spectral type study of the stars in NGC 2244 noted that spectra of HDE 259135 (B0.5V) showed double lines. The double lined nature was verified by spectra obtained at the Kitt Peak National Observatory (KPNO) by Heiser (1972). Radial velocities from these spectra and the early photometry led to the first period determination of 2.420 days. From the variety of photometric observations of V578 Mon obtained by the author and by D. S. Hall's collaborators (Anon. 1995), an apsidal motion period of approximately 30 years was estimated. A detailed study of the physical properties of the system was undertaken by Hensberge *et al.* (2000).

The current study is a summary of all the photometric data obtained by the author, from 1962 through the 2005–2006 season, at various observatories: Dyer Observatory (DO), Kitt Peak National Observatory (KPNO), and the Vanderbilt-Tennessee State University (TSU) 16-inch (APT) at Fairborn Observatory. The purposes of this study were (i) to obtain an improved orbital period of this eclipsing binary, (ii) to determine a better estimate of the apsidal motion period, and (iii) to show the light curve changes over time.

2. Observations

The author's photometric *UBV* data can be divided into three sets based on the observational epochs and the different observatories.

(i) 1962–1970 (HJD 2437698 to HJD 2440703) at DO; 1–2 observations per night.

(ii) 1967–1983 (HJD 2439503 to HJD 2445703) at KPNO; 1–3 observations per night.

(iii) 1994–2006 (HJD 2449638 to HJD 2453842) at APT; continuous observations on some predicted minima nights, and many nights with single observations.

All the data are in differential form, in the sense "variable – comparison." Virtually every night also had check star observations, in the sense "comparison – check." The comparison star, from Johnson's study of NGC 2244 (1962), was HD 46106 (= Johnson 5 type B1V) and the check star was either HD 46149 (= Johnson 4 type O8.5V), or HD 46223 (= Johnson 3 type O5e). Table 1 is a summary of the average observational errors from the differential check star observations at the different epochs and observatories.

3. Analysis

3.1. Times of minimum and period determination

The sporadic nature of the differential *B* data collected at DO and at KPNO resulted in a number of times when there were values that appeared to be near a minimum of the light variation. These minimal values of ΔB, listed in Table 2, indicated a probable orbital period for V578 Mon of about 2.408 days, which was later confirmed by the work of Hall and his collaborators (Anon. 1995). This period, together with the arbitrarily chosen KPNO HJD 2443158.8443 time of minimum, was used to predict times of minima for the observations undertaken with the APT. Differential *BV* data obtained at the APT resulted in six additional times of primary minimum, also listed in Table 2, as well as a number of times of secondary minimum. All the times of minima from the APT data were determined using the method of Kwee and van Woerden (1956).

The ΔB times of minimum were used in the following manner to determine a significantly better orbital period for V578 Mon: The two times of minima, HJD 2443158.84434 (KPNO) and HJD 2451554.77106 (APT), were separately iterated using trial periods until the sum of the $(O–C)^2$ was minimized for all fourteen values of the primary minima determined from the ΔB measurements. These results are 2.40848475 days (KPNO) and 2.40847965 days (APT), which gives an average period of 2.4084822 ± 0.0000026 days. This period was used with an epoch of HJD 2451554.77106 ± 0.00057 to calculate all the phases of

the light variations of V578 Mon from 1962 to 2006.

The apsidal motion period was determined by measuring (O–C)' deviations from thirteen times of primary minima around epoch HJD 2451554.77106. Least square fits were made to data over the range of cycles –6000 to –3000 and –1000 to +1000, giving slopes, shown in Figure 1, of 0.000055 ± 0.000010 and 0.000054 ± 0.000005, respectively. Since these two estimates are identical within their uncertainties, one can calculate the HJD's of each set at their (O–C)' values of 0.0. The difference of these HJD's is about 10,517 days. A similar analysis, using the deviations from epoch HJD 2443158.84434, gives a difference of about 11,680 days. Averaging these two differences results in an apsidal period of about 30.4 years, which is in good agreement with the value quoted by Hall and his collaborators (Anon. 1995).

3.2. Light curves

All DO and KPNO differential Δ*B* data are shown in Figure 2. Observations around primary minimum, near phase 0.07, indicate that the 1973 to 1978 data occur at slightly later phases than those of 1968 to 1971. On the other hand, the data from 1973 to 1978 at secondary minimum, near phase 0.54, occur at slightly earlier phases than observations from 1968 to 1971. Observations outside of eclipse show a post-primary shoulder from phase 0.13 to 0.20, then a slight increase to a maximum phase near 0.3 with no shoulder going into secondary eclipse, and then a very slight rise from phase 0.6 to 0.95. These outside-of-eclipse observations indicate that there are effects due to the ellipsoidal nature of the two stars, limb darkening, or reflection effects from the more luminous star onto the less luminous star.

The average *UBV* color indices at each minimum of the DO and KPNO observations are shown in Table 3. These colors indicate that the more luminous star is somewhat hotter than the less luminous star.

The APT observations around primary and secondary minima show variations indicative of apsidal motion. Figure 3a shows the variations in Δ*B* at primary minimum for the seasons of 1994/1995/1996 (=94/95/96), 1999/2000, and 2005/2006. The light curves show the primary minimum depth *increasing with time* and *increasing in phase* from the 94/95/96 observations to the 2005/2006 observations. Figure 3b shows the variations in Δ*B* at secondary minimum for the seasons of 94/95/96, 1999/2000, and 2005/2006. At secondary minimum both the depths and the phases are *decreasing with time*. The changes at the minima over the APT 11–12-year time interval lends support to the apsidal period of 30.4 years determined above in section 3.1.

4. Summary

The very long baseline of these observations of V578 Mon underscores the value of acquiring and analyzing data obtained over long time periods. The *UBV*

observations of this binary, obtained from 1962 to 2006, were used to determine a more significant orbital period. Color changes at minimum light indicate that the primary has a somewhat higher surface temperature than the secondary. Changes in the light at minima support the presence of an apsidal motion period of about 30.4 years. A further analysis of these observations has been undertaken by Garcia *et al.* (2010).

5. Acknowledgements

The author wishes to acknowledge the support from Vanderbilt University, the staffs of the Dyer Observatory and the Kitt Peak National Observatory, and Greg Henry of the TSU Center of Excellence. The author also wishes to thank the referee for many valuable suggestions and comments.

References

Anon. 1995, *Bull. Amer. Astron. Soc.*, **27**, 687.
Garcia, E., Stassun, K. G., Hebb, L., Heiser, A. 2010, *Bull. Amer. Astron. Soc.*, **42**, 283.
Hayford, P. 1932, *Lick Obs. Bull.*, **16**, 53.
Hardie, R. H. 1970, *Bull. Amer. Astron. Soc.*, **2**, 32.
Heiser, A. M. 1972, *Bull. Amer. Astron. Soc.*, **4**, 27.
Heiser, A. M. 1977, *Astron. J.*, **82**, 973.
Hensberge, H., Pavlovski, K., and Verschueren, W. 2000, *Astron. Astrophys.*, **358**, 553.
Johnson, H. L. 1962, *Astrophys. J.*, **136**, 1135.
Kwee, K. K., and van Woerden, H. 1956, *Bull. Astron. Inst. Netherlands*, **12**, 327.
Morgan, W. W., Hiltner, W. A., Neff, J. S., Garrison, R., and Osterbrock, D. E. 1965, *Astrophys. J.*, **142**, 974.

Table 1. Average errors, in magnitudes, from V578 Mon check star observations.

Observatory	*Errors in* ΔV	*Errors in* ΔB	*Errors in* ΔU
DO	±0.004	±0.007	±0.004
KPNO	±0.004	±0.004	±0.004
APT	±0.002	±0.001	—

Table 2. HJD times of minima of V578 Mon.

Year	*Observatory*	*Time of Minimum*	*Time of Min. Error*	ΔB *value*
1962*	DO	2437698.7496	± 0.0002	0.778
1962*	DO	2437739.6617	± 0.0002	0.773
1969*	DO	2440292.6882	± 0.0002	0.786
1973*	KPNO	2442014.83162	± 0.0002	0.808
1973*	KPNO	2442043.70033	± 0.0002	0.817
1976*	KPNO	2443105.90927	± 0.0002	0.790
1977*	KPNO	2443158.84434	± 0.0002	0.795
1977*	KPNO	2443488.86693	± 0.0002	0.788
1995#	APT	2449738.75624	± 0.00085	0.762
1995#	APT	2449750.79842	± 0.00152	0.762
2000#	APT	2451554.77106	± 0.00057	0.791
2005#	APT	2453712.83465	± 0.00076	0.799
2005#	APT	2453724.87717	± 0.00063	0.799
2005#	APT	2453741.73648	± 0.00111	0.800

* *Time of minimum is the observation time of the "minimal"* ΔB *measures.*
\# *Time of minimum is from Kwee and van Woerden (1956) analyses.*

Table 3. Differential *UBV* color indices of V578 Mon at minima.

Type	Δ *(*B – V*)*	Δ *(*U – B*)*
Primary	0.046 ± 0.002	0.030 ± 0.002
Secondary	0.045 ± 0.003	0.026 ± 0.006

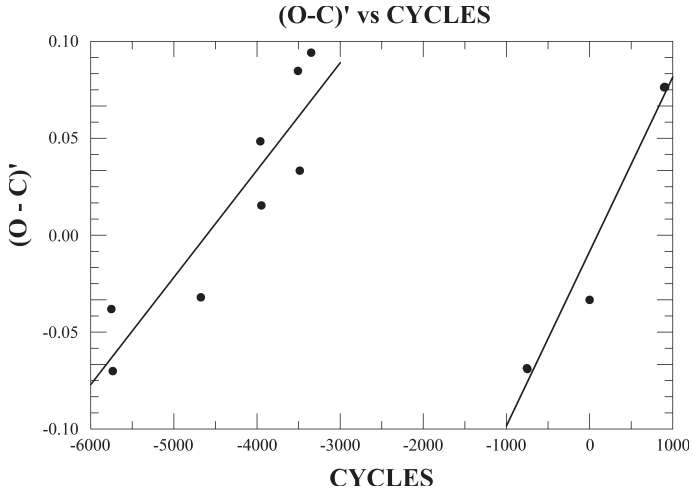

Figure 1. V578 Mon, deviations of the Table 2 times of minimum light as a function of the number of cycles, from the epoch HJD 2451554.77106.

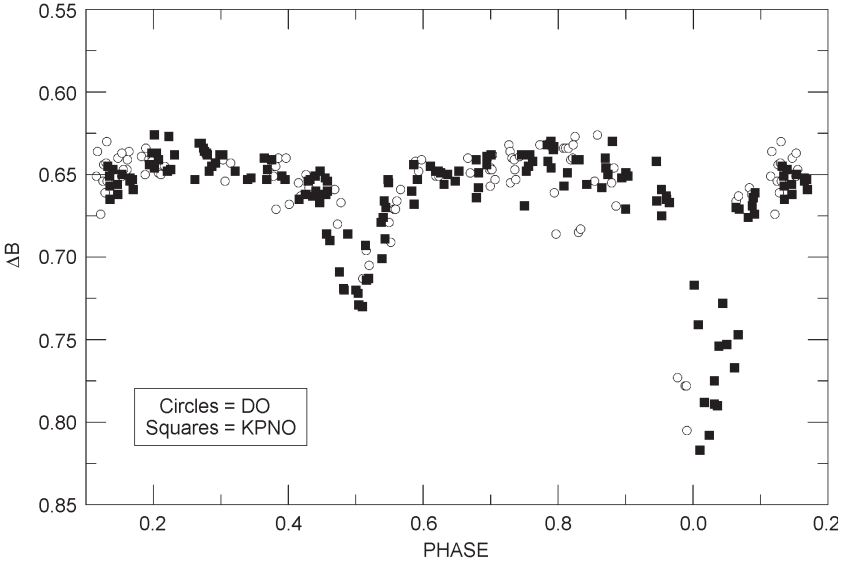

Figure 2. The differential *B* light curve for V578 Mon using the DO and KPNO data from 1968 through 1983.

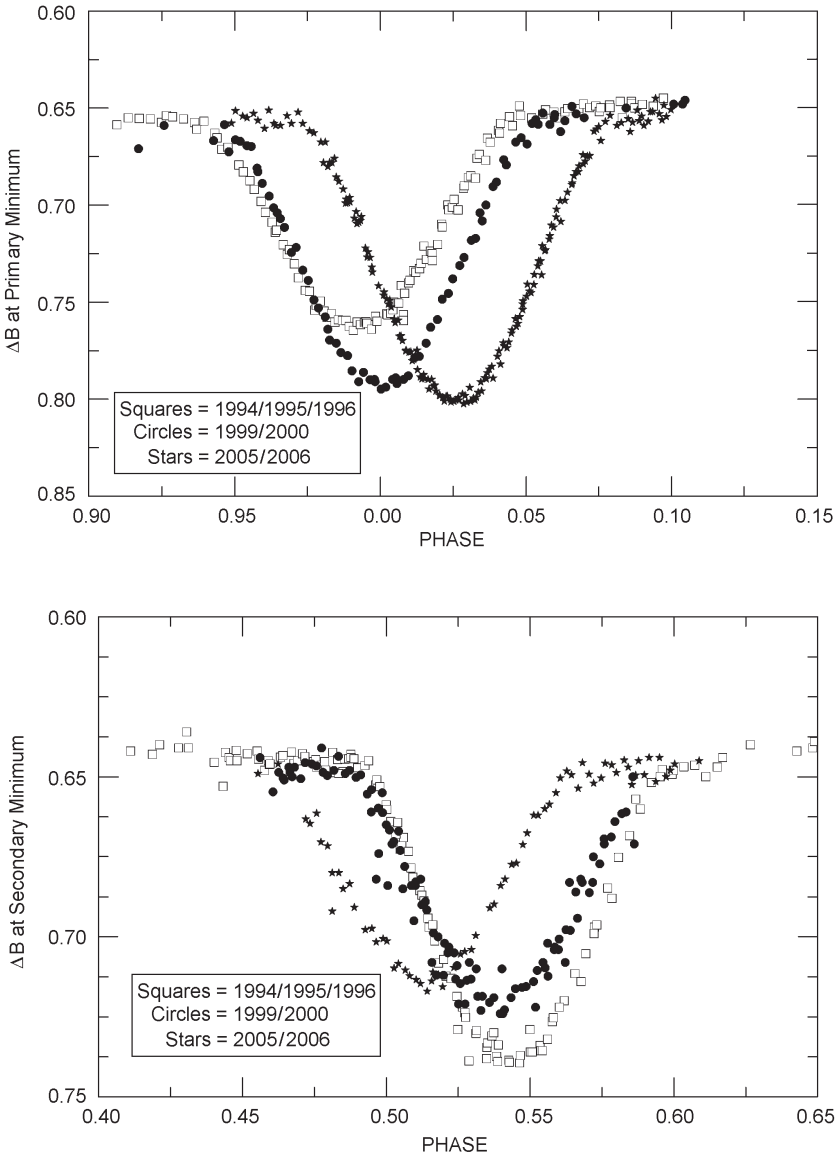

Figure 3. The APT differential *B* light curves around primary (top graph) and secondary (bottom graph) minimum for V578 Mon from 1994/1995/1996, 1999/2000, and 2005/2006. The curves show the increase in depth and phase over the indicated observing sessions.

RR Lyrae and Type II Cepheid Variables Adhere to a Common Distance Relation

Daniel J. Majaess
Saint Mary's University, Department of Astronomy and Physics, Halifax, Nova Scotia, B3H 3C3, Canada; dmajaess@ap.smu.ca

and

The Abbey Ridge Observatory, Stillwater Lake, Nova Scotia, Canada

Received October 30, 2009; revised December 21, 2009; accepted December 21, 2009

Abstract Preliminary evidence is presented reaffirming that SX Phe, RR Lyrae, and Type II Cepheid variables may be characterized by a common Wesenheit period-magnitude relation, to first order. Reliable distance estimates to RR Lyrae variables and Type II Cepheids are ascertained from a single *VI*-based reddening-free relation derived recently from OGLE photometry of LMC Type II Cepheids. Distances are computed to RR Lyrae ($d \simeq 260$ pc) and variables of its class in the galaxies IC 1613, M33, Fornax dSph, LMC, SMC, and the globular clusters M3, M15, M54, ω Cen, NGC 6441, and M92. The results are consistent with literature estimates, and in the particular cases of the SMC, M33, and IC 1613, the distances agree with those inferred from classical Cepheids to within the uncertainties: no corrections were applied to account for differences in metallicity. Moreover, no significant correlation was observed between the distances computed to RR Lyrae variables in ω Cen and their metallicity, despite a considerable spread in abundance across the sample. In sum, concerns regarding a sizeable metallicity effect are allayed when employing *VI*-based reddening-free Cepheid and RR Lyrae relations.

1. Introduction

The study of Cepheids and RR Lyrae variables has provided rich insight into countless facets of our Universe. The stars are employed: to establish distances to globular clusters, the Galactic center, and to galaxies exhibiting a diverse set of morphologies from dwarf, irregular, giant elliptical, to spiral in nature (Udalski *et al.* 2001; Kubiak and Udalski 2003; Pietrzyński *et al.* 2006; Macri *et al.* 2006; Matsunaga *et al.* 2006, 2009; Ferrarese *et al.* 2007; Feast *et al.* 2008; Groenewegen *et al.* 2008; Gieren *et al.* 2008; Scowcroft *et al.* 2009; Majaess *et al.* 2009c); to clarify properties of the Milky Way's spiral structure, bulge, and warped disk (Tammann 1970; Opolski 1988; Efremov 1997; Berdnikov *et al.* 2006; Majaess *et al.* 2009b); to constrain cosmological models by aiding to establish H_0 (Freedman and Madore 1996; Freedman *et al.* 2001; Tammann *et al.* 2002); to characterize extinction where such variables exist in the Galaxy and beyond

(Caldwell and Coulson 1985; Turner 2001; Laney and Caldwell 2007; Kovtyukh *et al.* 2008; Majaess *et al.* 2008a, 2009b, 2009c); to deduce the sun's displacement from the Galactic plane (Shapley 1918; Fernie 1968; Majaess *et al.* 2009a); and to trace the chemistry, dynamics, and ages of stellar populations (Turner 1996; Luck *et al.* 1998; Andrievsky *et al.* 2002a; Mottini 2006), etc.

An additional bond beyond the aforementioned successes is shared between RR Lyrae, Type II Cepheids, and SX Phe variables, namely that to first order the stars obey a common distance and Wesenheit period-magnitude relation.

2. Analysis and discussion

A Wesenheit period-magnitude diagram demonstrates the underlying continuity from SX Phe to W Vir variables (Figure 1). The Wesenheit function describing the LMC data is given by:

$$W_{VI} = V - \beta (V - I)$$

$$W_{VI} = -2.45\, log\, P_f + 17.28 \quad (1)$$

The relation is reddening-free and relatively insensitive to the width of the instability strip, hence the reduced scatter in Figure 1. Readers are referred to studies by van den Bergh (1968), Madore (1982), Opolski (1983), Madore and Freedman (2009), and Turner (2010) for an elaborate discussion on Wesenheit functions. The color coefficient used here, $\beta = 2.55$, is that employed by Fouqué *et al.* (2007). RR Lyrae variables pulsating in the overtone were shifted by $log\, P_f \sim log\, P_o + 0.13$ so to yield the equivalent fundamental mode period (e.g., see Soszyński *et al.* 2003; Gruberbauer *et al.* 2007). Soszyński *et al.* (2008) convincingly demonstrated that the RV Tau subclass of Type II Cepheids do not follow a simple Wesenheit relation that also encompasses the BL Her and W Vir regimes (see also Majaess *et al.* 2009a). RV Tau variables were therefore excluded from the derived Wesenheit function which characterizes variables with pulsation periods $\lesssim$ 15d (Equation 1).

A *VI*-based reddening-free Type II Cepheid relation (Majaess *et al.* 2009a) was used to compute the distance to RR Lyrae variables in the galaxies IC 1613 (Dolphin *et al.* 2001), M33 (Sarajedini *et al.* 2006), Fornax dSph (Bersier and Wood 2002; Mackey and Gilmore 2003), LMC and SMC (Udalski *et al.* 1998; Soszyński *et al.* 2003, 2009), and the globular clusters M3 (Benkő *et al.* 2006; Hartman *et al.* 2005), M15 (Corwin *et al.* 2008), NGC 6441 (Layden *et al.* 1999; Pritzl *et al.* 2003), M54 (Layden and Sarajedini 2000), ω Cen (Weldrake *et al.* 2007), and M92 (Kopacki 2001). The resulting distances are summarized in Table 1, along with estimates from classical and Type II Cepheids, where possible. The calibrators of the aforementioned relation were OGLE LMC Type II Cepheids (Udalski *et al.* 1999; Soszyński *et al.* 2008), with an adopted zero-point to the LMC established from classical Cepheids and other means (~ 18.50, Gibson 2000; Freedman *et al.* 2001; Benedict *et al.* 2002; Majaess *et al.*

2008a). The distances to classical Cepheids were estimated using a Galactic calibration (Majaess *et al.* 2008a) tied to a subsample of cluster Cepheids (e.g., Turner and Burke 2002) and new HST parallax measures (Benedict *et al.* 2007). Defining the relation strictly as a Galactic calibration is somewhat ambiguous, given that Milky Way Cepheids appear to follow a galactocentric metallicity gradient (Andrievsky *et al.* 2002a). The Majaess *et al.* (2008a) relation is tied to Galactic classical Cepheids that exhibit near solar abundances (Andrievsky *et al.* 2002a). Applying the Majaess *et al.* (2008a) relation to classical Cepheids observed in the LMC by Sebo *et al.* (2002) reaffirms the adopted zero-point ($(m-M)_0 = 18.44 \pm 0.12$, Figure 2). No correction was applied to account for differences in metallicity between LMC and Galactic classical Cepheids owing to the present results and contested nature of the effect (e.g., Udalski *et al.* 2001; Sakai *et al.* 2004; Pietrzyński *et al.* 2004; Macri *et al.* 2006; Bono *et al.* 2008; Scowcroft *et al.* 2009; Majaess *et al.* 2009c). A decrease of $\simeq 0.08$ magnitude would ensue if the correction proposed by Sakai *et al.* (2004) or Scowcroft *et al.* (2009) were adopted.

The distances cited in Table 1 to the globular clusters are consistent with those found in the literature (e.g., Harris 1996). A subsample of period distance diagrams demonstrate that the inferred distances are nearly constant across the entire period range examined (Figure 3). Moreover, distances computed to RR Lyrae variables in the SMC, M33, and IC 1613 agree with those inferred from classical Cepheids (Table 1). The results reaffirm that the slope and zero-point of *VI* reddening-free relations are relatively insensitive to metallicity (see also Udalski *et al.* 2001; Pietrzyński *et al.* 2004; Majaess *et al.* 2008a, 2009c). No corrections were made to account for differences in abundance. Consider the result for the SMC, which is founded on copious numbers of catalogued RR Lyrae and classical Cepheid variables (OGLE). SMC and Galactic classical Cepheids exhibit a sizeable metallicity difference (Δ[Fe/H] $\simeq 0.75$, Mottini (2006)). By contrast, SMC RR Lyrae variables are analogous to or slightly more metal-poor than their LMC counterparts (Udalski 2000). If the canonical metallicity corrections for RR Lyrae variables and classical Cepheids were equal yet opposite in sign as proposed in the literature (e.g., $\gamma - RR \simeq +0.3$ and $\gamma - Cep \simeq -0.3$ magnitude dex^{-1}), then the expected distances computed for SMC RR Lyrae variables and classical Cepheids should display a considerable offset (say at least $\simeq 0.25$ magnitude). However, that is not supported by the evidence, which instead implies a negligible offset separating the variable types (0.02 magnitude, Table 1). Similar conclusions are reached when analyzing distances to extragalactic RR Lyrae variables as inferred from a combined HST/HIP parallax for RR Lyrae (see Majaess *et al.* 2009c). In sum, comparing Cepheids and RR Lyrae variables at a common zero-point offers a unique opportunity to constrain the effects of metallicity. More work is needed here.

RR Lyrae variables in ω Cen provide an additional test for the effects of metallicity on distance, since the population exhibits a sizeable spread in

metallicity at a common zero-point ($-1.0 \geq$ [Fe/H] ≥ -2.4, Rey *et al.* (2000)). An abundance-distance diagram (Figure 4) compiled for RR Lyrae variables in ω Cen using *VI* photometry from Weldrake *et al.* (2007), and abundance estimates from Rey *et al.* (2000), offers further evidence implying that *VI*-based reddening-free distance relations are relatively insensitive to metallicity. A formal fit to data in Figure 4 is in agreement with no dependence and yields a modest slope of 0.1 ± 0.1 magnitude dex^{-1}. If that slope is real, metal-poor RR Lyrae variables are brighter than metal-rich ones. Uncertainties linked to the cited slope could be mitigated by acquiring additional abundance estimates and obtaining *VI* directly (see Weldrake *et al.* 2007). A minor note is made that although the variable in ω Cen designated V164 Cen is likely a Type II Cepheid (J2000 $13^h\,26^m\,14.86^s$ –47° 21' 15.17"), the variable designated V109 Cen may be anomalous or could belong to another variable class (J2000 $13^h\,26^m\,35.69^s$ -47° 32' 47.03", see numbering in Weldrake *et al.* 2007).

Equation 2 of Majaess *et al.* (2009a) was also employed to compute the distance to the brightest member of the variable class, RR Lyrae. *VI* photometry from The Amateur Sky Survey (Droege *et al.* 2006) was utilized, although concerns persist regarding the survey's zero-point and the star's modulating amplitude. Nevertheless, the resulting distance of $d \simeq 260$ pc is consistent with the star's parallax as obtained using HST ($d = 262 \pm 14$ pc, Benedict *et al.* 2002), and within the uncertainties of the HIP value (van Leeuwen *et al.* 2007; Feast *et al.* 2008). That reaffirms the robustness of the aforementioned relation to compute distances to variables of the RR Lyrae and Type II Cepheid class. RR Lyrae's phased *V* and *I* light-curves are displayed in Figure 5. An ephemeris from the GEOS RR Lyr database was adopted to phase the data (Boninsegna *et al.* 2002; Le Borgne *et al.* 2004, 2007), namely:

$$JD_{max} = 2442923.4193 + 0.5668378\,E \qquad (2)$$

The slope of the Wesenheit function derived from a combined sample of SX Phe, RR Lyrae, and Type II Cepheid variables detected in M3, ω Cen, and M15 is consistent with that determined from LMC RR Lyrae variables and Type II Cepheids (Figure 1). Presently, the distances computed to SX Phe variables discovered in M3 and ω Cen via the *VI* reddening-free Type II relation of Majaess *et al.* (2009a) are systemically offset. However, the new Wesenheit relation performs better (Equation 1). A reanalysis is anticipated once a sizeable sample of SX Phe variables become available. Yet meanwhile Equation 1 may be employed to evaluate simultaneously the distances to SX Phe, RR Lyrae, BL Her, and W Vir variables. Uncertainties are expected to be on the order of 5–15%. Indeed, the correction factor (ϕ) established by Majaess *et al.* (2009a) could be applied to Equation 1 to permit the determination of distances to the RV Tau subclass of Type II Cepheids.

Admittedly, further work is needed but the results are encouraging.

3. Summary and future work

A single *VI*-based reddening-free relation may be employed to simultaneously provide reliable distances to RR Lyrae variables and Type II Cepheids. The relation's viability is confirmed by demonstrating that distances to RR Lyrae variables in the globular clusters M3, M15, M54, ω Cen, M92, NGC 6441 (Figure 6), and galaxies IC 1613, M33, Fornax dSph, LMC, and SMC, agree with values in the literature and from other means (Table 1, see also Harris 1996). A distance was computed for the nearby star RR Lyrae ($d \sim 260$ pc) using mean *VI* photometry provided by The Amateur Sky Survey. The estimate is consistent with the HST parallax for the star ($d = 262 \pm 14$ pc, Benedict *et al.* 2002). The slope and zero-point of the *VI*-based relation appear relatively unaffected by metallicity to within the uncertainties (Table 1 and Figures 1, 3). That assertion is supported by noting that although RR Lyrae variables in ω Cen exhibit a sizeable spread in metallicity ($-1.0 \geq [Fe/H] \geq -2.4$, Rey *et al.* (2000)), no statistically significant effect was observed on the computed distances (Figure 4). Furthermore, the distances computed to RR Lyrae variables and classical Cepheids in the SMC, M33, and IC 1613 are consistent to within the uncertainties. No metallicity correction was applied. Finally, an underlying Wesenheit period-magnitude relation broadly unifies SX Phe, RR Lyrae, and Type II Cepheid variables of the population II instability strip, although somewhat imperfectly.

There remain numerous challenges and concerns to be addressed regarding the use of the distance indicators beyond the contested effects of metallicity (e.g., Udalski *et al.* 2001; Sakai *et al.* 2004; Pietrzyński *et al.* 2004; Macri *et al.* 2006; Bono *et al.* 2008; Scowcroft *et al.* 2009; Majaess *et al.* 2009c). For example, achieving a common photometric standardization is difficult and systemic offsets may be introduced, particularly across a range in color (e.g., Turner 1990; Saha *et al.* 2006). Yet another challenge is to establish a consensus on the effects of photometric contamination (e.g., blending, crowding) on the distances to variable stars in distant galaxies (Stanek and Udalski 1999; Macri 2001; Mochejska *et al.* 2000, 2001, Mochejska 2002; Freedman *et al.* 2001; Majaess *et al.* 2009c). Increasing the presently small number of galaxies with Cepheids observed in both the central and less-crowded outer regions is therefore desirable (e.g., Macri *et al.* 2006; Scowcroft *et al.* 2009). Unfortunately, a degeneracy complicates matters since the effects of metallicity and crowding may act in the same sense and be of comparable magnitude. Indeed, R (the ratio of total to selective extinction) may also vary as a function of radial distance from the centers of galaxies in tandem with the metallicity gradient. Efforts to disentangle the degeneracies are the subject of a study in preparation. Further research is warranted to examine the implications of anomalous values of R on the distances obtained from the standard candles (e.g., Macri *et al.* 2001b; Udalski 2003).

Lastly, the continued discovery of extragalactic SX Phoenicis, RR Lyrae, and Cepheids at a common zero-point shall bolster our understanding and enable firm

constraints to be placed on the metallicity effect (Szabados 2006a; Poretti *et al.* 2006; Majaess *et al.* 2009c). So too will obtaining mean multiband photometry, particularly *VI*, for such variables in the field and globular clusters (Clement *et al.* 2001; Pritzl *et al.* 2003; Schmidt *et al.* 2004, 2005a, 2005b, 2005c, 2009; Horne 2005; Matsunaga *et al.* 2006; Randall *et al.* 2007; Rabidoux *et al.* 2007; Corwin *et al.* 2008). A forthcoming study shall describe how related efforts are to be pursued from the Abbey-Ridge Observatory (ARO) (Lane 2007; Majaess *et al.* 2008b; Turner *et al.* 2009). AAVSO members drawn toward similar research may be interested in a fellow member's study entitled: "Using a Small Telescope to Detect Variable Stars in Globular Cluster NGC 6779" (Horne 2005). Modest telescopes may serve a pertinent role in variable star research (Percy 1980, 1986; Szabados 2003; Paczyński 2006; Turner *et al.* 2005, 2009).

4. Acknowledgements

I am grateful to D. Weldrake, D. Bersier, G. Kopacki, V. Scowcroft, L. Macri, B. Pritzl, K. Sebo, A. Mackey, T. Corwin, A. Dolphin, A. Sarajedini, J. Hartman, J. Benkő, A. Layden, A. Udalski, and I. Soszyński (OGLE), whose comprehensive surveys were the foundation of the research, to the AAVSO and M. Saladyga, Centre de Données astronomiques de Strasbourg, NASA, ADS, L. Berdnikov, L. Szabados, J. F. Le Borgne, W. Renz, N. Carboni, and the RASC. The following reviews and books facilitated the preparation of the work: Wallerstein and Cox (1984), Freedman and Madore (1996), Feast (1999, 2001, 2008), Fernie (1969, 1976, 2002), Hoffleit (2002), Wallerstein (2002), Szabados (2006b), Smith (2004), and Marconi (2009).

References

Andrievsky, S. M., Kovtyukh, V. V., Luck, R. E., Lepine, J. R. D., Maciel, W. J., and Beletsky, Y. V. 2002a, *Astron. Astrophys.*, **392**, 491.

Benedict, G. F., *et al.* 2002, *Astron. J.*, **123**, 473.

Benedict, G. F., *et al.* 2007, *Astron. J.*, **133**, 1810.

Benkő, J. M., Bakos, G. A., and Nuspl, J. 2006, *Mon. Not. Roy. Astron. Soc.*, **372**, 1657.

Berdnikov, L. N., Efremov, Y. N., Glushkova, E. V., and Turner, D. G. 2006, *Odessa Astron. Publ.*, **18**, 26.

Bersier, D., and Wood, P. R. 2002, *Astron. J.*, **123**, 840.

Boninsegna, R., Vandenbroere, J., Le Borgne, J. F., and The Geos Team 2002, in *Radial and Nonradial Pulsations as Probes of Stellar Physics*, eds. C. Aerts, T. R. Bedding, and J. Chirsensen-Dalsgaard, ASP Conf. Proc. 259, Astron. Soc. Pacific, San Francisco, 166.

Bono, G., Caputo, F., Fiorentino, G., Marconi, M., and Musella, I. 2008, *Astrophys. J.*, **684**, 102.

Caldwell, J. A. R., and Coulson, I. M. 1985, *Mon. Not. Roy. Astron. Soc.*, **212**, 879.
Clement, C. M., *et al.* 2001, *Astron. J.*, **122**, 2587.
Corwin, T. M., Borissova, J., Stetson, P. B., Catelan, M., Smith, H. A., Kurtev, R., and Stephens, A. W. 2008, *Astron. J.* **135**, 1459.
Dolphin, A. E., *et al.* 2001, *Astrophys. J.*, **550**, 554.
Droege, T. F., Richmond, M. W., Sallman, M. P., and Creager, R. P. 2006, *Publ. Astron. Soc. Pacific*, **118**, 1666.
Efremov, Y. N. 1997, *Astron., Lett.*, **23**, 579.
Feast, M. W. 1999, *Publ. Astron. Soc. Pacific*, **111**, 775.
Feast, M. W. 2001, arXiv:astro-ph/0110360.
Feast, M. W. 2008, arXiv:0806.3019.
Feast, M. W., Laney, C. D., Kinman, T. D., van Leeuwen, F., and Whitelock, P. A. 2008, *Mon. Not. Roy. Astron. Soc.*, **386**, 2115.
Fernie, J. D. 1968, *Astron. J.*, **73**, 995.
Fernie, J. D. 1969, *Publ. Astron. Soc. Pacific*, **81**, 707.
Fernie, J. D. 1976, *The Whisper and the Vision: The Voyages of the Astronomers*, Clarke, Irwin, and Co., Toronto.
Fernie, J. D. 2002, *Setting Sail for the Universe: Astronomers and Their Discoveries*, Rutgers Univ. Press, New Brunswick, NJ.
Ferrarese, L., Mould, J. R., Stetson, P. B., Tonry, J. L., Blakeslee, J. P., and Ajhar, E. A. 2007, *Astrophys. J.*, **654**, 186.
Fouqué, P., *et al.* 2007, *Astron. Astrophys.*, **476**, 73.
Freedman, W. L., and Madore, B. F. 1996, in *Clusters, Lensing, and the Future of the Universe*, eds. V. Trimble and A. Reisenegger, ASP Conf. Proc. 88, Astron. Soc. Pacific, San Francisco, 9.
Freedman, W. L., *et al.* 2001, *Astrophys. J.*, **553**, 47.
Gibson, B. K. 2000, *Mem. Soc. Astron. Ital.*, **71**, 693.
Gieren, W., Pietrzyński, G., Soszyński, I., Bresolin, F., Kudritzki, R.-P., Storm, J., and Minniti, D. 2008, *Astrophys. J.*, **672**, 266.
Groenewegen, M. A. T., Udalski, A., and Bono, G. 2008, *Astron. Astrophys.*, **481**, 441.
Gruberbauer, M., *et al.* 2007, *Mon. Not. Roy. Astron. Soc.*, **379**, 1498.
Harris, W. E. 1996, *Astron. J.*, **112**, 1487.
Hartman, J. D., Kaluzny, J., Szentgyorgyi, A., and Stanek, K. Z. 2005, *Astron. J.*, **129**, 1596.
Hoffleit, D. 2002, *Misfortunes As Blessings in Disguise: The Story of My Life*, AAVSO, Cambridge, MA.
Horne, J. D. 2005, *J. Amer. Assoc. Var. Star Obs.*, **34**, 61.
Kopacki, G. 2001, *Astron. Astrophys.*, **369**, 862.
Kovtyukh, V. V., Soubiran, C., Luck, R. E., Turner, D. G., Belik, S. I., Andrievsky, S. M., and Chekhonadskikh, F. A. 2008, *Mon. Not. Roy. Astron. Soc.*, **389**, 1336.
Kubiak, M., and Udalski, A. 2003, *Acta Astron.*, **53**, 117.
Lane, D. J. 2007, http://www.aavso.org/aavso/meetings/spring07present/Lane.ppt

Laney, C. D., and Caldwell, J. A. R. 2007, *Mon. Not. Roy. Astron. Soc.*, **377**, 147.
Layden, A. C., Ritter, L. A., Welch, D. L., and Webb, T. M. A. 1999, *Astron. J.*, **117**, 1313.
Layden, A. C., and Sarajedini, A. 2000, *Astron. J.*, **119**, 1760.
Le Borgne, J. F., Klotz, A., and Boer, M. 2004, *Inf. Bull. Var. Stars*, No. 5568, 1.
Le Borgne, J. F., *et al.* 2007, *Astron. Astrophys.*, **476**, 307.
Luck, R. E., Moffett, T. J., Barnes, T. G., and Gieren, W. P. 1998, *Astron. J.*, **115**, 605.
Mackey, A. D., and Gilmore, G. F. 2003, *Mon. Not. Roy. Astron. Soc.*, **345**, 747.
Macri, L. M. 2001, Ph.D. Thesis.
Macri, L. M., Stanek, K. Z., Sasselov, D. D., Krockenberger, M., and Kaluzny, J. 2001a, *Astron. J.*, **121**, 870.
Macri, L. M., *et al.* 2001b, *Astrophys. J.*, **549**, 721.
Macri, L. M., Stanek, K. Z., Bersier, D., Greenhill, L. J., and Reid, M. J. 2006, *Astrophys. J.*, **652**, 1133.
Madore, B. F. 1982, *Astrophys. J.*, **253**, 575.
Madore, B. F., and Freedman, W. L. 2009, *Astrophys. J.*, **696**, 1498.
Majaess, D. J., Turner, D. G., and Lane, D. J. 2008a, *Mon. Not. Roy. Astron. Soc.*, **390**, 1539.
Majaess, D. J., Turner, D. G., and Lane, D. J. 2009a, *Mon. Not. Roy. Astron. Soc.*, **398**, 263.
Majaess, D. J., Turner, D. G., and Lane, D. J. 2009b, *J. Amer. Assoc. Var. Star Obs.*, **37**, 179.
Majaess, D. J., Turner, D. G., and Lane, D. J. 2009c, arXiv:0909.0181.
Majaess, D. J., Turner, D. G., Lane, D. J., and Moncrieff, K. E. 2008b, *J. Amer. Assoc. Var. Star Obs.*, **36**, 90.
Marconi, M. 2009, arXiv:0909.0900.
Matsunaga, N., Feast, M. W., and Menzies, J. W. 2009, *Mon. Not. Roy. Astron. Soc.*, **397**, 933.
Matsunaga, N., *et al.* 2006, *Mon. Not. Roy. Astron. Soc.*, **370**, 1979.
Mochejska, B. J. 2002, Ph.D. Thesis.
Mochejska, B. J., Macri, L. M., Sasselov, D. D., and Stanek, K. Z. 2000, *Astron. J.*, **120**, 810.
Mochejska, B. J., Macri, L. M., Sasselov, D. D., and Stanek, K. Z. 2001, arXiv: astro-ph/0103440.
Mottini, M. 2006, Ph.D. Thesis.
Opolski, A. 1983, *Inf. Bull. Var. Stars*, No. 2425, 1.
Opolski, A. 1988, *Acta Astron.*, **38**, 375.
Paczyński, B. 2006, *Publ. Astron. Soc. Pacific*, **118**, 1621.
Percy, J. R. 1980, *J. Roy. Astron. Soc. Canada*, **74**, 334.
Percy, J. R. 1986, *The Study of Variable Stars Using Small Telescopes*, Cambridge Univ. Press, Cambridge, UK.

Pietrzyński, G., Gieren, W., Udalski, A., Bresolin, F., Kudritzki, R. -P., Soszyński, I., Szymański, M., and Kubiak, M. 2004, *Astron. J.*, **128**, 2815.
Pietrzyński, G., *et al.* 2006, *Astron. J.*, **132**, 2556.
Pritzl, B. J., Smith, H. A., Stetson, P. B., Catelan, M., Sweigart, A. V., Layden, A. C., and Rich, R. M. 2003, *Astron. J.*, **126**, 1381.
Poretti, E., *et al.* 2006, *Mem. Soc. Astron. Ital.*, **77**, 219.
Rabidoux, K., *et al.* 2007, *Bull. Amer. Astron. Soc.*, **39**, 845.
Randall, J. M., Rabidoux, K., Smith, H. A., De Lee, N., Pritzl, B., and Osborn, W. 2007, *Bull. Amer. Astron. Soc.*, **38**, 276.
Rey, S.-C., Lee, Y.-W., Joo, J.-M., Walker, A., and Baird, S. 2000, *Astron. J.*, **119**, 1824.
Saha, A., Thim, F., Tammann, G. A., Reindl, B., and Sandage, A. 2006, *Astrophys. J., Suppl. Ser.*, **165**, 108.
Sakai, S., Ferrarese, L., Kennicutt, R. C., Jr., and Saha, A. 2004, *Astrophys. J.*, **608**, 42.
Sarajedini, A., Barker, M. K., Geisler, D., Harding, P., and Schommer, R. 2006, *Astron. J.*, **132**, 1361.
Schmidt, E. G., Hemen, B., Rogalla, D., and Thacker-Lynn, L. 2009, *Astron. J.*, **137**, 4598.
Schmidt, E. G., Johnston, D., Langan, S., and Lee, K. M. 2004, *Astron. J.*, **128**, 1748.
Schmidt, E. G., Johnston, D., Langan, S., and Lee, K. M. 2005a, *Astron. J.*, **129**, 2007.
Schmidt, E. G., Johnston, D., Langan, S., and Lee, K. M. 2005b, *Astron. J.*, **130**, 832.
Schmidt, E. G., Langan, S., Rogalla, D., and Thacker-Lynn, L. 2005c, *Bull. Amer. Astron. Soc.*, **37**, 1334.
Scowcroft, V., Bersier, D., Mould, J. R., and Wood, P. R. 2009, *Mon. Not. Roy. Astron. Soc.*, **396**, 1287.
Sebo, K. M., *et al.* 2002, *Astrophys. J.* S, **142**, 71.
Shapley, H. 1918, *Astrophys. J.*, **48**, 279.
Smith, H. A. 2004, *RR Lyrae Stars*, Cambridge Univ. Press, Cambridge, UK, 166.
Soszyński, I., *et al.* 2002, *Acta Astron.*, **52**, 369.
Soszyński, I., *et al.* 2003, *Acta Astron.*, **53**, 93.
Soszyński, I., *et al.* 2008, *Acta Astron.*, **58**, 293.
Soszyński, I., *et al.* 2009, *Acta Astron.*, **59**, 1.
Stanek, K. Z., and Udalski, A. 1999, arXiv:astro-ph/9909346.
Szabados, L. 2003, in *The Future of Small Telescopes in the New Millennium. Vol. 3*, ed. T. D. Oswalt, Astrophys. Space Sci. Lib., 289, Kluwer, Dordrecht, 207.
Szabados, L. 2006a, *Commmun. Konkoly Obs.*, **104**, 105.
Szabados, L. 2006b, *Odessa Astron. Publ.*, **18**, 111.
Tammann, G. A. 1970, in *The Spiral Structure of Our Galaxy*, ed. W. Becker and G. T. Kontopoulos, IAU Symp. 38, 236.

Tammann, G. A., Reindl, B., Thim, F., Saha, A., and Sandage, A. 2002, in *A New Era in Cosmology*, eds. N. Metcalfe and T. Shanks, ASP Conf. Proc. 283, Astron. Soc. Pacific, San Francisco, 258.
Turner, D. G. 1990, *Publ. Astron. Soc. Pacific*, **102**, 1331.
Turner, D. G. 1996, *J. Roy. Astron. Soc. Canada*, **90**, 82.
Turner, D. G. 2001, *Odessa Astron. Publ.*, **14**, 166.
Turner, D. G. 2010, *Astrophys. Space Sci.*, **326**, 219.
Turner, D. G., and Burke, J. F. 2002, *Astron. J.*, **124**, 2931.
Turner, D. G., Majaess, D. J., Lane, D. J., Szabados, L., Kovtyukh, V. V., Usenko, I. A., and Berdnikov, L. N. 2009, in *Stellar Pulsation: Challenges For Theory and Observation*, AIP Conf. Proc. 1170, Amer. Inst. Physics, Melville, NY, 108.
Turner, D. G., Savoy, J., Derrah, J., Abdel-Sabour Abdel-Latif, M., and Berdnikov, L. N. 2005, *Publ. Astron. Soc. Pacific*, **117**, 207.
Udalski, A. 1998, *Acta Astron.*, **48**, 113.
Udalski, A. 2000, *Acta Astron.*, **50**, 279.
Udalski, A. 2003, *Astrophys. J.*, **590**, 284.
Udalski, A., Soszyński, I., Szymański, M., Kubiak, M., Pietrzyński, G., Woźniak, P., and Żebruń, K. 1999, *Acta Astron.*, **49**, 223.
Udalski, A., Szymański, M., Kubiak, M., Pietrzyński, G., Woźniak, P., and Żebruń, K. 1998, *Acta Astron.*, **48**, 1.
Udalski, A., Wyrzykowski, Ł, Pietrzyński, G., Szewczyk, O., Szymański, M., Kubiak, M., Soszyński, I., and Żebruń, K. 2001, *Acta Astron.*, **51**, 221.
van den Bergh, S. 1968, *J. Roy. Astron. Soc. Canada*, **62**, 145.
van Leeuwen, F., Feast, M. W., Whitelock, P. A., and Laney, C. D. 2007, *Mon. Not. Roy. Astron. Soc.*, **379**, 723.
Wallerstein, G. 2002, *Publ. Astron. Soc. Pacific*, **114**, 689.
Wallerstein, G., and Cox, A. N. 1984, *Publ. Astron. Soc. Pacific*, **96**, 677.
Weldrake, D. T. F., Sackett, P. D., and Bridges, T. J. 2007, *Astron. J.*, **133**, 1447.

Table 1. Distances to the sample.

Object	$(m - M)_0$ *(RR)*	$(m - M)_0$ *(TII)*[b]	$(m - M)_0$ *(TI)*	*Photometry*
IC 1613	24.40 ± 0.12	—	24.50 ± 0.12[a]	(6)
	—	24.52 ± 0.16 (n = 2)	24.35 ± 0.09	(9)
SMC	18.91 ± 0.08	18.85 ± 0.11	18.93 ± 0.10	(7, 8)
M33	24.54 ± 0.14	—	—	(9)
	—	24.54 (n = 1)	24.43 ± 0.14 (i) / 24.67 ± 0.07 (o)[c]	(10)
	—	24.5 ± 0.3	24.40 ± 0.17 (i)	(11)
Fornax dSph	20.53 ± 0.08	—	—	(5)
	20.57 ± 0.11	—	—	(4)
M54	17.15 ± 0.16	17.13 ± 0.06	—	(3)
M92	14.57 ± 0.12	—	—	(2)
NGC 6441	15.70 ± 0.06	15.69 ± 0.10	—	(1)
	15.74 ± 0.11	—	—	(16)
M3	15.04 ± 0.11	—	—	(12)
	15.04 ± 0.07	—	—	(15)
ω Cen	13.58 ± 0.14	—	—	(13)
M15	14.90 ± 0.11	—	—	(14)

Note: References: (1) Pritzl et al. 2003; (2) Kopacki 2001; (3) Layden and Sarajedini 2000; (4) Bersier and Wood 2002; (5) Mackey and Gilmore 2003; (6) Dolphin et al. 2001; (7) Udalski et al. 1998; (8) Soszyński et al. 2002; (9) Sarajedini et al. 2006; (10) Scowcroft et al. 2009; (11) Macri et al. 2001a; (12) Hartman et al. 2005; (13) Weldrake et al. 2007; (14) Corwin et al. 2008; (15) Benkő et al. 2006; (16) Layden et al. 1999.

[a]See discussion Dolphin et al. (2001). [b]Presently, the distance estimates for extragalactic Type II Cepheids should be interpreted cautiously owing to poor statistics and other concerns (Majaess et al. 2009c). [c]Distances to classical Cepheids occupying the outer (o) and inner (i) regions of M33.

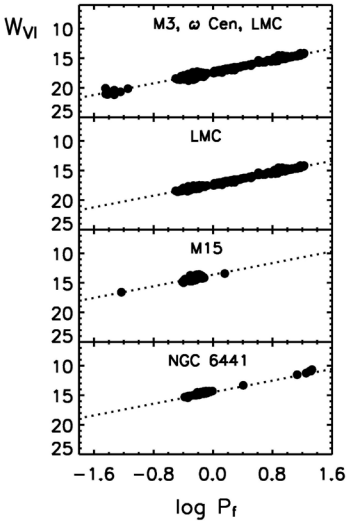

Figure. 1. Wesenheit diagrams demonstrate that SX Phe, RR Lyrae, and Type II Cepheid variables follow a common period-magnitude relation. Variable stars belonging to the globular clusters ω Cen and M3 were shifted in magnitude space to match the LMC. The over-plotted relation is Equation (1) after adjusting the zero-point. The fundamental mode period is plotted (log P_f).

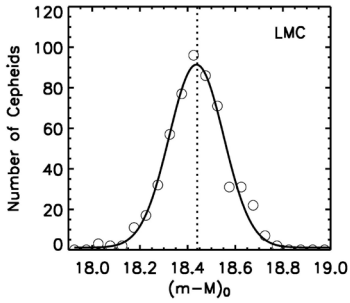

Figure. 2. Applying the *VI* reddening-free distance relation of Majaess *et al.* (2008a) to classical Cepheids observed in the LMC by Sebo *et al.* (2002) yields a distance modulus of $(m - M)_0 = 18.44 \pm 0.12$.

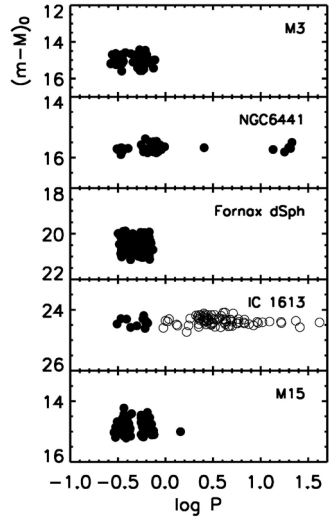

Figure. 3. Period-distance diagrams for a subsample of objects studied. Filled circles represent RR Lyrae variables and Type II Cepheids, while open circles denote classical Cepheids.

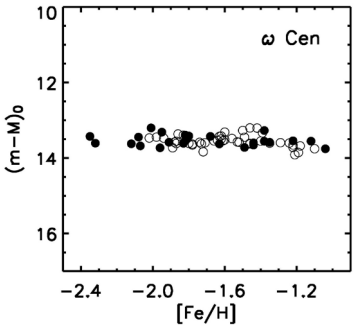

Figure. 4. Abundance-distance diagram for RR Lyrae variables in the globular cluster ω Cen. Open and filled circles are data points with metallicities inferred from $[Fe/H]_{hk}$ and $[Fe/H]_{\Delta S}$ methods (see Rey *et al.* 2000). A formal fit yields a modest slope of 0.1 ± 0.1 mag dex^{-1} and implies that metal-poor RR Lyrae variables are brighter than metal-rich ones. The fit is also in agreement with no correlation.

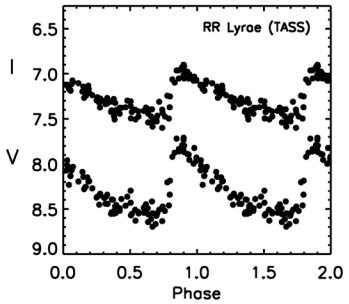

Figure. 5. *V* and *I* light-curves for RR Lyrae phased using equation 2. The *V*-band photometry is offset by +0.5 magnitude. The distance to RR Lyrae using The Amateur Sky Survey photometry is $d \simeq 260$ pc (see text).

Figure. 6. The metal rich globular cluster NGC 6441 observed through a 10-inch telescope (left) and the Hubble Space Telescope (right). Image by Noel Carboni.

Possible Misclassified Eclipsing Binary Stars Within the Detached Eclipsing Binary Light Curve Fitter (DEBiL) Data Set

Martin Nicholson
3 Grovelands, Daventry, Northamptonshire NN11 4DH, England

Received February 3, 2009; revised March 9, 2009, September 17, 2009; accepted September 23, 2009; martin_piers_nicholson@yahoo.co.uk

Abstract The dangers inherent in using fully automated data processing for large data sets are exemplified by examining the eclipsing binary stars identified via the Detached Eclipsing Binary Light curve fitter. The software may have confused eclipsing binaries with other types of low amplitude variable stars and it is estimated that over a quarter of the 10,862 variable stars listed may have been misclassified.

1. Introduction

The Detached Eclipsing Binary Light Curve Fitter (DEBiL; Devor 2005) was used to process 218,699 light curves from the galactic bulge fields of the Optical Gravitational Lensing Experiment (OGLE) survey (Udalski *et al.* 1997). A total of 10,862 binary stars were identified and details of these variable stars were made available via the VIZIER service (Ochsenbein *et al.* 2000) operated by Centre de Données astronomiques de Strasbourg (http://vizier.u-strasbg.fr/viz-bin/VizieR?-source=J/ApJ/628/411).

The data processing pipeline used by DEBiL involved passing the light curves through a series of analytical programs designed to create a more rigorous level of scrutiny at each tier. By eliminating light curves that failed to match the pre-set criteria for a given step it proved possible to focus computational resources on the ever-shrinking pool of candidate variable stars that reached the later tiers. A measure of the success of the technique was that step five of the process was only required for 10% of the light curves.

The light curve analysis involved six stages:

1. Determining the period.
2. Filtering out non-periodic curves.
3. Making an initial "guess" for the binary star parameters.
4. Filtering out non-eclipsing (pulsating) stars.
5. Fitting the parameters of a detached eclipsing binary star to the data.
6. Filtering out unsuccessful fits.

The limitations of DEBiL were explored in some detail by Devor (2005).

Light curves with very similar primary and secondary minima and light curves with no detectable secondary minima were particularly difficult for the software to analyse. The similarity between the light curves of some eclipsing and some non-eclipsing variable stars also created analytical problems.

Pribulla *et al.* (2009) further describe the difficulties associated with classifying low amplitude variable stars with periods between 0.1 and 0.5 day. Detailed study showed that most were δ Sct, RR Lyr, SX Phe, or γ Dor types, although some were contact binaries seen at low inclination angles. A further complication was the presence of companions to close binaries that might alter the observed light curve and the color of the combined system. Since the frequency of such companions "may be approaching 100%" the use of period-color diagrams as an analytical tool as suggested by Duerbeck (1997) may be invalid.

2. Objectives

A preliminary examination of the DEBiL data showed that over one in six of the variable stars listed had a period of over ten days. This compares with a figure of about one in sixteen for all the eclipsing binary stars listed in International Variable Star Index (VSX; Watson *et al.* 2007). This raised the suspicion that many of the stars listed in the catalogue were pulsating variables, as referred to by Devor (2005), rather than eclipsing binaries. It was also noted during the preliminary examination that only small scale variation—less than 0.2 magnitude—could be seen in the first ten light curves of long period variable stars that were examined in detail.

- Objective 1—to examine a random sample of stars to see if any of the variable stars listed as eclipsing binary stars had been misclassified
- Objective 2—to examine the characteristics of any misclassified variable stars to see if any such stars were spread equally throughout the entire DEBiL catalogue or if they shared one or more common features

3. Data and results

3.1. Experiment 1

A sample of twenty stars was selected from the entries in the DEBiL catalogue using the random number facility in MICROSOFT EXCEL. The prime aim of this experiment was to see if the phase diagram obtained for each star in the sample were consistent with the claim that the star was an eclipsing binary. Any attempt to identify the nature of the variability of any star not thought to be correctly classified was a secondary consideration and it was recognized that without additional information such identifications would be problematic.

Each star had its phase diagram generated using the software package PERANSO (Vanmunster 2007). These were then compared with phase diagrams for stars

known to belong to each of the three main sub-types of eclipsing binaries: EA, EB, and EW. The "saw tooth" shape of the phase diagrams obtained for seven of the twenty stars is quite unlike what would be expected for an eclipsing binary being more like those obtained from a pulsating or rotating ellipsoidal variable star. The phase diagram for an eclipsing binary of type EB or type EW is in the form of a continuous curve rather than as straight lines that come to a relatively sharp maximum or minimum. The comparison results were as follows:

Category	/20	Star #
Star is confirmed as an eclipsing binary with a close match between the period obtained via PERANSO and the period quoted in the catalogue.	13	1, 2, 3, 4, 7, 8, 10, 12, 13, 14, 15, 17, 19
Star appears not to be an eclipsing variable but there is a close match between the period obtained via PERANSO and the period quoted in the catalogue.	2	11, 16
Star appears not to be an eclipsing variable and the true period is half the period quoted in the catalogue.	5	5, 6, 9, 18, 20

It appeared to be the low amplitude variable stars that were particularly prone to misclassification by the software. All the variable stars with an amplitude > 0.20 magnitude were correctly classified whereas all the variable stars with an amplitude < 0.15 magnitude seem to have been misclassified. Unfortunately the on-line DEBiL database does not include the amplitude of variation and this can only be determined by examination of the individual light curves.

The results for the individual stars are summarized in Table 1 and phase plots for the possible misclassified variable stars are shown in Figures 1 to 7 inclusive.

3.2. Experiment 2

Ten DEBiL catalogue variable stars with quoted periods of over ten days were examined in detail using the software package peranso, with the following results:

Category	/10	Star #
Star is confirmed as an eclipsing binary with a close match between the period obtained via PERANSO and the period quoted in the catalogue.	0	
Star appears not to be an eclipsing variable but there is a close match between the period obtained via PERANSO and the period quoted in the catalogue.	8	22, 23, 24, 25, 26, 28, 29, 30
Star appears not to be an eclipsing variable and the true period is half the period quoted in the catalogue	2	21, 27

None of the supposed eclipsing binary stars had their classification confirmed since the shape of the phase diagrams obtained were quite unlike what would be expected for an eclipsing binary, being far more like those obtained from a pulsating variable star. The results for the individual stars are summarized in Table 2 and a specimen light curve and phase plot for a possibly misclassified star are provided in Figures 8 and 9.

4. Possible improvements to the Detached Eclipsing Binary Light Curve Fitter

A) Mis-classification of long period variable stars—Visual examination of the light curve and/or phase diagram of a small sample of the supposed long period binary stars identified by the automated data processing pipeline would have revealed possible errors in the algorithms being used. A simple filtering process could then have removed all such entries from the entire data set prior to publication.

B) Mis-classification of low amplitude variable stars—Pribulla *et al.* (2009) have described in some detail the difficulties associated with classifying low amplitude, short period variable stars. Obtaining spectra of candidate close binary systems was a key diagnostic tool but this technique was not used by Devor (2005) to check the operation of the algorithms within the Detached Eclipsing Binary Light curve fitter. Doubtless this was due to the large number of stars being examined.

C) Alternative approaches (1)—Eyer and Blake (2005) report an estimated classification error of 7% in the system they used with candidate variable stars from the All-Sky Automated Survey. The AUTOCLASS algorithm was able to generate results of this level of reliability using just four parameters— period, amplitude, phase difference, and amplitude ratio. Crucially, they discovered that adding parameters "...often does not improve the classification." Testing the algorithm on a sub-sample of the data as a prelude to refining the methodology was seen as desirable.

D) Alternative approaches (2)—The O'Connell effect (Wilsey and Beaky 2008) is the name given to the situation where there is an obvious difference between the two maxima in the light curves of an eclipsing system. Evidence of the O'Connell effect in the phase diagram of a variable star would be evidence of a binary, rather than a pulsating system. The article on the Detached Eclipsing Binary Light curve fitter (Devor 2005) makes no mention of using the O'Connell effect as a diagnostic tool.

5. Data access

Additional data relating to the possibly misclassified variable stars discussed in this paper can be downloaded from http://www.martin-nicholson.info/debil.xls. This file will also be archived and made available through the AAVSO ftp site at ftp://ftp.aavso.org/public/datasets/jnichm381.xls.

6. Summary

Over a quarter of the 10,862 variable stars listed in the DEBiL data set may have been misclassified and therefore the results published through VIZIER and subsequently imported into VSX need to be reviewed on a star-by-star basis.

7. Acknowledgements

This publication makes use of data products from The Two Micron All Sky Survey (Skrutskie *et al.* 2006), which is a joint project of the University of Massachusetts and the Infrared Processing and Analysis Center/California Institute of Technology, funded by the National Aeronautics and Space Administration and the National Science Foundation.

This research has made use of the VIZIER catalogue access tool, CDS, Strasbourg, France.

References

Devor, J. 2005, *Astrophys. J.*, **628**, 411.

Duerbeck, H. W. 1997, *Inf. Bull. Var. Stars*, No. 4513, 1.

Eyer L., and Blake C. 2005, *Mon. Not. Roy. Astron. Soc.*, **358**, 30.

Ochsenbein, F., Bauer, P., and Marcout, J. 2000, *Astron. Astrophys., Suppl. Ser.*, **143**, 23.

Pribulla, T., *et al.* 2009, *Astron J.*, **137**, 3655.

Skrutskie, M. F., *et al.* 2006, *Astron. J.*, **131**, 1163.

Udalski, A., Kubiak, M., and Szymański, M. 1997, *Acta Astron.*, **47**, 319.

Vanmunster, T. 2007, PERANSO period analysis software, http://www.peranso.com

Watson, C. L., Henden, A. A., and Price, A. 2007, *J. Amer. Assoc. Var. Star Obs.*, **35**, 414 (http://www.aavso.org/vsx/)

Wilsey, N. J., and Beaky, M. 2008, 23rd National Conference on Undergraduate Research, Dept. of Physics, Truman State Univ., Kirksville, MO, http://ncur.uwlax.edu/ncur2009/search/Display_NCUR.aspx?id=22667

Table 1. Details of initial random sample of twenty alleged eclipsing binary variable stars.

#	Name 2MASS J+#	Coordinates (J2000) h m s ° ‘ “	P(d)	Max	Min	Type
1	17284257-3925541	17 28 42.67 –39 25 53.2	0.359269	17.55	18.20	E
2	USNO-B1.0 0626-0704390	17 35 14.56 –27 19 55.8	1.233624	17.30	18.00	E
3	17471489-3456036	17 47 15.14 –34 56 01.4	0.658254	18.20	19.20	E
4	17474381-3450025	17 47 44.00 –34 50 03.2	1.015786	18.00	20.00	E
5	17504498-2954194	17 50 44.99 –29 54 19.0	76.29	14.74	14.82	P or R
6	17522545-3007032	17 52 25.44 –30 07 02.9	77.17	14.15	14.20	P or R
7	17522871-2938464	17 52 28.86 –29 38 47.1	0.288474	17.50	18.30	E
8	17540469-2944267	17 54 04.44 –29 44 24.6	1.098334	17.40	17.80	E
9	17574170-3110322	17 57 41.67 –31 10 31.5	36.17	14.09	14.17	P or R
10	17581939-2931358	17 58 19.41 –29 31 35.9	2.492962	17.50	18.20	E
11	17585070-2853195	17 58 50.72 –28 53 19.8	18.48	15.25	15.45	P or R
12	17590652-2909521	17 59 06.83 –29 09 52.7	0.775588	17.10	17.50	E
13	USNO-B1.0 0597-0652956	18 01 03.50 –30 15 35.1	0.589852	17.60	18.05	E
14	USNO-B1.0 0599-0653161	18 02 05.41 –30 05 05.4	10.342666	16.20	16.40	E
15	18021452-2856098	18 02 14.25 –28 56 11.2	3.937071	15.60	15.75	E
16	18023615-2957242	18 02 36.15 –29 57 23.7	12.67	15.35	15.50	P or R
17	18025968-3008587	18 02 59.45 –30 08 59.6	1.504424	14.80	14.95	E
18	18031230-2844088	18 03 12.31 –28 44 09.0	3.07	14.43	14.53	P or R
19	USNO-B1.0 0631-0688583	18 07 43.72 –26 52 27.8	0.502161	17.20	17.65	E
20	18103207-2637252	18 10 32.19 –26 37 26.7	0.171283	15.35	15.50	P or R

Table 2. Details of sample of ten alleged eclipsing binary variable stars with stated period > 10 days.

#	Name 2MASS J+#	Coordinates (J2000) h m s ° ‘ ‘‘	P(d)	Max	Min	Type
21	17531352-3256558	17 53 13.58 –32 56 55.5	188.71	14.01	14.06	P
22	17543116-2954252	17 54 31.13 –29 54 25.1	42.52	14.30	14.34	P
23	17543988-3304246	17 54 39.91 –33 04 24.6	56.95	15.30	15.42	P
24	17552582-2945223	17 55 25.82 –29 45 22.1	20.94	15.22	15.30	P
25	18015211-2828088	18 01 52.13 –28 28 08.8	55.40	14.80	14.90	P
26	18023379-2936335	18 02 33.79 –29 36 33.1	193.05	12.75	12.84	P
27	USNO-B1.0 0601-0660319	18 02 40.78 –29 49 08.7	49.40	15.44	15.61	P
28	USNO-B1.0 0615-0647851	18 04 37.91 –28 28 17.9	49.99	15.72	15.90	P
29	18050781-2745460	18 05 07.80 –27 45 46.5	10.40	14.62	14.70	P
30	18074728-3204384	18 07 47.24 –32 04 37.8	25.80	14.98	15.08	P

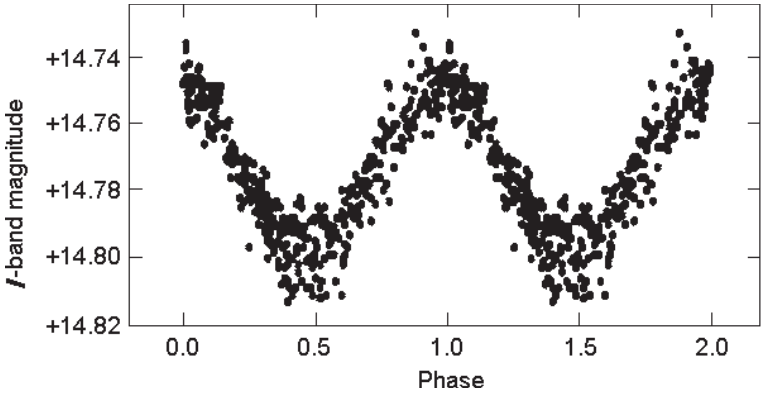

Figure 1. Phase diagram for star #5, 2MASS J17504498-2954194.

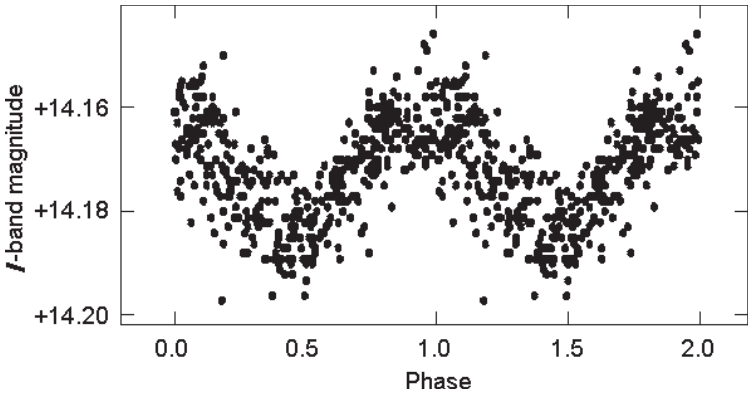

Figure 2. Phase diagram for star #6, 2MASS J17522545-3007032.

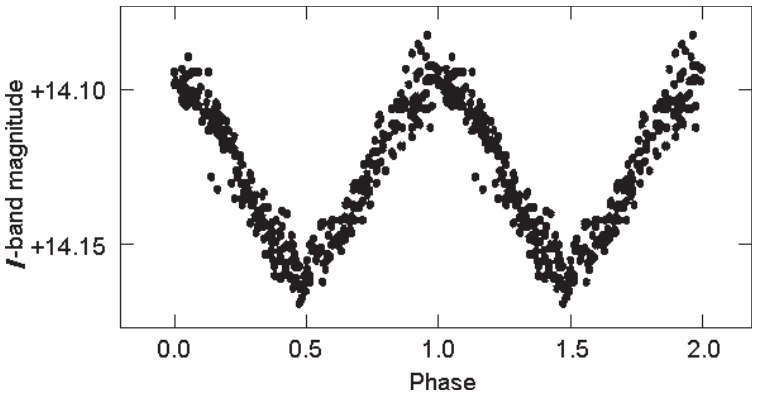

Figure 3. Phase diagram for star #9, 2MASS J17574170-3110322.

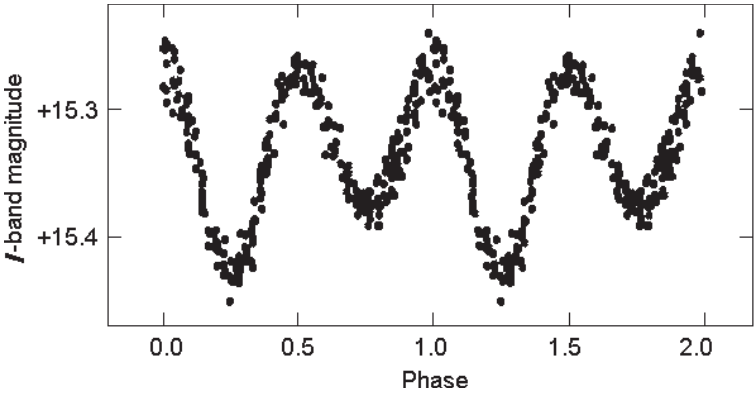

Figure 4. Phase diagram for star #11, 2MASS J17585070-2853195.

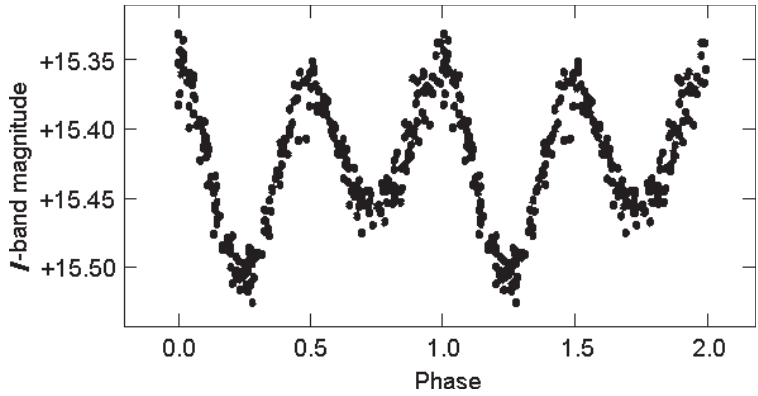

Figure 5. Phase diagram for star #16, 2MASS J18023615-2957242.

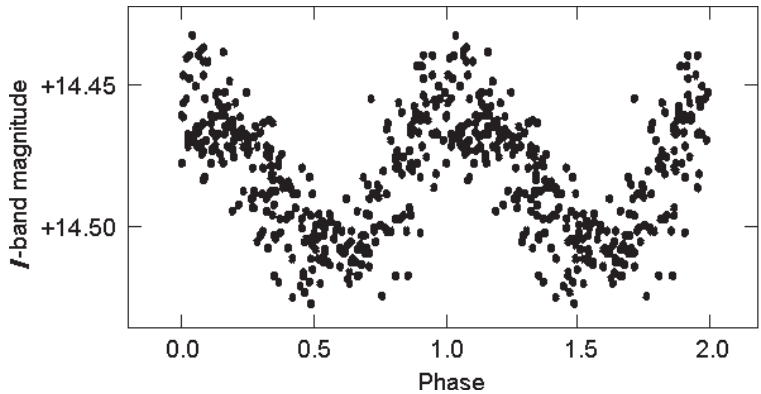

Figure 6. Phase diagram for star #18, 2MASS J18031230-2844088.

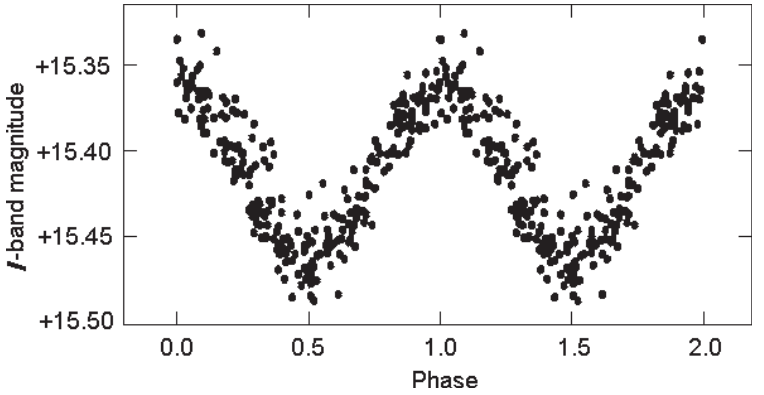

Figure 7. Phase diagram for star #20, 2MASS J18103207-2637252.

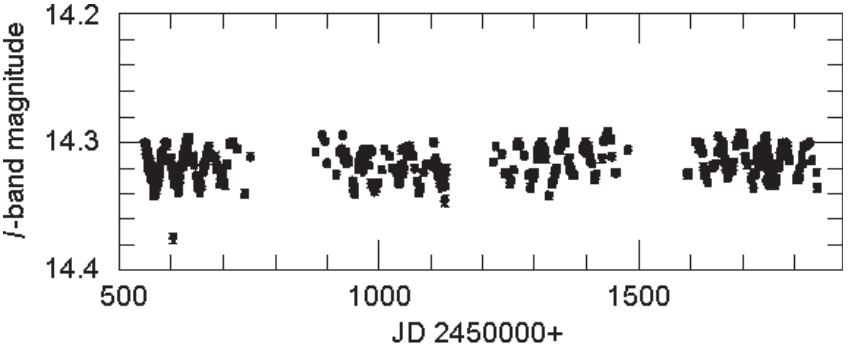

Figure 8. Light curve for star #22, 2MASS J17543116-2954252.

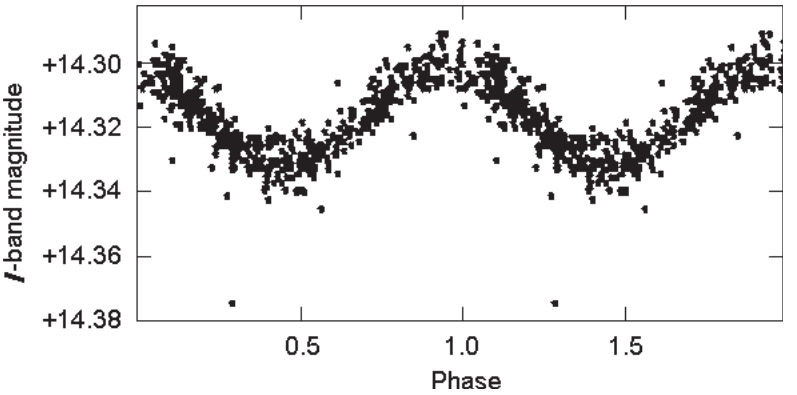

Figure 9. Phase diagram for star #22, 2MASS J17543116-2954252.

The VSS RASNZ Variable Star Charts: a Story of Co-Evolution

Alan Plummer
Linden Observatory, 105 Glossop Road, Linden, NSW 2778, Australia; info@alplummer.com.au

Mati Morel
6 Blakewell Road, Thornton, NSW 2322, Australia; mmorel7@bigpond.com

Received September 21, 2009; accepted October 7, 2009

Abstract The background and history of the *Charts for Southern Variables* of the Variable Star Section of the Royal Astronomical Society of New Zealand (VSS RASNZ) is presented. It is seen that while there are some common origins with the charts of the AAVSO, they have undergone their own unique and important development. After much effort the two organizations' chart resources are now compatible and complementary. Some more general but nonetheless important history of the VSS is also mentioned.

1. Introduction

1,302 charts with good sequences now exist for southern variables, courtesy of the Variable Star Section—now Variable Stars South—of the Royal Astronomical Society of New Zealand (VSS RASNZ). The charts have been published as *Charts for Southern Variables* in 27 Series between 1958 and 2008 (Table 1), with the earlier charts and sequences more recently revised.

We add a southern hemisphere perspective to the historical work done by Malatesta and Scovil (2005) which covers the early history of the AAVSO charts. The AAVSO certainly did—and do—offer charts for southern objects, but naturally their priority lies in the north. After much in common in the early years, it fell to those under the southern sky to do the labor needed. After many decades the two chart systems are now formally linked, with the southern comparison star sequences having being entered into the AAVSO's Variable Star Plotter (VSP). This current work is excerpted and expanded from a presentation to the 2009 Conference of the RASNZ held in Wellington, New Zealand (Morel and Plummer 2009).

2. The Variable Star Section

The Section was formed in 1927 by Frank Bateson, on his return from a four-year stay in Sydney, Australia, in response to requests from professional and amateur astronomers. At first it was a sub-section of the Southern Variable Star Section of the New South Wales Branch of the British Astronomical Association (now the Sydney City SkyWatchers). From June 30, 1928, the successful sub-

section became an observing section of the Astronomical Society of New Zealand (Bateson, 1958a), later to become the RASNZ.

It is worth noting some historically important decisions, the consequences of which still reverberate in astronomy today. In the early 1950s a decision was made by Bateson to concentrate less on Miras and to observe all dwarf novae brighter than magnitude 13.5 at maximum. This was at a time when there was very little professional interest in these objects (Bateson 1990). Look to any current text on cataclysmic variables and the fruits of this decision can be seen (see for instance Livio and Shaviv 1983 and Warner 1995).

The International Astronomical Union (IAU) 1956 Dublin session formally asked the VSS and the AAVSO to work more closely together. In 1957 the two directors met—the AAVSO's Margaret Mayall and Frank Bateson—whereupon it was agreed that VSS be freed from observing LPVs north of –20°. in order to concentrate on southern objects. This was with the important exception of U Gem stars and the like, because New Zealand filled an important longitude gap. Furthermore, the two organizations were asked to standardize charts and sequences (Bateson 1959). As will be seen below, this has only just been completed in the first years of the 21st century.

3. Charts and sequences

Every organization that starts its own series of charts has a precursor, drawing upon similar work done elsewhere. This is true of the VSS as much as the AAVSO. An early compiler of variable star charts around the year 1900 was Rev. Johann Georg Hagen, S.J. of Georgetown Observatory, Washington, DC. For a detailed account of his and other early advocates of variable star observing see Malatesta and Scovil (2005). These charts are now hard to locate; however, a set does exist in the State Library of New South Wales, Australia.

Hagen's charts are described, but not reproduced, in the pages of the *Astrophysical Journal* (Anon. 1897; Hagen 1898; Parkhurst 1907). A specimen chart, U Puppis, is available for download from the ADS Serials and Journals server, but the reproduction is poor and distorted. Shown in Figure 1 is the Hagen U Pup chart from his *Atlas Stellarum Variabilium,Series I* (Hagen 1899), reproduced from a copy in the AAVSO library. The original charts have a grid, printed in red, the purpose of which was that when viewed under red light at the telescope, the grid would vanish.

Hagen's listings of magnitudes were not really sequences as they are understood today, but simply visual estimates for every field star, and none were ever published in the *Astrophysical Journal*. At this time it is not known whether or not these charts were used by the VSS, but more likely early southern observers used charts from the AAVSO or the British Astronomical Association.

Campbell and Pickering (1913) published useful comparison star sequences for ninety-two variable stars south of –30°, and some of the VSS charts were

made from Campbell and Pickering's photographs with these values marked on them. The AAVSO appears to have reproduced Campbell and Pickering's original charts for these southern stars. The weaknesses of these sequences are summarized by Bateson (1958a) as follows:

1. Sequences often not as bright as the target at maximum.
2. Sequences often not as faint as target at minimum.
3. Consecutive stars in the sequences sometimes differ in brightness by far more than desirable.
4. Many differences in assigned and "apparent" magnitudes, and occasional wrong identifications.
5. All sequences unreliable under 11th magnitude.

The *Cape Photographic Durchmusterung* (CPD; Gill and Kapteyn 1895–1900) survey was used to plot some basic charts, and another cause of problems was the fact that the film was blue sensitive, so that red stars disappeared below about 10th magnitude while blue stars of magnitude 11.0–11.5 were present.

While the use of the *Cordoba Durchmusterung* (CoD; Thome 1892–1932) would have been preferable for making charts for visual observers, this survey, in five parts, was long out of print for most parts. By 1965 Bateson had overcome this problem in collaboration with Ignas Stranson of Queensland, Australia. The latter had very skillfully constructed his own Schmidt camera, aperture 7-inch and focal length 434-mm, which he used to photograph many southern variable star fields between 1965 and 1972. His prints were used extensively to provide accurate detail on the charts down to 13.5v, from Series Three onwards.

For lack of good sequences many VSS program stars, particularly long period variables, had only lettered comparison stars. The old observations of these stars await a future date to be reduced to numerical values and entered into the VSS RASNZ data base.

In the period 1974–2004 one of us (MM) was focused on preparing charts for the VSS under Frank Bateson's direction. At first, the concept of an overall index or compilation of sequences such as now exists never really arose. As far back as 1966 Bateson stated "...After publication of all charts in this Series a separate publication will provide data on all comparison stars" (Bateson *et al.* 1966). There were some efforts made in 1994 after the *Guide Star Catalog* (Space Telescope Science Inst.1992) became available, however nothing of enduring value then materialized.

4. The beginning of modernization

In 2003 the AAVSO initiated their Comparison Star Database project. The aim was to document over 70,614 comparison stars on 4,128 charts, with the ultimate aim to have an updatable database which could be accessed by computer

and used to create charts, on demand, by their Variable Star Plotter (VSP) system (Malatesta *et al.* 2007). While the work of documenting the AAVSO charts was divided up among about a dozen members, they were not surprisingly most familiar with northern skies.

The progress of the AAVSO work was followed closely, and it appeared that the extensive southern charting work of the VSS RASNZ was barely on the radar. In June 2005 it was decided that if documenting the VSS charts were to be done at all, if would have to be done by someone intimately familiar with their creation. Thus began Project Snapshot.

5. Project Snapshot 2005–2007

The plan was simple: to document all visual comparison stars used or selected by observers and shown on published VSS charts. With the availability of several modern all-sky surveys with reliable *BV* data it appeared quite feasible to convert all of the existing VSS sequences to the international *BV* standard, to clear the backlog of letter-only sequences, and to update old visual magnitudes.

Starting with the very first charts issued by the VSS, each chart was compared with a GUIDE8® display on a PC, to obtain the most precise astrometric position of each lettered comparison star or magnitude on the chart. The *USNO-A2.0 Catalog* (Monet *et al.* 1992) was used to extend the on-screen display beyond magnitude 14–15 when required. Particular care was needed when comparing a precise computer display with paper charts which often used telescopic field sketches, made by hand and eye alone.

Figure 2 compares the original hand drawn VSS chart 1 with the new version. The old chart is perfectly good and served very well for decades. However, it can not be doubted that the revised chart 1 serves the observer better.

Prior to 2001 quite a few VSS stars had photoelectric (p.e.) *V* sequences determined and published by a variety of authors. Nevertheless it was felt wise to check existing p.e. sequences against *All Sky Automatic Survey 3* (ASAS-3; Pojmański 2002) measures as any discrepant data could be identified and resolved. ASAS-3 has been extensively used in Project Snapshot.

It took about two years to go through 1,302 charts, compile the data, and type them all into EXCEL spreadsheets, of which there are now twenty-seven different volumes, corresponding to twenty-seven issues of *Charts for Southern Variables*. By mid-2007 Project Snapshot was essentially completed. One final task remained. At the suggestion of Arne Henden, Director of the AAVSO, between October 2008 and January 2009 the Snapshot files were converted into a format which could be loaded into the AAVSO's Variable Star Database, and hence be utilized for online plotting of charts via the VSP system.

The ASAS-3 magnitudes used in Project Snapshot are not the perfect solution, as ASAS-3 only delivers one color—*V*. One would prefer at least *B–V* as well, as there may unknowingly be very red stars in the sequences, a circumstance best

avoided. Until the AAVSO's mooted All-Sky Photometric Survey gets up and running in a year or two observers have to make the best of what's available. This new survey hopefully will return reliable data much fainter than the cutoff point of ASAS-3, 13.5V or so.

6. Conclusion

It is fitting that the VSS and AAVSO chart resources are now complementary and compatible. One might say that the vision of the 1956 IAU Dublin session was a long time being realized. As both organizations move into the future with the inevitable new astronomical discoveries and better measures, a close working relationship serves everyone well.

References

Anonymous. 1897, *Astrophys. J.*, **6**, 441.

Bateson, F. M. 1958a, *J. Roy. Astron. Soc. Canada*, **52**, 241.

Bateson, F. M. 1958b, *The Observation of Variable Stars*, privately printed, Rarotonga, Cook Islands.

Bateson, F. M. 1959, *J. Roy. Astron. Soc. Canada*, **53**, 1.

Bateson, F. M. 1990, *J. Amer. Assoc. Var. Star Obs.*, **19**, 156.

Bateson, F. M., Jones, A. F., and Stranson, I. 1966, *Charts for Southern Variables, Series 3*, Astronomical Research, Ltd., Tauranga, New Zealand.

Campbell, L., and Pickering, E. C. 1913, *Ann. Harvard Coll. Obs.*, **63**, 143.

Gill, D., and Kapteyn, J. C. 1895–1900, *Cape Photographic Durchmusterung, Ann. Cape Obs.*, **3** (1895, Part I: zones –18 to –37 degrees); **4** (1897, Part II: zones –38 to –52 degrees); **5** (1900, Part III: zones –53 to –89 degrees).

Hagen, J. G. 1898, *Astrophys. J.*, **8**, 160.

Hagen J. G. 1899, *Atlas Stellarum Variabilium, Series I*, F. L. Dames, Berlin.

Livio, M., and Shaviv, G., eds. 1983, *Cataclysmic Variables and Related Objects*, Proc. 72nd Colloq., Haifa, Israel, August 9–13, 1982, D. Reidel, Dordrecht.

Malatesta, K. H., and Scovil, C. E. 2005, *J. Amer. Assoc. Var. Star Obs.*, **34**, 81.

Malatesta, K. H., Simonsen, M. A., and Scovil, C. E. 2007, *J. Amer. Assoc. Var. Star Obs.*, **35**, 377.

Monet, D., *et al.* 1998, *USNO-A V2.0 Catalog of Astrometric Standards*, U.S. Naval Observatory, Flagstaff, AZ.

Morel, M., and Plummer, A. 2009, *South. Stars*, **48**, 19.

Parkhurst, J. A. 1907, *Astrophys. J.*, **25**, 361P.

Pojmański, G. 2002, *Acta Astron.*, **52**, 397.

Space Telescope Science Institute 1992, *The Guide Star Catalog*, Version 1.1, STScI, Baltimore.

Thome, J. M. 1892–1932 *Cordoba Durchmusterung, Resultados del Observatorio Nacional Argentino*, **16** (1892, Part I: –22 to –32 degrees), **17** (1894, Part II: –34 to –42 degrees), **18** (1900, Part III: –42 to –52 degrees), **21** (Part I) (1914, Part IV, –52 to –62 degrees), **21** (Part II) (1932, Parv V: –62 to –90 degrees).

Warner, B. 1995, *Cataclysmic Variable Stars*, Cambridge Astrophysics Series, Cambridge Univ. Press, Cambridge and New York.

Table 1. Series comprising *Charts for Southern Variables*.

Chart Numbers	*Series Number*	*Compilers*	*Year Published*
1–12*	1*	F. M. Bateson, A. F. Jones	1958
13–43	2	F. M. Bateson, A. F. Jones	1960
44–100	3	F. M.Bateson, A. F.Jones, I. Stranson	1966
101–150	4	F. M.Bateson, A. F.Jones, I. Stranson	1967
151–200	5	F. M.Bateson, A. F.Jones, I. Stranson	1968
201–250	6	F. M.Bateson, A. F.Jones, I. Stranson	1970
251–300	7	F. M.Bateson, A. F.Jones, I. Stranson	1971
301–350	8	F. M.Bateson, M. Morel, R.Winnett	1976
351–400	9	F. M.Bateson, M. Morel, R.Winnett	1977
401–449	10	F. M.Bateson, M. Morel, R.Winnett	1979
450–500	11	F. M.Bateson, M. Morel, B.Sumner, R.Winnett	1979
501–551	12	F. M.Bateson, M. Morel, B.Sumner, R.Winnett	1980
552–600	13	F. M.Bateson, M. Morel, B.Sumner, R.Winnett	1981
601–649	14	F. M.Bateson, M. Morel, B.Sumner	1982
650–700	15	F. M.Bateson, M. Morel	1982
701–750	16	F. M.Bateson, M. Morel	1983
751–800	17	F. M.Bateson, M. Morel	1984
801–851	18	F. M.Bateson, M. Morel	1985
852–900	19	F. M.Bateson, M. Morel	1986
901–947	20	F. M.Bateson, M. Morel	1988
948–1002	21	F. M.Bateson, M. Morel	1990
1003–1053	22	F. M.Bateson, M. Morel	1990
1054–1104	23	F. M.Bateson, M. Morel	1992
1105–1154	24	F. M.Bateson, M. Morel	1995
1155–1203	25	F. M.Bateson, M. Morel	1997
1204–1251	26	F. M.Bateson, M. Morel, B. Sumner	1999
1252–1302	27	M. Morel	2008

**Note: The first twelve charts were not numbered. These were named "Series 1" some time after the publication of Series 2. The first twelve (unnumbered) were issued with a booklet to assist novice members of the VSS, titled* The Observation of Variable Stars *(Bateson, 1958b).*

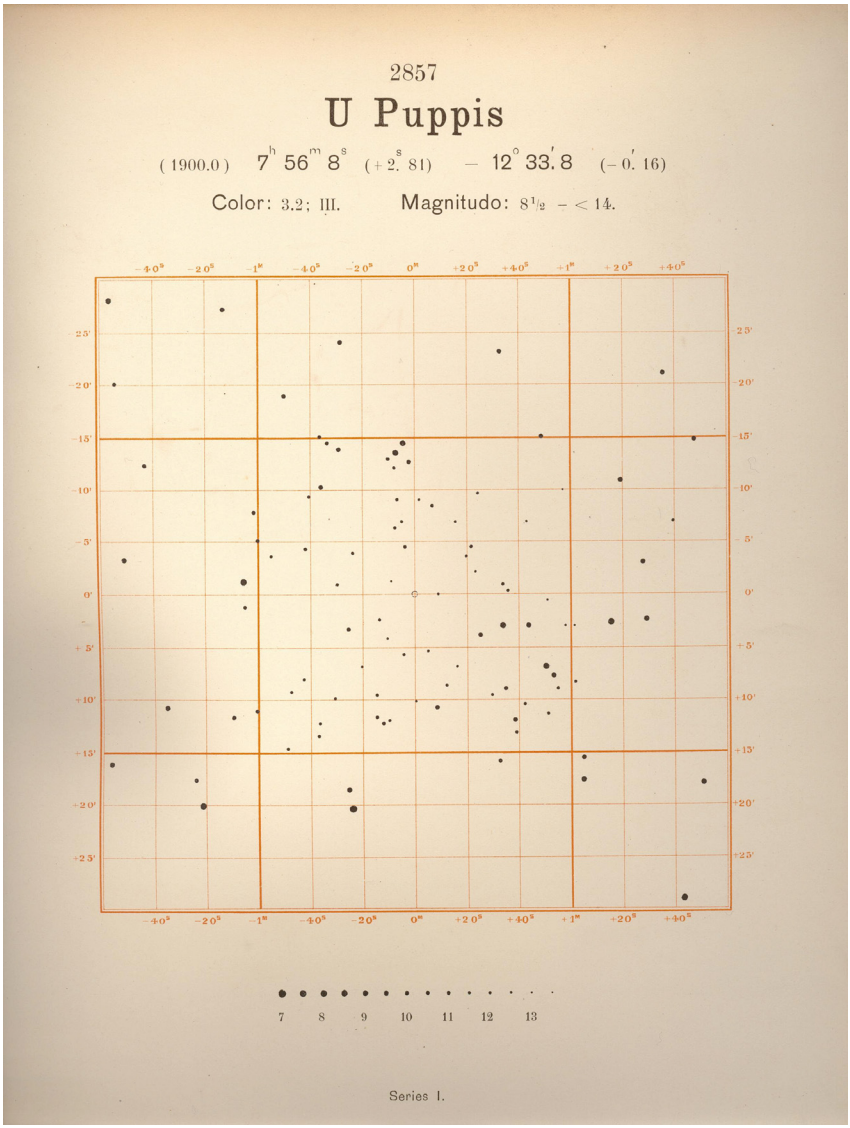

Figure 1. Chart for U Pup from *Atlas Stellarum Variabilium*, Series I (Hagen 1899).

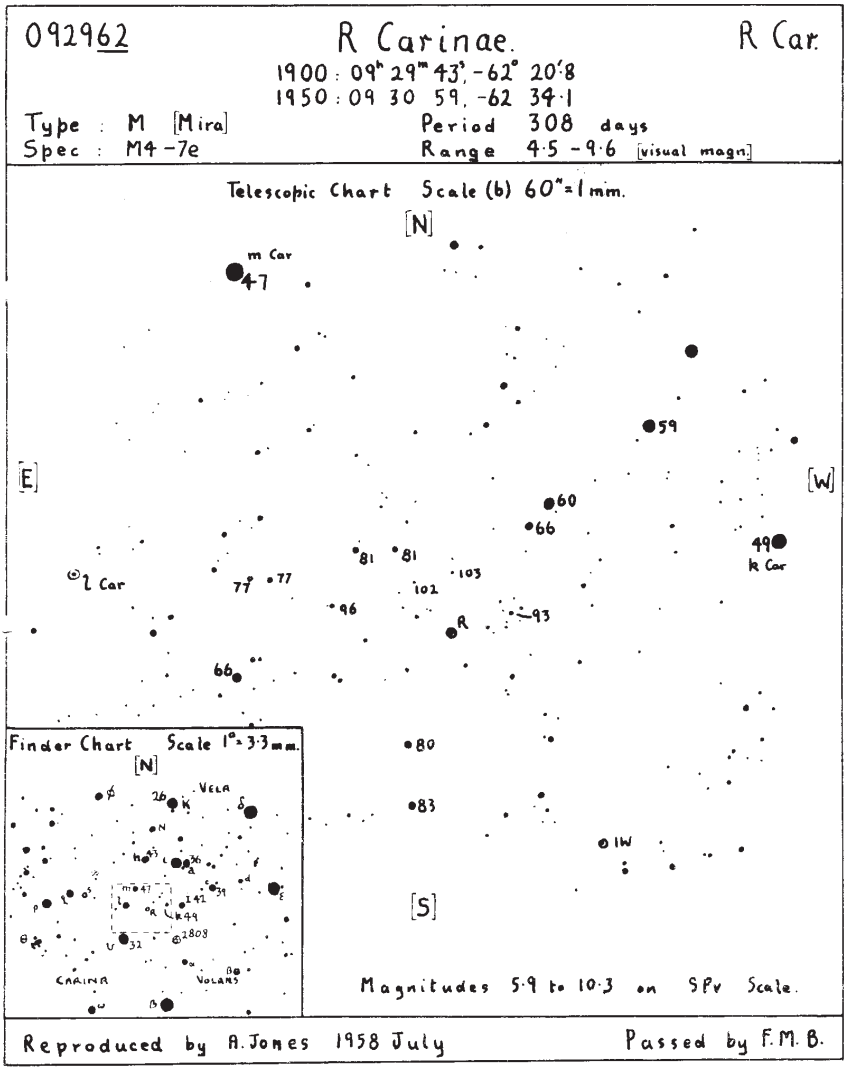

Figure 2a. The original VSS Chart 1 for R Car.

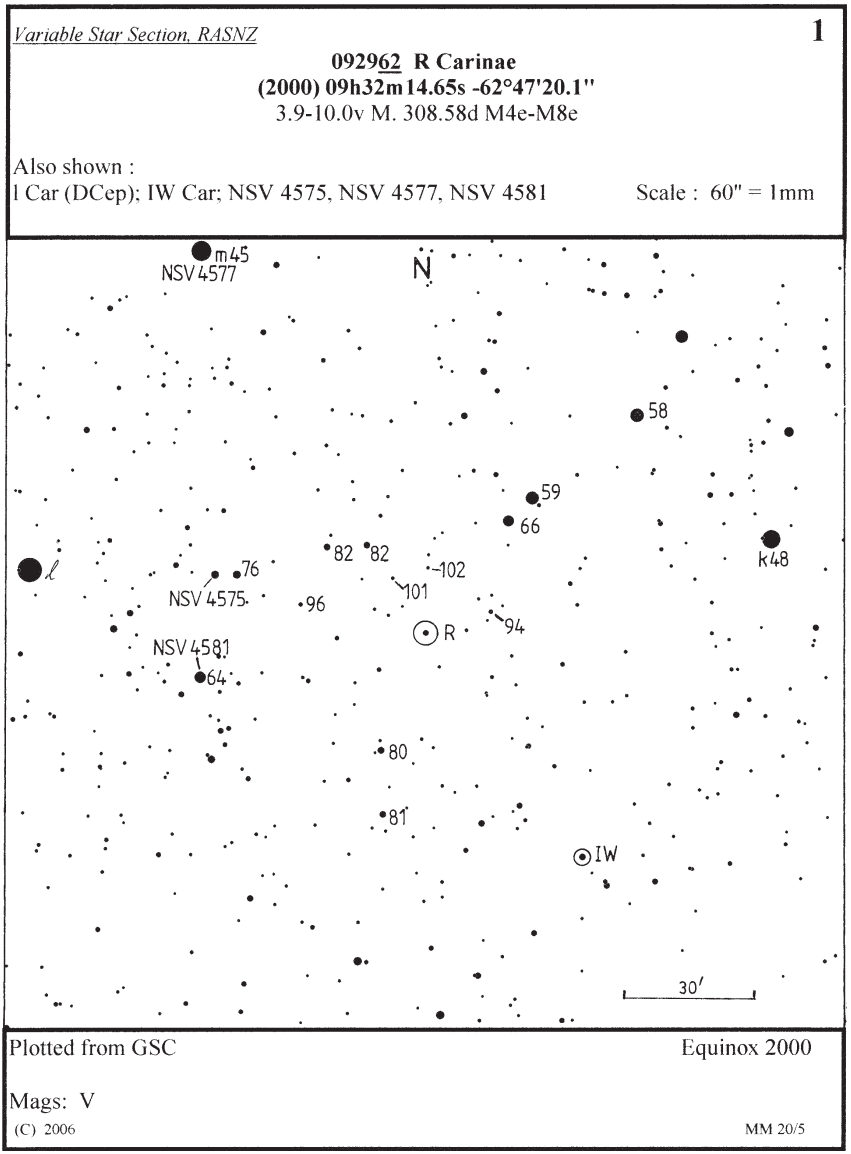

Figure 2b. The revised VSS Chart 1 for R Car.

Documenting Local Night Sky Brightness Using Sky Quality Meters: An Interdisciplinary College Capstone Project and a First Step Toward Reducing Light Pollution

Jennifer Birriel
Department of Mathematics, Computer Science, and Physics, Morehead State University, Morehead, KY 43051; j.birriel@morehead-st.edu

Jaclyn Wheatley
Ashland, Inc., 3499 Blazer Parkway, Lexington, KY 40509; jaclyn_wheatley@yahoo.com

Christine McMichael
School of Public Affairs, Morehead State University, Morehead KY 40351; c.mcmichael@moreheadstate.edu

Received October 30, 2009; revised January 28, 2010; accepted January 29, 2010

Abstract The advent of inexpensive, hand-held light meters allows science students the opportunity to document night sky brightness in their local communities as a first step toward ultimately reducing local light pollution. We report our preliminary results of one college student's interdisciplinary capstone project documenting sky brightness in the local campus community. The student produced two maps of sky brightness readings in the Morehead, Kentucky, area using the Unihedron Sky Quality Meter (SQM) and the Unihedron Sky Quality Meter with Lens (SQM-L). Typical night sky brightness measurements within town ranged from suburban to city on the Bortle Scale of visual brightness. We end with a discussion of opportunities for future student contributions to this project.

1. Introduction

Light pollution studies provide K–16 students an excellent opportunity to participate in interdisciplinary research projects (Percy 2002; Alvarez del Castillo 2004). Topics in light pollution span a multitude of disciplines: science, technology, environment, economics, society, and culture. As such, documenting and monitoring light pollution makes an exemplary capstone project for graduating college students. Furthermore, light pollution abatement discussions are more effective when based on quantitative arguments and so capstone projects such as these are both important and necessary.

At many colleges and universities, students are required to do a capstone project to complete their education. These are expected to be intensive, active learning projects. At Morehead State University, mathematics and science students are required to complete a directed research project to fulfill the capstone

requirement. In mathematics, the capstone research project is adminstered through a three-credit hour course administered over a fifteen-week semester. Students are required to conduct a research investigation, write a formal paper, and give an oral presentation on their work. Within the broader framework of the University's general education standards, the mathematics capstone course has several learning objectives. These include the ability to:

1. locate, select, organize, and present mathematical information in an appropriate manner;

2. communicate mathematical reasoning effectively in both written and spoken forms;

3. use appropriate mathematical language to communicate ideas;

4. think and reason logically by evaluating, analyzing, and synthesizing information;

5. use technology as a tool to help solve non-trivial real-world problems;

6. express problems in multiple representational forms (e.g., graphical, algebraic, physical model);

7. develop a curiosity and appreciation for mathematics as a dynamic, accessible, and essential tool to model particular phenomena in daily life.

This particular list of objectives is specific to Morehead State University (MSU) mathematics students. However, several of these objectives are common to the capstone course in the physical sciences here at MSU. In addition, these objectives are common to most capstone experiences in the disciplines of both mathematics and science at many institutions of higher learning.

Using hand-held light meters to document night sky brightness on the campus and in the surrounding local community effectively addresses most of these learning objectives. For example, documenting night sky brightness quantitatively requires the use of technology (here a hand-held light meter and a GPS device) and mathematics to address the non-trivial, real world problem of light pollution and effectively meets objectives 5 and 7. The presentation of data measurements in terms of both a logarithmic measure in the astronomical magnitude system and plotted as function of geographic location, addresses objectives 4 and 6. Finally, objectives 1 through 3 are met when the student makes the oral and written presentations.

In addition to meeting these specific course goals, this project has strong interdisciplinary aspects. For example, a student should first research natural

sources of night sky brightness since "natural" light levels serve as a baseline for comparison with light pollution levels. These studies expose the student to astronomical sources of light and how such sources are quantified. The student should also do some research to put the problem into context and while doing so learns about plant, animal, and human ecology. In addition, the student can examine other aspects of light pollution such as the economic and environmental impact of the wasted energy associated with light pollution.

2. Data collection methods

All sky brightness measurements were obtained using the Unihedron Corporation Sky Quality Meter (SQM) and SQM-L. The SQM has a full cone angle of 84 degrees and the SQM-L has a lens that narrows the full observation cone down to 20 degrees. Both devices have the same sensor; the only difference is the lens. Each device measures sky brightness in visible light (from blue to red) in mag/arcsec^2. Both devices also measure temperature in both °C and °F; however, all photometric measurements are automatically corrected for temperature effects. Previous groups have reported the uncertainty of SQM measurements to be on the order of ±0.2 mag/arcsec^2 (e.g., Smith *et al.* 2008; Cinzano 2005).

Measurements of night sky brightness were made in accordance with the "Globe at Night" protocol (http://www.globeatnight.org/learn_SQM.html). All measurements were made when the sky was free of clouds (as confirmed using current conditions as found on the "Weather Channel" web site) and moonlight. All data collection commenced at least one hour after sunset. The SQM and SQM-L were allowed to reach ambient temperature before any measurements were taken. All measurements were made away from obstructions (buildings, trees, walls) and at least 7.6m away from lighting fixtures. When taking brightness measurements, the student (JW) held the meters at arm's length above her head. At each location, the student took a GPS reading and then obtained a measurement of sky brightness and ambient temperature with both the SQM and the SQM-L. All results were recorded by hand using a flashlight and notebook. Measurements for the main part of town, which includes the university, were taken on the night of January 21, 2009. (On this date, there was no snow cover on the ground.) Readings on the southern side of town and up along the main route (KY 32, which runs north and east from town) were made on April 24, 2009.

3. Sky brightness around Morehead, Kentucky

The city of Morehead (pop. 5,914) is located in Rowan County in northeastern Kentucky. Nestled in the foothills of the central Appalachian Mountains, Morehead is characterized by largely forested, hilly, and highly dissected terrain where elevation ranges between 208m and 404m. Similar (general) geologic patterns are found throughout the area.

Maps of sky brightness can be created using the GPS readings and the mapping and display facilities of Google Earth (Smith *et al.* 2008). This is a good option for those groups interested in simple displays of sky brightness data. In our case, we choose to use a GIS-based mapping approach because we expect that it will ultimately be particularly useful for not only educating people about light pollution patterns and trends in Morehead and Rowan County, but because it provides a framework in which to explore factors that may be contributing to light pollution (e.g., street lights, buildings), to delineate areas that are currently being impacted by light pollution (e.g., wildlife habitat), and to predict how future development may aggravate the problem.

We used ArcMap 9.2 from Environmental Systems Research Institute (ESRI) to create two air photo-based maps showing each device's brightness readings collected within the City of Morehead. In ArcMap, device readings were overlain on a summer 2006 National Agricultural Imagery Program (NAIP) aerial photo obtained from the Kentucky Division of Geographic Information in order to visualize the correspondence between ground locations and each set of sky brightness measurements.

Examination of the SQM map (Figure 1) reveals that night sky brightness within the town itself varies dramatically, from as bright as 12.9 mag/arcsec^2 near the local car dealership to as dark as 20.5 mag/arcsec^2 in steep-sided valleys. Measurements made near commercial venues such as the local strip malls and plazas tended to be among the brightest sites. Shadowing by the surrounding hill sides (e.g., Smith *et al.* 2008) is evident at a number of locations in local "hollows" (i.e., the area between two hills). Sites at the edge of town also have lower readings due to distance effects (e.g., Pike 1976; Berry 1976). In fact, a measurement taken at nearby Cave Run Lake some 20km away benefits from both distance and hillside shielding: average SQM readings at this remote location were 21.7 mag/arcsec^2.

Readings taken with the SQM-L (Figure 2) indicate that the main part of town and campus are in fact quite bright: most readings are significantly brighter than 19 mag/arcsec^2. Using the Sky Brightness Nomogram (http://www.darkskiesawareness.org/img/sky-brightness-nomogram.gif) provided by the International Year of Astronomy's Dark Skies Awareness website, it is clear that most of the town ranks between 6 (bright suburban sky) and almost 8 (city sky) on the Bortle Scale (Bortle 2001)!

A comparison of Figures 1 and 2 reveals a striking difference in meter readings. This is to be expected, given the much larger field of view of the SQM versus the SQM-L. The cone of the SQM is large enough that readings are significantly influenced by street lights, buildings, and trees. Thus, all future measurements will be made using the SQM-L.

4. Summary and future

This student's work effectively documented night sky brightness in Morehead, Kentucky, during the first half of 2009. She presented her work at the state-wide meeting of the Kentucky Association of Physics Teachers in Louisville, Kentucky, on March 7, 2009, to an audience of college faculty and students and high school faculty. Later, in May 2009, she spoke to a local audience of Morehead State University students and faculty at her capstone presentation. Together, these presentations afforded the student meaningful "community engagement" activities.

As the city and county continue to grow, future students will monitor the evolution of light pollution using the Unihedron Sky Quality Meter and create additional maps. The aim is to continue to educate both the campus community and local residents and leaders about light pollution and its negative economical, ecological, and aesthetic effects—with the goal of reducing overall light pollution in the area. Towards this end, both measurements and maps will be shared with appropriate university, business, and government entities—as well as local residents—to help support the development and implementation of more effective and efficient lighting policies throughout the community.

5. Acknowledgement

The authors would like to thank the anonymous referee for the many helpful suggestions that helped improve the quality and focus of this paper.

References

Alvarez del Castillo, E. M. 2004, *J. Amer. Assoc. Var. Star Obs.*, **32**, 55.
Berry, R. 1976, *J. Roy. Astron. Soc. Canada*, **70**, 97.
Bortle, J. 2001, *Sky & Telescope*, **101**, 126.
Cinzano, P. 2005, *ISTIL Internal Report*, No. 9, 1.4.
Percy, J. R. 2002, *J. Roy. Astron. Soc. Canada*, **96**, 24.
Pike, R. 1976, *J. Roy. Astron. Soc. Canada*, **70**, 116.
Smith, M. G., Warner, M., Orellana, D., Munizaga, D., Sanhueza, P., Bogglio, H., and Cartier, R. 2008, in *Preparing for the 2009 International Year of Astronomy*, eds. M. G. Gibbs, J. Barnes, J. G. Manning, and B. Partridge, ASP Conf. Ser., **400**, Astron. Soc. Pacific, San Francisco, 152.

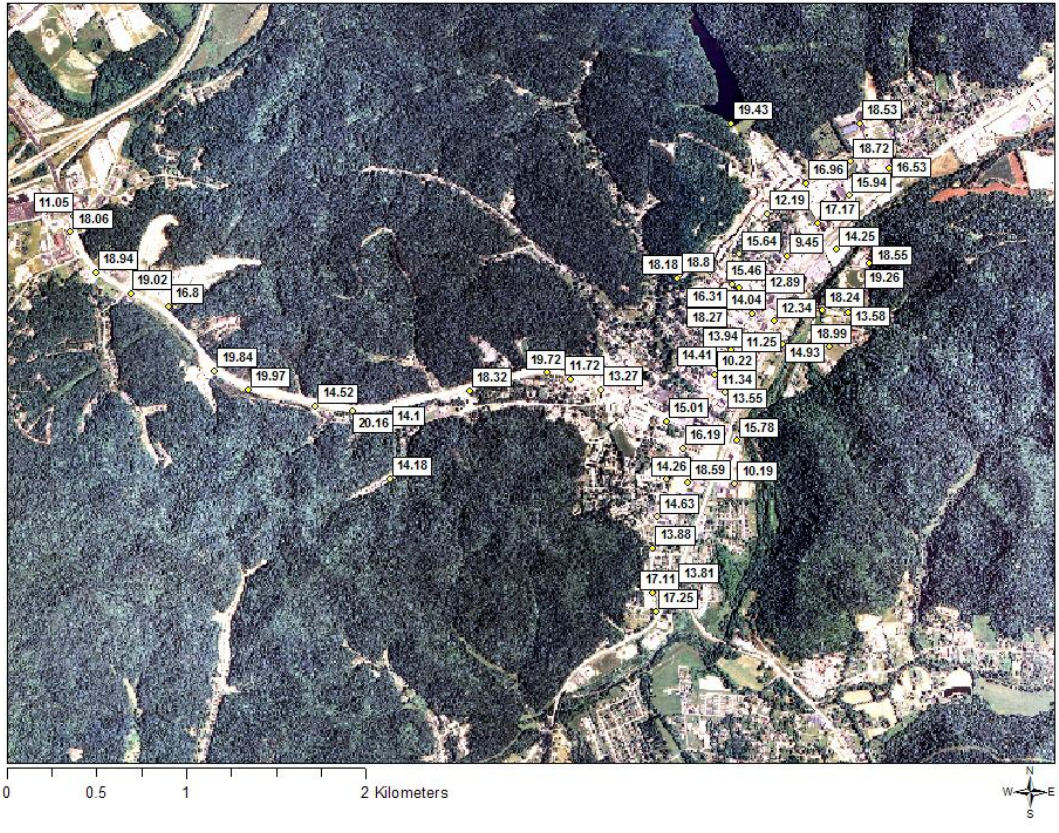

Figure 1. Night sky brightness readings for Morehead, Kentucky, using the first generation Unihedron Sky Quality Meter (SQM) with an 84-degree cone. The readings are in magnitudes per square arc second with an uncertainty of about ±0.2 mag/arcsec^2.

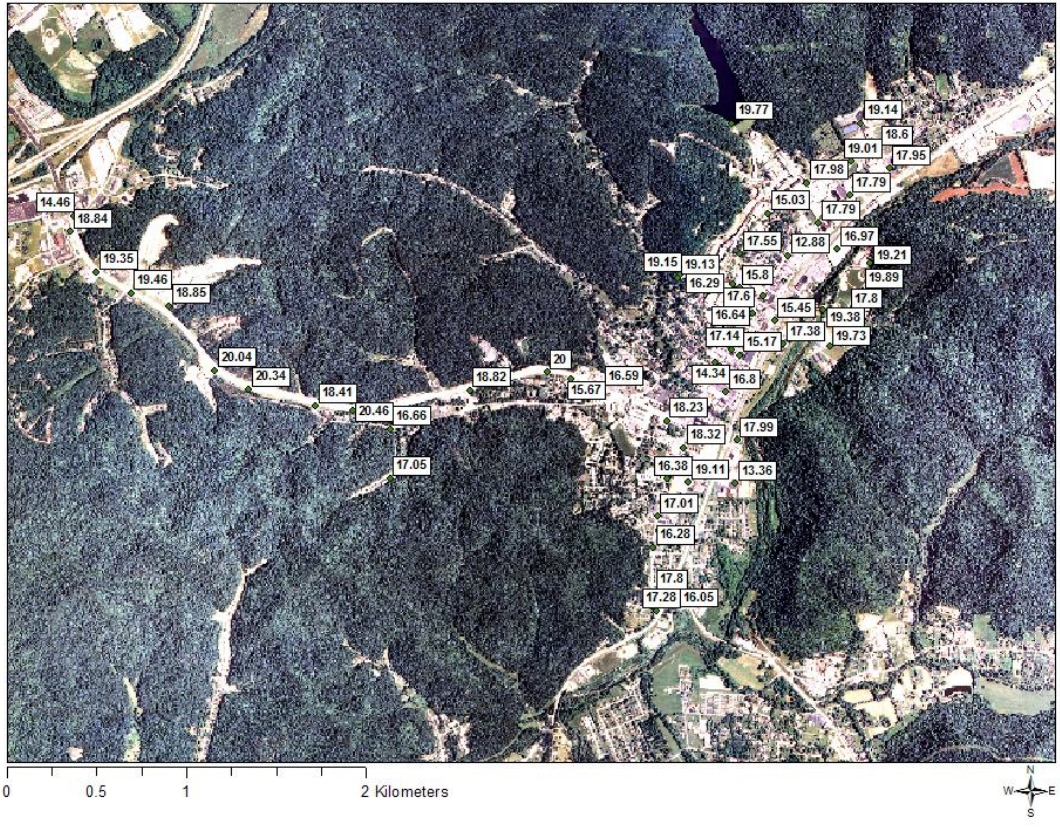

Figure 2. Night sky brightness readings (in magnitudes per square arc second ±0.2 mag/arcsec^2) for Morehead, Kentucky, using the Unihedron SQM-L with a lens that narrows the sampling cone down to 20 degrees.

Abstracts of Papers and Posters Presented at the 98th Annual Meeting of the AAVSO, Held in Newton, Massachusetts, November 6–7, 2009

Scientists Look at 2012: Carrying on Margaret Mayall's Legacy of Debunking Pseudoscience

Kristine Larsen
Physics and Earth Sciences, Central Connecticut State University, 1616 Stanley Street, New Britain, CT 06053; larsen@ccsu.edu

Abstract In 1941 Margaret Mayall, the future director of the AAVSO, and Harvard colleague Bart Bok authored a critical study of astrology and its impact on society entitled "Scientists Look at Astrology." They chastised the scientific community for thinking the debunking of astrology to be "below the dignity of scientists." In contrast, they opined that it is one of the duties of scientists to "inform the public about the nature and background of a current fad, such as astrology, even though to do so may be unpleasant." Fast-forward 68 years in the future, and the astronomical community now faces a pseudoscientific enemy just as insidious as astrology, yet just as ignored by the general professional and amateur community as astrology had been when Mayall and Bok took up the charge in 1941. The pseudoscience in question is the well-publicized "prediction" that the Mayan calendar will end on December 21, 2012, causing the end of civilization in concert with one of a number of possible astronomical calamities, including (but not limited to) the gravitational pull of the center of the Milky Way (somehow enhanced by an "alignment" with our solar system), the near-approach by a mythical 10th planet (often named Nibiru), large-scale damage to the planet by solar flares larger than those ever recorded, or the shifting of the earth's axis of rotation (often confused with a proposed sudden and catastrophic reversal of the earth's magnetic polarity). As a scientific and educational organization, the AAVSO and its members have a responsibility to follow in Mayall's footsteps, shining the light of reason and knowledge on the dark corners of ignorance which far too often permeate the Internet, radio and television programming, and recent films, most notably 2012. This talk will highlight some of the basic premises of the 2012 hysteria and suggest ways that the AAVSO and its members can use variable stars and the history of the AAVSO to counteract some of the astronomical misinformation which is increasingly promulgated by proponents of the 2012 pseudoscience.

The Z CamPaign

Michael Simonsen
2615 S. Summers Road, Imlay City, MI 48444; mikesimonsen@aavso.org

Abstract Z Cam type dwarf novae are described as being those CVs that sometimes after an outburst do not return to their original brightness, but instead, get hung up on the way to quiescence in what is called a "standstill." If it doesn't exhibit standstills it isn't a Z Cam star. There is no strong agreement between the various CV catalogs as to which few dozen or so stars are actually Z Cam type systems. If any significant percentage of the number of Z Cams eventually proves not to be Z Cam, the remaining few represent a fairly rare and unique class of stars worthy of further investigation. We will describe a campaign to observe many of the known and suspected Z Cam stars and the science goals we hope to achieve through this campaign.

T Ursae Minoris: From Mira to ???

Grant Foster
146C Mechanic Street, Westbrook, ME 04092; tamino_9@hotmail.com

Abstract T UMi is known to have decreased its period and amplitude dramatically, perhaps due to a helium shell flash. Most recently, its amplitude has dropped below the limit defining the class of Mira-type variables, and it now shows signs of multimode pulsation, the two modes having the period ratio observed in many semiregular variables. We suggest that T UMi is no longer a Mira-type variable, instead it is presently behaving like a member of the SRb class.

Variability "Profiles" for T Tauri Variables and Related Objects From AAVSO Visual Observations

John Percy
Samantha Esteves
Jou Glasheen
Alfred Lin
Marina Mashintsova
Sophia Wu
Department of Astronomy and Astrophysics, University of Toronto, Toronto, ON M5S 3H4, Canada; john.percy@utoronto.ca

Abstract T Tauri variables are young sun-like stars in various stages of their birth. The AAVSO has accumulated observations of T Tauri variables and related objects for several decades, but only recently have some of the observations been

validated and analyzed (Percy and Palaniappan 2006 JAAVSO 35, 290). Here, we report the analysis of many additional variables, using Fourier and self-correlation analysis. A few variables showed periodic behavior, but self-correlation analysis makes it possible to construct a "variability profile"—amount of variability versus time scale—for all the stars, not just the periodic ones. We will show several examples, and discuss the significance of the results. We will discuss an interesting but spurious low-amplitude one-year periodicity which occurs in a few of the stars, and a possible spurious low-amplitude one-month periodicity.

We thank the AAVSO observers who made the measurements, the AAVSO Headquarters staff—especially Elizabeth Waagen—who validated them, and the Natural Sciences and Engineering Research Council of Canada for support.

GALEX and Optical Light Curves of LARPs

Paula Szkody
University of Washington, Department of Astronomy, Box 351580, Seattle, WA 98195; szkody@astro.washington.edu

Abstract Low Accretion Rate Polars are expected to have little to no accretion and therefore flat light curves. But GALEX and ground-based data show otherwise. I will present our UV and optical light curves of three systems (WX LMi, SDSS1031+20 and SDSS1212+01) and the results of our modeling efforts for WX LMi.

Kepler Observations of Variable Stars

Steve B. Howell
WIYN/NOAO, 950 N. Cherry Avenue, Tucson, AZ 85726; howell@noao.edu

Abstract The NASA Kepler mission was launched in March 2009 and has begun science operations. While its primary goal is to detect exo-planets—particularly Earth-like planets—light curves of variable stars will be a great by-product. Kepler exo-planet target stars as well as guest observer targets are already showing a wide variety of variability from classical types to new and bizarre variables. This talk will highlight light curves of some variables already observed, focusing on a few spectacular examples, as well as discussing ways in which AAVSO members can get Kepler light curves of their very own.

Rapid Cadence Monitoring of ε Aurigae

Gary Billings
2320 Cherokee Drive NW, Calgary, Alberta T2L 0X7, Canada; obs681@gmail.com

Abstract Rapid cadence (every 42 seconds) photometry of ε Aur in September 2009, using a V-filtered 50 mm *f*/2.8 camera lens and an SBIG ST-7E camera, does not show short period brightness variations significantly different from those of the comparison star η Aurigae. On a scale of minutes to hours, the only variations detected are attributable to scintillation and differences in atmospheric extinction.

BVRI Photometry of W Ursae Majoris Binary Systems and Lessons Learned

Andy Howell
3522 NW 18th Avenue, Gainesville, FL 32606; andyho@mindspring.com

Abstract Six years ago, a multi-color *BVRI* survey of W UMa binary systems was begun. This was the first time the author undertook multi-color photometry. Although he had done *V*-band photometry in the past, there were many new things he had to learn. Data of thirty-five W UMa binaries was collected on nine nights during Nov/Dec 2003 when the sky was suitable for all-sky photometry. The equipment used was an 11-inch Schmidt-Cassegrain with ST-9E camera and *BVRI* filters. Approximately 1,520 CCD images were obtained. The data then waited six years to be reduced. A major reason for the delay was overcoming procrastination in reducing this rather large data set. An efficient, accurate process had to be developed. First, Mira AL was used to extract the instrumental magnitudes. Then, the data were entered into a filemaker pro relational database where air mass values were obtained from the AAVSO web site. The final step in the reduction process was to use Minitab statistical software to transform instrumental magnitudes into standard magnitudes. Publication of the scientific results is forthcoming. This work was partially supported by a grant from NASA administered by the American Astronomical Society.

Debris Disks in the AB Doradus Moving Group

Mimi Hang
Mount Holyoke College, 50 College Street, South Hadley, MA 01075; marykdk@yahoo.com

Abstract The field of planetary science is quickly developing due to our appetite to learn more about the formation of our solar system and about planets

around other stars. After the Jovian planets formed in our own solar system, it is believed that our solar system underwent a period of high dust production. For example, our terrestrial planets are thought to have formed from collisions between planetary embryos which includes the large collision that formed our moon when our solar system was ~50 Myr. These collisions formed more dust which swirled around our sun to become a debris disk. We can apply the model here to other star systems. Collisions between planetary embryos of other star systems must also produce high dust production and the dust grains are warmed by stellar light. These dust grains emit thermal infrared radiation which can be detected using space-based infrared telescopes such as the Spitzer Space Telescope (SST). However, it is important to note that the majority of these debris disks are not spatially resolved with current telescopes.

The goal of this project was to figure out if there were any debris disks around the stars in the AB Dor moving group. In this project, the moving group AB Doradus was chosen because at 50 Myr and only 20 pc away from Earth, the stars in this association make for an extraordinary laboratory for inquiry of the end-stages of planetary formation. Data was obtained from the Spitzer Space Telescope's FEPS Legacy MIPS observations. The approach was to: 1) reduce Spitzer data to measure the brightness of the stars at 24 and 70 microns, 2) estimate the brightness of the stellar photosphere at those wavelengths and finally, 3) to look for an excess in the infrared emission which would indicate thermal radiation from dust grains. The study revealed that about 21% of the stars measured in AB Dor have debris disks. However, only the star system of HIP 18859 had an excess at both 24 and 70 microns. Therefore, only HIP 18859 is guaranteed to have a debris disk based on the result of this study.

Hawaii Student/Teacher Astronomy Research (HI STAR) Outcomes

Mary Ann Kadooka
University of Hawaii, Institute for Astronomy, 2680 Woodlawn Drive, Honolulu, HI 96822; marykdk@yahoo.com

Abstract Outcomes of Hawaii Student/Teacher Research (HI STAR) program are: 1. Support grade 7–11 students in Hawaii to conduct authentic astronomy research projects worthy of Science Fair entry. 2. Provide HI STAR alumni pursuing science and mathematics majors in college with summer research opportunities. 3. Establish an astronomy mentoring program to support the students undertaking Science Fair projects. We will discuss how we have been able to realize these goals due to having passionate, motivated 12–16 year old students, dedicated astronomer mentors, committed parents and teachers and other supporters for our program. Our major grant funding is over, but we will continue HI STAR. We continue to expand our program. We will have our HI STAR alumnus, Mimi

Hang, now a sophomore at Mt. Holyoke College, discuss her research on Debris Disks in the AB Doradus Moving Group. She was fortunate enough to work at the Space Telescope Science Institute operated for AURA for NASA as an undergraduate researcher this past summer.

Estimate of the Limiting Magnitudes of the Harvard College Observatory Plate Collection

Edward J. Los
7 Cheyenne Drive, Nashua, NH 03063

Abstract This paper provides estimates of the number of plates in the Harvard College Observatory plate collection which show a given object. The estimate is a function of magnitude and sky location and is based on the analysis of 6,041 plates scanned under the "Digital Access to a Sky Century @ Harvard" program and transcriptions of 199,921 plate centers of the approximately 530,000 plates in the HCO collection. We find that the deepest plates are in the region of the Milky Way and the Magellanic Clouds.

Intrinsic Variability of Eclipsing Variable β Lyrae Measured With a Digital SLR Camera

Donald F. Collins
WWC 6017, P.O. Box 9000, Asheville, NC 28815; dcollins@warren-wilson.edu

Abstract Continued observations of β Lyr with a DSLR camera with a standard-issue zoom lens (focal length: 55 mm; *f*/5.6) on an unguided tripod clearly show the well-known eclipse light curve where the magnitude drops about 0.6 magnitude every 12.94 days. After the eclipse light curve is subtracted the data show a definite intrinsic variability with a cycle time ~280 days. These observations were begun in June 2008 and are continuing through the present. The portability of the equipment and quick observation time should encourage many observers to make these observations while reserving telescopes for observing fainter objects. It is desired to obtain several years of similar observations of β Lyr in order to understand the cause of the intrinsic variability. The wide field of view using photographic lenses as opposed to telescopes, while advantageous for bright stars, presents special problems in obtaining suitable flat fields and measuring for atmospheric extinction. The use of electroluminescent film as a source for flat fields will be evaluated. Problems correcting for atmospheric extinction will also be discussed.

Making Good Plots With EXCEL

Michael Koppelman
University of Minnesota, 1523 Valders Avenue N., Golden Valley, MN 55427; michael@clockwork.net

Abstract Microsoft EXCEL is used by many amateur and professional astronomers for data analysis. EXCEL also has plotting capabilities which are often used in their default settings, which create plots that are hard to read and contain many violations of good style. Based on the work of Edward Tufte, I will present examples of good plots and bad plots and demonstrate how to make a good plot with Microsoft EXCEL.

Mrs. Fleming's "Q" Stars

Barbara L. Welther
295 Salem Street, Woburn, MA 01801; barbara.welther@gmail.com

Abstract At Harvard in the 1890s, Williamina Fleming developed an alphabetical classification system for the photographic spectra of "normal" stars. In her system she used the letter "Q" for stars whose line patterns didn't resemble the prototypes. After she published a preliminary catalog of spectral types for more than 10,000 stars, she studied the "peculiar" stars and published several papers on them in The Harvard Circulars. This paper will present the development of her classification system and her discovery of many variable stars and novae by the peculiarities in their photographic spectra.

The Park in the Sky

John Pazmino
979 East 42nd Street, Brooklyn, NY 11210; john.pazmino@ferc.gov

Abstract Parks in towns are favorite spots for stargazing. They commonly have open sky exposure, quiet surrounds, trees to block local lights, proximity to conveniences and transport. In New York City the prime park for astronomy is Central Park through the Top of the Lawn clear sky star viewing sessions on weekends. When a new park opens, astronomers inquire after its utility for stargazing. This was the case on Manhattan when the new High Line opened in June of 2009. But this park is a bit different than the typical center-city park. It's a park in the sky, built on an abandoned elevated railway. The slides shows High Line by day and evening to illustrate its history and features. These demonstrate how the High Line in its few months of its operation became a new habitat for stargazers on each clear evening.

NOTES